Using fluorescence to understand mycobacterial heterogeneity at a single cell level

by

Trisha Parbhoo

Thesis submitted in partial fulfilment of the requirements for the degree of Master of Science in Molecular Biology at the Faculty of Medicine and Health Sciences, University of Stellenbosch

Supervisor: Prof. Samantha Sampson

Co-supervisor: Dr Jomien Mouton

March 2017

DECLARATION

By submitting this thesis/dissertation electronically, I declare that the entirety of the work contained therein is my own, original work, that I am the sole author thereof (save to the extent explicitly otherwise stated), that reproduction and publication thereof by Stellenbosch University will not infringe any third party rights and that I have not previously in its entirety or in part submitted it for obtaining any qualification.

March 2017 _____

ABSTRACT

Tuberculosis remains a major worldwide health threat. Among those infected there is risk of *Mycobacterium tuberculosis*, the causative agent of tuberculosis, developing into an asymptomatic dormant state. Cell-to-cell phenotypic variation is known to contribute to the establishment of diverse colonization states to evade host immune responses. There are major knowledge gaps regarding dormant or viable but non-culturable (VBNC) bacteria as they are difficult to isolate and heterogeneous populations are not reflected by colony forming unit plating. This has led to the application of single-cell techniques, such as flow cytometry, which offers a rapid, high-throughput tool to analyse the physiological and biochemical characteristics of bacteria at a single cell level in *M. tuberculosis.* Here we discussed various applications of flow cytometry for further understanding the physiological nature of bacterial systems. We aim to provide a better understanding of these physiological states of mycobacteria, and this thesis describes efforts to develop tools towards this aim.

To identify and enumerate live and dead *Mycobacterium smegmatis* within a heterogeneous population we optimised the LIVE/DEAD BacLight Bacterial Viability and counting kit, exploiting flow cytometry. *M. smegmatis* was quantified by means of standardization beads, and the kit shows promise for developing a rapid, culture-free counting method for mycobacteria, ultimately replacing colony forming unit (CFU) plating. Efforts were initiated for applying this method to bacteria exposed to various anti-tuberculosis antibiotics, as well as for bacteria spiked into artificial sputum, which will require further investigation.

In addition, flow cytometry was applied together with a recently developed Fluorescence Dilution (FD) reporter system, to enable measurement of differentially replicating mycobacteria in macrophage infection models. Previous studies have reported *M. smegmatis* to be rapidly killed upon uptake into macrophages. In contrast, results from our lab using a *M. smegmatis* macrophage infection model uncovered an unexpected sub-population of apparently dividing *M. smegmatis*. The nature of this population was explored using a fluorescently labelled anti-tuberculosis cell-surface binding antibody in combination with FD, for determination of whether the replicating population was intra- or extracellular of the macrophage. However, further investigation will need to be performed to determine the location of this population.

The findings of this study suggest the feasibility of a real-time tool to distinguish and enumerate live and dead cells within a heterogeneous mycobacterial population. Additionally, FD in combination with

other markers offers a promising technique for studying population-wide adaptation to environmental stress, or even to anti-tuberculosis drugs.

OPSOMMING

Tuberkulose bly 'n wêreldwye gesondheidsbedreiging. Tussen diegene wat met *Mycobacterium turbuculosis* besmet is, die veroorsakende agent van tuberkulose, is daar 'n verdere risiko dat die bakterium in 'n asimptomatiese dormante staat kan ontwikkel. Sel-tot-sel fenotipiese variasies is bekend daarvoor om by te dra tot die vestiging van diverse kolonisasie toestande om die gasheer se immuunreaksie te ontduik. Daar is groot kennisgapings tussen dormante, ook bekend as lewensvatbaar maar nie-kultuurbare bakterieë, omdat dit moeilik is om hulle te isoleer en heterogene bevolkings word nie weerspieël deur enkele kolonievormende eenheide nie. Dit het gelei tot die toepassing van enkelseltegnieke, soos vloeisitometrie, wat 'n vinnige, hoë-deurset instrument is om die fisiologiese en biochemiese eienskappe van bakterieë op 'n enkelselvlak te analiseer. Hier bespreek ons verskeie toepassings van vloeisitometrie vir verdere begrip van die fisiologiese aard van die bakteriële stelsel. Ons doel is om 'n beter begrip van hierdie fisiologiese toestande van mikrobakterieë te voorsien. Hierdie tesis beskryf pogings om gereedskap te ontwikkel vir hierdie doel.

Om lewende en dooie *Mycobacterium smegmatis* te identifiseer binne 'n heterogene bevolking, het ons die LIVE/DEAD BacLight Bakteriese Lewensvaatbaarheid protokol in parallel met vloeisitometrie gebruik. *M. smegmatis* was gekwantifiseer by wyse van gestandariseerde krale, en die tegniek wys belowende resultate vir die ontwikkeling van ‘n vinnige, kultuur-vrye metode om mikrobakterieë te tel, in plaas van om kolonievormende eenhede te plaat. Pogings is geïnisieer vir die toepassing van hierdie metode op bakterieë wat blootgestel is aan verskeie anti-tuberkulose antibiotika, asook bakterieë in kunsmatige speeksel, wat verdere ondersoek vereis.

Daarbenewens is vloeisitometrie saam met die onlangse ontwikkelde Fluoresensie Verwatering (FV) rapporteerstelsel gebruik, om ons in staat te stel om lesings van differensiële repliserende mikrobakterieë in 'n makrofaag infeksiemodel vas te stel. Vorige studies het aangedui dat *M. smegmatis* vinnig doodgemaak is tydens opname in makrofage. In teenstelling hiermee, het die resultate van ons labaratorium se *M. smegmatis* macrofaag infeksiemodel, 'n onverwagte sub-bevolking van repliserende *M. smegmatis* blootgestel. Die aard van die bevolking was ondersoek met behulp van 'n fluoreserend gemerkte anti-tuberkulose seloppervlakbindende teenliggaam in kombinasie met FV, wat gebruik was om te bepaal of die repliserende bevolking intra- of ekstrasellulêr van die makrofaag is. Daar sal egter verdere ondersoek uitgevoer moet word om die ligging van hierdie bevolking te bepaal.

Die bevindinge van hierdie studie dui op die lewensvatbaarheid van 'n ware tyd instrument wat tussen lewende en dooie selle kan onderskei in 'n heterogene mikobakteriële bevolking. Daarbenewens bied

die gebruik van FV, in kombinasie met ander merkers, 'n belowende tegniek te wees vir die bestudering van bevolking-wye aanpassing op omgewingstres, of op anti-tuberkulose dwelms.

ACKNOWLEDGEMENTS

I would like to express my sincere gratitude to my supervisors and mentors, Prof Samantha Sampson and Dr Jomien Mouton who have always offered their guidance, support, motivation and valuable advice throughout my Masters research and writing of this thesis.

Thank you to the lab members of the Host Pathogen Mycobactomics group for their support, assistance and contribution in any way toward this research.

The National Research Foundation (NRF) for their funding.

I warmly thank my parents, brother, loved ones and friends for their support in all aspects of my life, for their upliftment and encouragement.

TABLE OF CONTENTS

Declaration ... ii
Abstract ... iii
Opsomming ... v
Acknowledgements ... vii
List of Abbreviations ... xi
List of Figures ... xiii
List of Tables ... xv
Chapter 1: ... 1
General introduction ... 1
1.1 Background ... 1
1.2 Problem statement ... 2
1.3 Aims ... 2
1.4 Structure of thesis ... 3
Chapter 2: ... 1
Literature review – Mycobacterial flow cytometry ... 1
2.1 Mycobacterium tuberculosis background and challenges ... 1
2.1.1 Tuberculosis burden ... 1
2.1.1 Overview of dormant tuberculosis ... 1
2.2 Challenges for control of tuberculosis ... 2
2.2.1 Tuberculosis diagnosis and treatment ... 2
2.3 Flow cytometry to overcome challenges in mycobacterial research ... 3
2.3.1 Flow cytometry instrumentation ... 3
2.3.2 Advantages of bacterial flow cytometry ... 5
2.3.3 Limitations of bacterial flow cytometry ... 5
2.4 Practical application of flow cytometry to *M. tuberculosis* diagnosis and treatment monitoring ... 6
2.4.1 Counting ... 6
2.4.2 Susceptibility testing ... 6
2.4.3 Drug discovery ... 7
2.5 Application of flow cytometry to *M. tuberculosis* basic research ... 8
2.5.1 Fluorescent probes to determine physiological aspects of cellular components ... 8
2.5.2 Membrane potential ... 10
2.5.3 Membrane integrity ... 11
2.5.4 Metabolic activity ... 12
2.5.5 Cell cycle determination ... 14
2.5.6 Targeting cell surface components ... 14

2.5.7 Analysis of gene expression 15
2.6 Conclusion 16
Chapter 3: 17
Development of a next-generation fluorescence dilution reporter plasmid 17
3.1 Introduction 17
3.2 Materials and Methods 21
3.2.1 Bacterial strains, plasmid DNA and media 21
3.2.2 Generating a next-generation dual fluorescent reporter 22
3.2.3 Fluorescence screening by theophylline induction 25
3.3 Results 26
3.3.1 Rationale 26
3.3.2 First cloning strategy 26
3.3.3 Screening colonies by monitoring basal and induced fluorescence 30
3.3.4 Alternative cloning strategies 32
3.4 Discussion 34
3.4.1 Fluorescent reporter proteins 34
3.4.2 Determining induction of pToiGc 35
3.4.3 Aspects to consider for improving expression 37
3.5 Conclusion 39
Chapter 4: 40
Characterization of differentially replicating *M. smegmatis* upon macrophage infection 40
4.1 Introduction 40
4.2 Materials and Methods 42
4.2.1 Bacterial strains and media 42
4.2.2 Preparation of the conjugated antibody 42
4.2.3 Labelling *M. smegmatis* with the conjugate 43
4.2.4 Mammalian cell culture 44
4.2.5 Flow cytometric sample preparation and acquisition 46
4.3 Results 47
4.3.1 Rationale 47
4.3.2 Reproduction of previous experimental conditions and results 47
4.3.3 Determination of the optimal antibody binding to *M. smegmatis* 49
4.3.4 Applying the optimized antibody conjugate to *M. smegmatis*-infected macrophages 54
4.3.5 Testing antibody binding on an attenuated strain of *M. tuberculosis* 58
4.4 Discussion 59
4.4.1 Replication dynamics of infected *M. smegmatis* reveals population heterogeneity 59
4.4.2 Optimization of binding of the labelling complex 59
4.4.3 Adaptation to host environment 60

4.4.4 Limitations 62
4.4.5 Future work 62
4.5 Conclusion 63
Chapter 5: 64
Application of flow cytometric methods for mycobacterial viability discrimination and cell enumeration 64
5.1 Introduction 64
5.2 Materials and Methods 66
5.2.1 Bacterial strains, media and plasmids 66
5.2.2 Preparation of bacterial samples for flow cytometry 66
5.2.3 Flow cytometric acquisition 67
5.2.4 Sample preparation for transmission electron microscopy (TEM) 68
5.2.5 Staining of *M. smegmatis* recovered from mock sputum 69
5.2.6 Determination of the minimum inhibitory concentration (MIC) 69
5.3 Results 70
5.3.1 Rationale 70
5.3.2 Optimization of the BacLight Live/Dead Bacterial Viability and Counting kit 70
5.3.3 Enumeration of mixed suspensions of live and heat-killed bacteria 79
5.3.4 TEM microscopy: Morphology of live and heat-killed cells 81
5.3.5 Application of the optimized staining method in an attenuated strain of *Mycobacterium tuberculosis* 82
5.3.6 Validation of staining using *M. smegmatis* recovered from mock sputum 83
5.4 Discussion 86
5.4.1 Overview 86
5.4.2 Killing methods 86
5.4.3 PI and SYTO9 affinity 86
5.4.4 Influence of mycobacterial cell wall properties on uptake of dyes 87
5.4.5 Applying the BacLight kit for enumeration of *M. smegmatis* 89
5.4.6 Applying the BacLight kit to *M. smegmatis* recovered from mock sputum 89
5.4.7 Assessing the effect of antibiotics (INH/RIF) on *M. smegmatis* using the BacLight kit 90
5.4.8 Heterogeneity in the live population 91
5.4.9 Limitations 91
5.4.10 Further work 92
5.5 Conclusion 93
Chapter 6: 94
General conclusion 94
References 96

LIST OF ABBREVIATIONS

VBNC	Viable but non-culturable
MDR	Multi-drug resistant
FCS	Forward scatter
SSC	Side scatter
FACS	Fluorescence-Activated Cell Sorting
CTC	5-cyano-2,3-ditolyl tetrazolium chloride
Rpfs	Resuscitation-promoting factors
PI	Propidium iodide
EtBr	Ethidium bromide
FDA	Fluorescein diacetate
FDA	Food and Drug Administration
2-NBDG	2-[N-(7-nitrobenz-2-oxa-1,3—diazol-4-yl)amino]-2-deoxyglucose
EdU	5-ethynyl-2'-deoxyuridine
IPTG	Isopropyl-beta-D-thiogalactopyranoside
PS	Phosphatidylserine
7-AAD	7-aminoactinomycin D
PBP	Penicillin-binding proteins
MIC	Minimum inhibitory concentration
PBS	Phosphate buffered saline
EDTA	Ethylenediaminetetraacetic acid
PMT	Photomultiplier tube
SP	Short pass
LP	Long pass
TEM	Transmission electron microscopy
NHLS	National Health Laboratory Service
RIF	Rifampicin
INH	Isoniazid
NALC	N-acetyl-L-cysteine
NALC-NaOH	NALC-sodium hydroxide
CFU	Colony forming unit
FD	Fluorescence dilution
BCG	*Bacillus Calmette-Guérin*

bp	Base pair
nm	Nano meter
LB	Luria-Bertani
OADC	Oleic acid-albumin-dextrose-catalase supplement
TE	Tris-EDTA
µl	Micro litre
NEB	New England Biolabs
OD	Optical density
SOC	Super Optimal Broth
CAF	Central Analytical Facility
WT	Wildtype
GFP	Green fluorescent protein
RFU	Relative fluorescence units
PCR	Polymerase chain reaction
UTR	Untranslated region
3’	3 prime
5’	5 prime
RBS	Ribosome binding site
Sec	Second
pT	Plus theophylline
MFI	Mean fluorescence intensity
mT	Minus theophylline

LIST OF FIGURES

Fig 2.1. Schematic of flow cytometry instrumentation. 4
Fig 2.2. Various fluorescent probes can be selected for targeting different physiological processes of the cell. 11
Fig 3.1. The theophylline riboswitch. 20
Fig 3.2. Cloning design of the first cloning strategy. 26
Fig 3.3. Amplification of tdTomato. 27
Fig 3.4. Restriction enzyme digestion. 27
Fig 3.5. Verification of pSTom. 28
Fig 3.6. Restriction enzyme digestion of pTiGc. 29
Fig 3.7. Confirmation of the presence of GFP. 29
Fig 3.8. Testing of single colour controls. 30
Fig 3.9. Fold change of tdTomato expression in $pToiGc_{11}$ and $pToiGc_{12}$. 31
Fig 3.10. Cloning design for both alternative cloning strategies. 32
Fig 3.11. Fold change of tdTomato for $pSTom_{2.6}$, $pSTom_{2.10}$, $pSTom_{3.8}$ and $pSTom_{3.12}$. 33
Fig 4.1. Measurement of bacterial replication using fluorescence dilution. 41
Fig 4.2. Formation of the antibody conjugate 43
Fig 4.3. Confirmation of induction 48
Fig 4.4. Population-wide and summative *M. smegmatis* replication dynamics upon macrophage infection. 49
Fig 4.5. Workflow for preparing samples with the labelling complex as suggested by the Zenon Labelling kit. 50
Fig 4.6. Increasing ratios of antibody:bacteria improved labelling. 51
Fig 4.7. Comparison between fixation methods. 52
Fig 4.8. Saturation of binding at 2 µg. 52
Fig 4.9. Fluorescence was enhanced and binding improved using the 6:1 ratio. 53
Fig 4.10. *M. smegmatis*::pTiGc displayed optimal binding to the antibody conjugate using 3 µg antibody. 53
Fig 4.11. Optimized workflow for labelling bacteria with the antibody conjugate. 54
Fig 4.12. Gating strategy. 55
Fig 4.13. The heterogeneous bacterial population at 24h in lysed and non-lysed macrophages. 56
Fig 4.14. Possible scenarios for labelling with the antibody conjugate. 57
Fig 4.15. Labelling *M. tuberculosis* with the antibody conjugate. 58

Fig 5.1. Staining of SYTO9 and PI. 64
Fig 5.2. Organism specific differences contribute to the variation in staining. 70
Fig 5.3. Workflow for the BacLight Live/Dead Bacterial Viability and Counting kit. 71
Fig 5.4. Using 70% ethanol as a killing method resulted in a large proportion of cell debris. 71
Fig 5.5. Testing killing methods 72
Fig 5.6. Testing heat-killing. 72
Fig 5.7. Workflow of data analysis 73
Fig 5.8. Modifications to the protocol by lengthening the incubation time for SYTO9 improved binding. 74
Fig 5.9. Fixing stained samples affected bacterial numbers. 75
Fig 5.10. Batch fixing samples improved bacterial numbers. 75
Fig 5.11. The addition of 1 mM EDTA improved grouping of live cells 76
Fig 5.12. Optimizing dye ratios 77
Fig 5.13. Samples were analysed 24h post preparation. 78
Fig 5.14. Single-stained controls were compared at 0h and 24h post preparation. 78
Fig 5.15. Optimized workflow for sample preparation with the BacLight Live/Dead Bacterial Viability and Counting kit. 79
Fig 5.16. Identification of the bead population 79
Fig 5.17. Enumeration of mixed samples 80
Fig 5.18. Correlation of cell counts for flow cytometry and plating 81
Fig 5.19. TEM images displaying morphology of live, live + 1 mM EDTA and heat-killed M. smegmatis. 82
Fig 5.20. Applying the optimized staining method to *M. tuberculosis*. 83
Fig 5.21. Applying the optimized staining to *M. smegmatis* recovered from mock sputum. 84
Fig 5.22. *M. smegmatis* treated with NALC resulted in no intermediary population. 84
Fig 5.23. NALC treated sputum displayed the intermediary population. 85
Fig 5.24. Live and dead *M. smegmatis* were differentiated following recovery from mock sputum. . 85

LIST OF TABLES

Table 2.1. Characteristics of various fluorescent probes utilized in bacterial flow cytometry 8
Table 3.1. Bacterial strains and vectors used in this study 21
Table 3.2. Primers used to generate the dual fluorescent reporter 22
Table 3.3. PCR reaction components and cycling conditions 23
Table 3.4. Properties of orange-red fluorescent reporters 35
Table 4.1. Bacterial strains and vectors used in this study 42
Table 4.2. LSRFortessa laser configuration 46
Table 4.3. Mean fluorescence intensity of Alexa Fluor 405 for the live bacteria 58
Table 5.1. FACS Canto II laser configuration 68

Chapter 1:

GENERAL INTRODUCTION

1.1 BACKGROUND

The ability of *Mycobacterium tuberculosis,* the causative agent of tuberculosis, to adapt in the host contributes to tuberculosis being one of the leading pulmonary infectious diseases in the world. According to the latest World Health Organization (WHO) tuberculosis report, 9.6 million individuals are estimated to contract tuberculosis annually, causing 1.5 million deaths globally each year (World Health Organization, 2015). As infection with *M. tuberculosis* progresses, the bacilli experience various degrees of environmental stressors such as temperature change, nutrient deprivation or exposure to toxic agents which has shown to cause a loss of culturability (Oliver, 2010). *M. tuberculosis* responds to these adverse conditions by entering into a dormant state, as a survival strategy. This dormant state results in the infection to persist in a clinically asymptomatic state, with the ability to reactivate. This may include a physiologically viable but non-culturable (VBNC) subpopulation, which is characterised by a loss of growth on solid media, while remaining metabolically active. The VBNC population may also harbour persistent bacteria, which are multi-drug tolerant, despite the majority of the population being genetically susceptible to antibiotics (Chao and Rubin, 2010). Persisters are able to survive high concentrations of antibiotic exposure, whilst remaining genetically clonal as the bacterial population. This is in contrast to drug-induced tolerance, which is acquired through genetic mutations (Brauner *et al*., 2016). Cell-to-cell variation contributes to the phenotypic heterogeneity within the host, this plays a key role in the detection and subsequent management of these populations. It is estimated that 37% of new cases were undiagnosed (World Health Organization, 2015), which may be as a result of individuals experiencing infection in an asymptomatic dormant state. There is a growing appreciation that bacterial populations are more heterogeneous than previously thought, and understanding this heterogeneity may assist to develop effective interventions. In this thesis we have developed tools to exploit the power of flow cytometry to understand mycobacterial heterogeneity at a single cell level.

This range in varying conditions promotes diverse physiological changes within *M. tuberculosis*, which makes analysing these populations very complex. Flow cytometry allows rapid, real-time quantitative analysis of a large amount of bacteria at a single cell level to provide information on the physiological and biochemical characteristics of bacteria within a heterogeneous population, as elaborated in chapter 2.

In combination with flow cytometry, a novel technique termed Fluorescence Dilution (FD) was developed in our lab for use in mycobacteria (Mouton *et al.*, 2016). This technique utilizes a dual-reporter system; a constitutive reporter to track the viable bacteria, and an inducible reporter for the measurement of bacterial replication. To improve upon the existing system, we aimed to develop a next-generation dual-reporter plasmid, by replacing the inducible TurboFP635 reporter, currently incorporated into the FD system, with the tdTomato reporter, for which suitable lasers for flow cytometry are more widely accessible than for TurboFP635. FD was used for identification of differentially replicating *Mycobacterium smegmatis* in macrophage infection models, which surprisingly revealed a replicating *M. smegmatis* population. *M. smegmatis* has previously been shown to not survive within the macrophage environment (Kuehnel *et al*., 2001; Prakash *et al*., 2010), therefore this replicating population was further investigated to determine whether this population was intra- or extracellular of the macrophage, using FD in combination with an anti-*M. tuberculosis* antibody.

A major hurdle to TB research and diagnosis is the slow growth rate of *M. tuberculosis*. Traditional cell counting techniques, such as the plate count method relies on the ability of viable cells to grow on solid media and was considered the ideal method for the enumeration and identification of actively growing bacterial cells. This is however hindered by the lengthy time needed for *M. tuberculosis* to form visible colonies (3-4 weeks). To address this, we optimised and developed a flow-cytometric-based method for distinguishing and enumerating live and dead bacteria within a heterogeneous population.

1.2 Problem statement

A rapid and accurate method is required for identification and enumeration of the various physiological states of mycobacteria within a heterogeneous population.

1.3 Aims

Aim 1: To develop and validate the next-generation dual-reporter plasmid.

Aim 2: To develop a rapid flow cytometric method for live/dead mycobacterial discrimination and cell enumeration.

Aim 3: To apply the dual-fluorescent plasmid, in combination with fluorescence dilution and an anti-mycobacterial antibody to characterize differentially replicating *M. smegmatis* in macrophage infection models.

1.4 STRUCTURE OF THESIS

Chapter 1:

The general introduction sets the scope of the thesis by establishing the significance of a heterogeneous mycobacterial population with mention to the knowledge gaps and impact on a clinical setting.

Chapter 2:

The literature review summarizes the advancement of flow cytometry for bacterial systems, by addressing potential applications and various fluorescent dyes for understanding the physiological state of mycobacteria.

Chapter3:

This chapter concentrated on developing a next-generation dual-reporter plasmid for application using the fluorescence dilution technique specifically for mycobacteria.

Chapter 4:

This chapter introduces a flow cytometric method developed for rapidly and accurately distinguishing and enumerating live and dead *M. smegmatis* in a heterogeneous population.

Chapter 5:

As *M. smegmatis* does not readily survive the macrophage environment, this chapter focussed on determining whether an unexpected replicating population was intra- or extracellular of the macrophage, using a novel technique termed fluorescence dilution in combination with a mycobacterial specific antibody.

CHAPTER 2:

LITERATURE REVIEW – MYCOBACTERIAL FLOW CYTOMETRY

2.1 MYCOBACTERIUM TUBERCULOSIS BACKGROUND AND CHALLENGES

2.1.1 Tuberculosis burden

Mycobacterium tuberculosis, the etiological agent of tuberculosis was first discovered in 1882 by Robert Koch and remains one of the leading causes of death worldwide (Sakula, 1982). According to the World Health Organization (WHO) global tuberculosis report 2015, it is estimated that 9.6 million people contracted tuberculosis in 2014 alone, of which 1.5 million people were killed (World Health Organization, 2015). Despite the development and implementation of the appropriate treatment regimen, majority of cases are not reported, therefore contributing to the rise in multi-drug resistant (MDR) tuberculosis.

Additionally, latent infection is estimated to account for a third of the world's population, although the lifetime risk for reactivation is approximately 5-10%. However, several risk factors such as HIV infection, malnutrition and diabetes are known to increase progression into the active state (World Health Organization, 2015).

2.1.1 Overview of dormant tuberculosis

M. tuberculosis adapts to the host cell environment by inducing an asymptomatic dormant state during harsh environmental instability. This allows the bacilli to withstand stressful conditions by being able to persist for many years in the host with the potential to resuscitate and cause active tuberculosis. The dormant bacterial state comprises of subpopulations of viable but non-culturable (VBNC) bacteria and persister cells. VBNC cells are characterized by a loss of growth on selective laboratory media, whilst still metabolically active. Persister cells are thought to be genetically identical to the non-persister population, but display a drug-tolerant phenotype with the potential to regrow when the stress is alleviated (Lewis, 2010; Pinto *et al.*, 2011). Currently, most drug therapies are targeted at actively replicating bacteria, therefore the ability to detect and distinguish between the active and dormant states of tuberculosis is essential for more effective treatment regimens. The factors influencing drug distribution in the host is largely unknown, although alterations in the cell

wall composition of dormant states may affect the permeability and transport mechanisms of anti-tuberculosis drugs (Dartois, 2014).

2.2 CHALLENGES FOR CONTROL OF TUBERCULOSIS

Historically, traditional cell counting techniques were considered the ideal method for confirmation of active tuberculosis based on microbiological or histopathological features. This strategy, overall, is inadequate for the detection of bacteria in dormant infection, presumably due to their low numbers and non- or minimally replicating nature. In addition, the plate count method relies on the ability of viable cells to grow on solid media. This poses a huge risk to public health as VBNC cells are not accounted for, thus leading to an underrepresentation of the total amount of viable cells in an environmental or clinical sample (Li *et al*., 2014). However, this is particularly problematic for *M. tuberculosis*, where their lengthy doubling time translates into 3-4 weeks to form visible colonies on agar plates (Breeuwer and Abee, 2000). The broad range of physiological states of bacteria enhances the underlying cell-to-cell phenotypic variation, thus contributing to the heterogeneity that exists within mycobacterial populations.

2.2.1 Tuberculosis diagnosis and treatment

Routine tuberculosis testing is carried out throughout the world with the main objective of identifying active disease in patients. However, the distinction between active and dormant infection is critical for the clinical management of patients. The sputum smear microscopy test is a key inexpensive, yet simple diagnostic tool for the identification of acid-fast bacilli in patients' sputum. This technique however, requires a minimum of 10 000 bacterial cells per ml of sputum and is unable to detect drug susceptibilities (Keeler *et al*., 2006; Lawn and Wilkinson, 2006). GeneXpert is able to identify *M. tuberculosis* and resistance to rifampicin in paucibacillary sputum and extrapulmonary samples (Pandey *et al.*, 2017) The impact of infection has a detrimental effect, especially when individuals are co-infected with HIV. For example, observation of Ziehl-Neelsen stained sputum samples performs poorly in immunocompromised individuals (Holani *et al*., 2014). Additionally, the collection of good quality samples required for diagnosis represents a limitation in areas with a high HIV co-infection rate as these patients produce inferior quality sputum, which may affect analysis or diagnosis (Steingart *et al*., 2006).

M. tuberculosis infections can in most cases be successfully resolved with the use of at least four antibiotics during a standard 2 month course, followed by two antibiotics for a further 4 months. However, the prevalence of multi-drug resistant (MDR) tuberculosis has increased during the last decade. Due to the extreme slow growth of *M. tuberculosis,* alternative and more rapid methods of susceptibility tests is required. It is estimated that only 25% of new MDR-TB cases each year are

detected (World Health Organization, 2015). Failure to diagnose drug resistance not only leads to unsuitable treatment that results in a detrimental outcome to the patient; it could enhance resistance and transmission within the community, ultimately worsening the situation (Zumla *et al.*, 2012). Further complications affecting treatment results could be due to the presence of non-tuberculosis strains present in patients' sputum, the facilities needed to handle highly infectious agents and the varying range of bacterial densities in sputum samples. New diagnostic approaches would need to combine specificity, sensitivity, speed, biosafety and reliable determination of resistance to the standard anti-tuberculosis drugs administered (Piuri *et al.*, 2009).

Application of these characteristics to incorporate patient specific immune defence response could improve treatment for *M. tuberculosis* infection. It is of utmost importance to apply a reliable detection method for the enumeration of a heterogeneous bacterial population as this could aid in the improvement of patient specific treatment. Additionally, the understanding of the mechanism of dormant infection may provide valuable insight into the physiology of mycobacterial cells, which may assist in the development of rapid and specific novel detection methods.

2.3 FLOW CYTOMETRY TO OVERCOME CHALLENGES IN MYCOBACTERIAL RESEARCH

There is an increasing need for alternative techniques that allow real-time quantitative analysis of bacterial numbers and its physiological state. One approach is to harness the multiple advantages of flow cytometry. There is promising evidence suggesting flow cytometry as a promising tool for clinical studies due to its many advantages in comparison to available immune-based tests (Hendon-Dunn *et al*., 2016; Sester *et al*., 2011).

2.3.1 Flow cytometry instrumentation

Flow cytometry is a technique involving rapid multiparametric analysis of individual cells by combining fluidics, optics and electronic parameters. The fluidics system delivers cells individually at a rate of a few thousand per second in a fluid stream to the laser intercept for analysis (Fig 2.1). This involves the simultaneous measurement of multiple characteristics of cells, which includes the relative sizes of cells, their granularity and fluorescence intensity. The ability of flow cytometers to measure both intrinsic and extrinsic properties of cells for the determination of cell viability is not only achieved through light scattering, but also by the use of various fluorescent reporters. These can be heterologously expressed or introduced through staining techniques. Measurement of these characteristics depends on the optics system which most commonly consists of a blue (488 nm) Argon ion laser, although multiple lasers may be used depending on the model of the flow cytometer used. This beam is focused on the cell at the laser intercept, causing the cell to scatter the laser light in all

angles. Light scattered at acute angles is measured by forward scatter (FSC) and light scattered at right angles (90°) is measured by side scatter (SSC). FSC provides information on the size of the cell, whereas SSC is related to the internal granularity of the cell. The combination of FSC and SSC can also be used to distinguish different types of cells, such as mammalian cells (Freud *et al.*, 2005), bacteria (Gunasekera *et al.*, 2000) and plant cells (Sliwinska *et al.*, 2005). For bacteria, these lasers are able to excite naturally fluorescent bacteria or bacteria labelled with probes to track various cellular components or processes (Ambriz-Aviña *et al.*, 2014; Tracy *et al.*, 2010). The light scattering signals yield qualitative data concerning cell size or granularity, whereas the fluorescence signals yield quantitative information regarding the analysis of intracellular components such as nucleic acids, proteins, lipids, membrane potential and ion fluxes, or the expression of surface antigens (Nuding, 2013).

The electronics system directs the light signals obtained from the lasers to the appropriate photomultiplier tubes (PMT) detectors using optical filters, where it is converted into electronic signals using computer-based algorithms. The electrical signals, known as an event are processed by linear and logarithmic amplifiers to measure the fluorescent signals. These signals will generate a series of numbers and plots when analysed by flow cytometry software to yield the ability of how cells scatter the incident laser light to emit fluorescence.

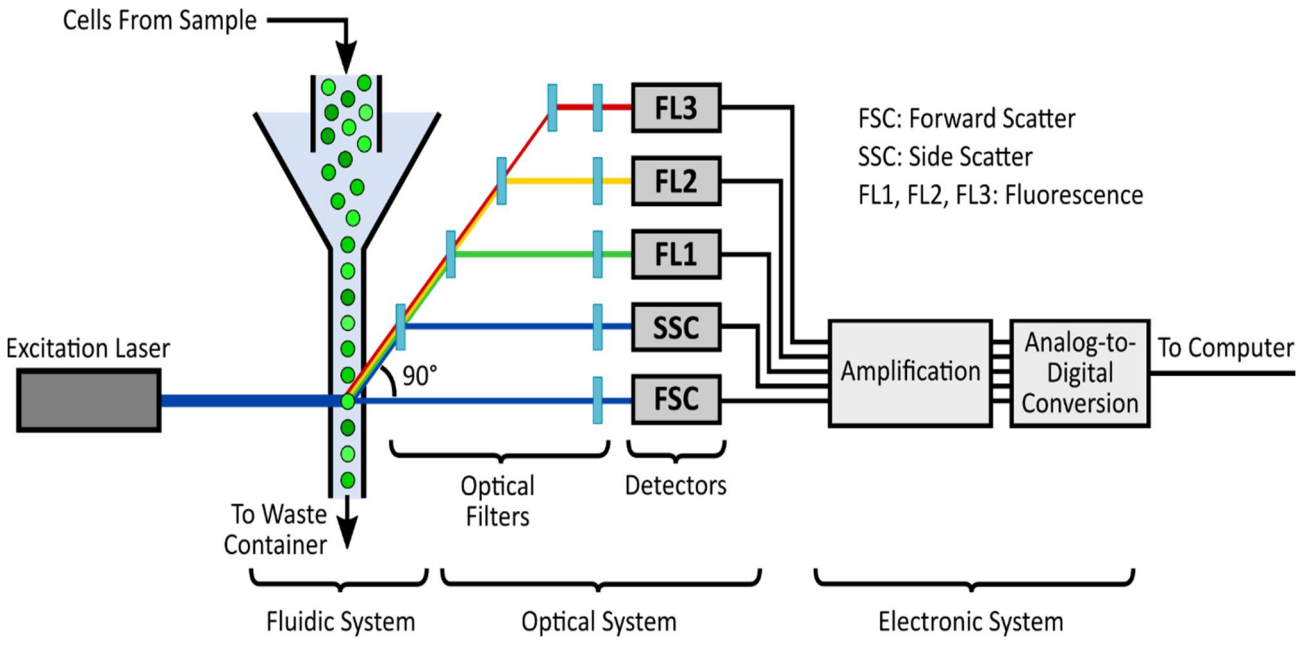

Fig 2.1. Schematic of flow cytometry instrumentation. Cells are passed through the fluidic system, where their size (FSC), granularity (SSC) and fluorescence intensity (FL1, FL2, FL3) is measured in the optical system. These signals are relayed into electronic signals to measure the light scattering abilities of the cells to emit fluorescence (Figure from Castillo-Hair, 2016).

Flow cytometers can also be equipped with a cell-sorting function for Fluorescence-Activated Cell Sorting (FACS) analysis, where cells with desirable phenotypic and physiological properties can be

identified, captured and sorted into tubes for subsequent analysis or subculturing for molecular, functional and clinical applications (Perez and Nolan, 2006). When cells with desirable characteristics are detected, the sorter expels a charge onto the cell as it passes through and generates an electrostatic field which deflects cells into collection tubes. Cells can be sorted at a rate of 40 000 cells per second (Herzenberg *et al*., 2002) and has previously been used to isolate bacteria in varying physiological states (Claudi *et al*., 2014; Morishige *et al*., 2015). FACS has not extensively been exploited to analyse complex phenotypes, but there is immense potential regarding the analysis of the physiological aspect of such phenotypes which could benefit medical and industrial sectors.

2.3.2 Advantages of bacterial flow cytometry

In a bacterial population, the application of flow cytometry allows the rapid and direct analysis of a large number of bacteria at a single cell level. The combination of fluorescent probes targeting different cellular targets can also be exploited to provide information on the physiological and biochemical characteristics of bacteria, which in turn allows the determination of population heterogeneity as there are many complex phenotypes within a single population (Chao and Rubin, 2010; Vives-Rego *et al*., 2000). In addition, this highly sensitive technique allows the detection of low bacterial numbers, which is expected for VBNC populations (Ambriz-Aviña *et al*., 2014). Bacterial species known to enter the VBNC state (Li *et al*., 2014; Oliver, 2010; Ramamurthy *et al*., 2014), share many general characteristics with viable cells. For example, they maintain an active membrane potential and cellular integrity, however they undergo various physiological, metabolic and molecular changes, including a change in cellular morphology, cell wall and membrane composition, metabolism, gene expression and virulence potential (Du *et al*., 2007; Keer and Birch, 2003).

2.3.3 Limitations of bacterial flow cytometry

The potential of flow cytometry for bacterial systems has not yet been fully exploited, due to the challenges posed by the smaller sizes of bacterial cells, decreased protein and nucleic acid content, lack of fluorescent markers and originally being developed for mammalian cells, and the overall lack of experience in applying this technique to bacteria. Bacterial membranes are also less permeable to fluorescent dyes than mammalian cells and due to bacteria having such effective efflux pumps, many fluorescent dyes are pumped out (Tracy *et al*., 2010). Therefore, more precise instrument calibration and higher signal amplification is required for analysing bacterial samples (Braga *et al*., 2003). Bacteria that have most often been analysed using flow cytometry include *Escherichia coli* and *Staphylococcus aureus* due to their presence as single cells and generally uniform morphology. However, some bacteria naturally grow in intertwining chains of different lengths, for example *Streptococcus pyogenes*, which will ultimately lower the accuracy of the results obtained using flow cytometry.

Bacterial cells therefore need to be disaggregated either by chemical, mechanical or ultrasonic treatment to obtain single cells *(Braga et al.*, 2003). Despite the limitations in the application of flow cytometry to investigate bacterial systems, significant progress has been made for its development (Hong *et al.*, 2015; Langemann *et al*., 2016).

In this review we will address the diversity and broad range of applications flow cytometry can be exploited for bacterial systems, for understanding of *M. tuberculosis* at an applied and basic research level.

2.4 PRACTICAL APPLICATION OF FLOW CYTOMETRY TO *M. TUBERCULOSIS* DIAGNOSIS AND TREATMENT MONITORING

2.4.1 Counting

Flow cytometric detection, identification and susceptibility testing can offer more valuable advantages by identifying and analysing heterogeneous subpopulations at a single-cell level. Antibiotic-treated *M. tuberculosis* has shown to contribute to population heterogeneity, and these populations may not be detected by the plate count method. Flow cytometry, using a variety of viability and metabolic activity dyes has shown to discriminate between these varying physiological states in response to anti-tuberculosis drugs (Hendon-Dunn *et al.*, 2016), therefore these varying populations can be rapidly enumerated using standardization beads (Chapter 5). Currently, a mycobacterial counting method using flow cytometry has not been reported, with exception to Burdz *et al*., who attempted to count the loss of viable *M. tuberculosis* following recovery from different sputum decontamination methods (Burdz *et al.*, 2003). Despite, their flow cytometry counts not corresponding to plate counts, this proves the range in applications counting will be useful for *M. tuberculosis,* using flow cytometry. Due to the slow growth of *M. tuberculosis,* this will be valuable for susceptibility testing of existing or novel anti-tuberculosis drugs.

2.4.2 Susceptibility testing

Within a heterogeneous culture *M. tuberculosis* can be detected by constructing recombinant mycobacteriophages containing fluorescent reporters to generate fluoromycobacteriophages, which specifically infect and replicate in mycobacteria. These can be used in antibiotic susceptibility testing as fluoromycobacteriophages are able to discriminate between drug sensitive and drug resistant *M. tuberculosis* strains by the absence or presence of fluorescence, respectively (Piuri *et al*., 2009). For example, the construction of the reporter mycobacteriophage ϕ^2GFP10 allows for phenotypic drug resistance testing to rifampin in *M. tuberculosis* clinical sputum samples at less than 10^4 bacilli/ml (paucibacillary concentrations). In addition, detection remained sensitive in HIV-infected patients in

comparison to GeneXpert (O'Donnell *et al*., 2015). This is especially important for evaluating acid-fast bacilli smear-negative sputum samples of HIV infected individuals (Boehme *et al*., 2010), which is known for its poor quality.

A rapid flow cytometry-based method was recently developed for the determination of antibiotic activity of rifampicin and isoniazid against *M. tuberculosis*. Based on the mode of action of these antibiotics, the fluorescent dyes calcein violet acetoxymethyl (AM) and SYTOX-green were used to determine the susceptibility of a bacterial population post antibiotic exposure. This resulted in differential susceptibility phenotypes, including subpopulations of injured cells and delayed killing post exposure (Hendon-Dunn *et al.*, 2016). These subpopulations will not only be undetected by conventional assays, but would most probably be unculturable. Conventional assays under-represent the actual state of the bacterial population, as they provide no detail in the alteration of morphology of individual bacterial cells after antibiotic treatment nor the change in expression of surface proteins (Nuding, 2013). Therefore, flow cytometry offers a valuable method for distinguishing the mode of action of drugs and can therefore be applied to identify effective drugs.

2.4.3 Drug discovery

In VBNC cells of *M. smegmatis,* a substantial increase in resistance to hygromycin and doxycycline was observed in comparison to stationary phase cultures grown for 48 hours (Anuchin *et al*., 2009). Novel antibiotics could also be applied in combination with various fluorescent probes for the determination of its mode of action, killing effect and susceptibility on bacterial populations, similar to the application of flow cytometry to assess the response of *M. tuberculosis* to antibiotics with different modes of action (Hendon-Dunn *et al.*, 2016). For example, the mode of action of the antimicrobial tachyplesin I on *E. coli,* using PI and carboxyfluorescein confirmed simultaneous cell membrane damage and intracellular esterase inactivation (Hong *et al*., 2015).

Additionally, the identification of novel antituberculosis compounds could be discovered. For example, bedaquiline, which is a novel inhibitor of mycobacterial ATP synthase was discovered by screening compound libraries against *M. smegmatis* (Andries *et al.*, 2005). To detect antibiotic binding sites on the cell surface, antibiotics conjugated to fluorescent reporters can be used to determine cell wall biosynthesis or antibiotic resistance in *M. tuberculosis* using flow cytometry. For example, penicillin is used to detect penicillin-binding proteins (PBP) on the cell surface of *S. aureus* and *Enterococcus faecalis* (Jarzembowski *et al*., 2008).

Therefore the identification of more effective antimicrobials and the susceptibility testing thereof can be applied using multiparametric flow cytometry in combination with various fluorescent probes

targeting membrane potential, metabolic activity and membrane integrity. Due to the rise in the amount of MDR and XDR *M. tuberculosis* strains (World Health Organization, 2015), response to antibiotic susceptibility testing at a single-cell level will be beneficial. This will allow the detection of susceptible and resistant cells more rapidly, as well as the determination of the minimal inhibitory concentration (MIC) of antimicrobials in clinical isolates, thus decreasing the time needed for outcomes of these results.

2.5 APPLICATION OF FLOW CYTOMETRY TO *M. TUBERCULOSIS* BASIC RESEARCH

2.5.1 Fluorescent probes to determine physiological aspects of cellular components

A broad range of fluorescent probes are available to assess the physiological state and target various specific cellular components in microorganisms. For example, fluorescent dyes with different cell permeability attributes can be used to differentiate between different cell membrane integrities. Fluorescent dyes are characterized by their different excitation and emission spectra (Table 2.1). This allows for multiparametric measurements, as distinct excitation and emission spectra allows the discrimination of each fluorescent dye (Joux and Lebaron, 2000). The fluorescent probes and the methods used to label cells have greatly improved in bacterial systems, although it is still underused. By combining dyes that target different cellular characteristics, a more accurate representation of the physiological state of a population can be simultaneously obtained. For example, with the use of nucleic acid dyes both membrane integrity and metabolic activity can be determined as this simultaneously provides information on whether an intact cell is actively metabolizing.

A challenge however, is selecting a combination of fluorophores with limited spectral overlap. This will allow minimal compensation, whilst maintaining the accuracy and quality of the data. The brightness of a fluorophore may also be affected by background fluorescence, such as cellular autofluorescence, non-specific staining or instrument noise. These properties will differ between cell types and the interaction of the fluorophores when dual-stained. The use of dyes may affect cell physiology and it is therefore not recommended for long-term study of bacteria (Maglica *et al*., 2015). The following sections briefly explores several commonly used bacterial flow cytometry dyes, more of which are listed in Table 2.1.

Table 2.1. Characteristics of various fluorescent probes utilized in bacterial flow cytometry

Cellular target sites	Fluorescent dyes	Excitation (nm)	Emission (nm)	Cell permeant	References
Metabolic activity 1. Esterases	Fluorescein diacetate	473	514	Yes	Diaper *et al*., 1992
	Calcein AM	495	515	Yes	López-Amorós *et al*., 1998
	DyLight 488	493	518	Yes	Robertson and Vora, 2012
2. Tetrazoliums	5-cyano-2,3-ditolyl tetrazolium chloride (CTC)	450	630	Yes	Stellmach and Severin, 1987
Membrane potential	$DiBAC_4$	493	516	Yes	Jepras *et al.,* 1997
	$DiOC_2(3)$	482	497	Yes	Novo *et al*., 2000
	$DiOC_5(3)$	482	497	Yes	Ordóñez and Wehman, 1993
	$DiOC_6(3)$	484	501	Yes	Rottenberg and Wu, 1998
	Rhodamine 123	507	529	Yes	Shleeva *et al.*, 2002
Membrane integrity	SYTO 9	485	498	Yes	Langsrud and Sundheim, 1996
	Propidium iodide	488	617	No	Langsrud and Sundheim, 1996
	SYTOX green	504	523	No	Roth *et al*., 1997
	7-AAD	546	647	No	Koopman *et al*., 1994
	Calcein AM	495	515	Yes	Comas and Vives-Rego, 1998
	Calcein Blue AM	360	445	Yes	Bunthof *et al*., 2001
	CyTRAK orange	515	615	Yes	Edward, 2009
	DAPI	350	470	Yes	Sauvat *et al*., 2015
	DRAQ5	646	697	Yes	Bernander *et al*., 1998
	Hoechst 33342	350	461	Yes	Sauvat *et al*., 2015
	SYTO 13	488	509	Yes	Mason *et al*., 1998
	SYTOX blue	444	480	No	Müller and Nebe-von-Caron, 2010
	Thiazole Orange	510	530	Yes	Bunthof *et al*., 2001
	TO-PRO-3	642	661	No	Kerstens *et al.,* 2014
	YO-PRO-3	612	631	No	Sandilos *et al.,* 2012
	YOYO-1	491	509	No	Marie *et al*., 1996
Cell cycle determination	Acridine orange	502	525	Yes	Mason and Lloyd, 1997
	Annexin V FITC	494	518	No	Lee *et al*., 2006
	Annexin V Alexa Fluor 488	495	519	No	Lönnbro *et al.,* 2008
	Dextran Texas Red	595	615	Yes	Zenk *et al*., 2009

2.5.2 Membrane potential

In the cell, maintenance of the membrane potential is necessary for the synthesis of ATP and the regulation of intracellular pH. In bacterial cells with damaged membranes or cells killed due to heating, freezing or exposure to beta-lactam antibiotics, the membrane potential diminishes to zero (Novo *et al*., 2000). This criteria is vital for understanding the impact of anti-tuberculosis drugs on intracellular ATP levels and bacterial energy metabolism and how this translates into antibacterial activity, as this could either inhibit ATP synthase or cause a disruption in the electrochemical gradient (Andries *et al*., 2005). Metabolically active bacteria generate an electrochemical potential by ATP hydrolysis. The selective permeability of cell membranes to a variety of cations and anions, results in polarized cells that are electrically negative on the inside of the cytoplasmic membrane with respect to the exterior (Tracy *et al*., 2010). The cationic cyanines $DiOC_2(3)$, $DiOC_5(3)$, $DiOC_6(3)$ and Rhodamine 123 (Rh123) thus accumulates in polarized cells (Fig 2.2), whereas the bis-oxonol dye, $DiBAC_4$, only enters upon cell depolarization (As reviewed in Langemann et al., 2016; Nuding, 2013).

$DiOC_2(3)$ (3,3′-diethyloxacarbocyanine iodide) penetrates the cytosol and fluoresces green in all bacterial cells, but in bacterial cells with active membrane potentials the dye molecules self-associate at the higher cytosolic concentrations, causing fluorescence to shift towards red emission. Applying $DiOC_2(3)$ to evaluate the adaptation and resistance of *M. tuberculosis* to acid stress has shown to be oxygen or nitrate dependant. During hypoxia *M. tuberculosis* is able to use nitrate as an electron acceptor to maintain a lower level of ATP, thus contributing to the viability of persistent bacteria (Rao *et al*., 2008; Tan *et al*., 2010). The use of membrane potential dyes has received little application with regards to treatment that naturally causes a disruption in the cell membrane of *M. tuberculosis* (e.g., antibiotics and surfactants) and is inconclusive. However, a drawback of some membrane potential dyes is the requirement of a pre-treatment step by the addition of EDTA to permeabilize the outer membrane of gram negative bacteria. Metabolic activity is dependent on an intact cell membrane in order to maintain an electrochemical gradient to generate a membrane potential. Therefore, this step may introduce bias as it could enhance the toxic effects of compounds when studying drug interactions as it allows antimicrobials to penetrate the cell more easily (Joux and Lebaron, 2000).

$DiOC_6(3)$ accumulates within the mitochondrial matrix according to the extent of the membrane potential and has mainly featured in studies on mitochondrial functionality during apoptosis in *M. tuberculosis* (Sánchez *et al.*, 2012; Vermes *et al.*, 2000).

Staining dormant *M. tuberculosis, M. bovis* and *Rhodococcus rhodochrous* with Rh123 followed by addition with supernatant of growing cultures has previously been used to show that the growth factor activity of resuscitation-promoting factors (Rpfs) within growing cultures is able to restore growth to that of bacteria growing exponentially (Shleeva *et al*., 2002).

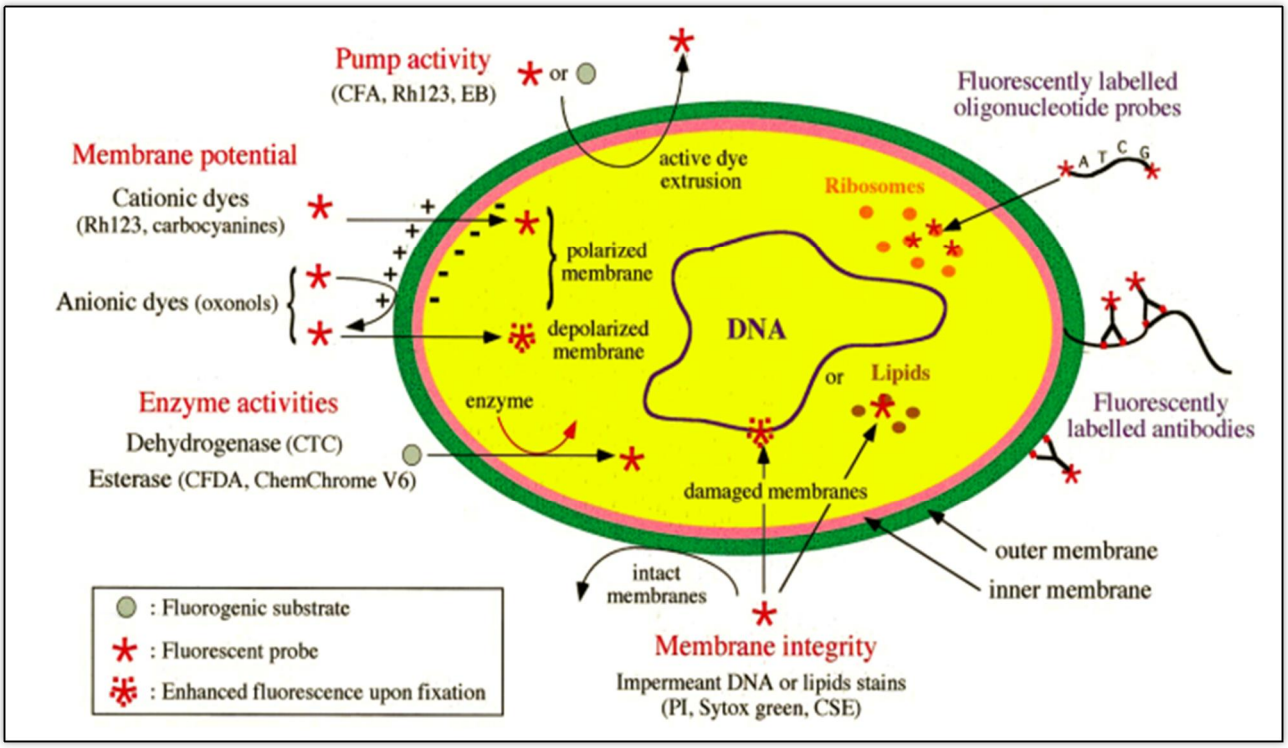

Fig 2.2. Various fluorescent probes can be selected for targeting different physiological processes of the cell. Figure from Joux and Lebaron (2000).

2.5.3 Membrane integrity

The most common way to detect cell viability is by monitoring exclusion or retention of membrane integrity dyes. To simultaneously detect live and dead cells, two nucleic acids stains that differ in spectral characteristics and their ability to penetrate intact bacterial cell membranes are used. The high concentration of nucleic acid within cells enhances the fluorescence upon binding of the dye.

Nucleic acid dyes vary in their selectivity for staining either DNA or RNA. Some dyes lack selectivity and are able to stain both DNA and RNA, as in the case with the cell membrane impermeant dyes Ethidium bromide (EtBr) and propidium iodide (PI). Most commonly used, PI, a red fluorescent dye is able to penetrate cells with damaged membranes. SYTO9, a green fluorescent dye penetrates cells with both intact and damaged membranes and its emission is known to contribute to the excitation of PI by an energy transfer (Langsrud and Sundheim, 1996). Studies using PI and SYTO9 have been applied to *M. tuberculosis* to assess viability after long-term cryopreservation (Shu *et al.,* 2012) and

identification of antibiotic-injured cells through the addition of ethidium monoazide, resulting in the inhibition of SYTO9 intercalation due to cleavage of bacterial DNA (Soejima *et al.*, 2009).

However, cell death can be a debatable topic as processes other than plasma membrane permeabilization may be the cause of cellular death, such as dysfunctional membrane potential and the activation of cysteine proteases by caspases (Sauvat *et al.*, 2015). For this reason YO-PRO-3, a carbocyanine fluorochrome is used to provide an indication of caspase activation by permeating the plasma membrane through pannexin 1 (PANX1) channels, since caspase-3 activates these channels before the onset of plasma membrane permeabilization (Sandilos *et al.*, 2012). Sauvat *et al.*, (2015) applied a co-staining approach using the fluorescent probes YO-PRO-3, $DiOC_6(3)$, Hoechst 33342 and DAPI to quantify viable cells with an intact plasma membrane, closed PANX1 channels and therefore high membrane potential. Hoechst 33342 is often used to determine nuclear physiology which can be viewed with a fluorescence microscope, and the cell permeant dye DAPI can be used to assess the DNA content within a cell to track ploidy or cellular division. Although this approach was applied in mammalian cells, it could be a useful application in bacterial cells.

The combination of dyes available to assess membrane integrity can contribute greatly to the understanding of the physiology of heterogeneous bacterial populations. However, bacterial efflux mechanisms in some species may prevent the uptake of certain dyes that they usually would have been permeable to (Davey and Kell, 1996), or varying permeabilities to certain dyes among different bacterial species may occur, as seen with the commonly used probe PI (Berney *et al.*, 2007; Stiefel *et al.*, 2015).

2.5.4 Metabolic activity

The ability of cells to synthesize enzymes and maintain them in active form (such as esterases or dehydrogenases) provides a measure of metabolic activity. Esterase activity can be detected through the use of lipophilic, uncharged and non-fluorescent fluorogenic substrates. Once the dye enters the cell, non-specific esterases cleave the substrate and release a polar fluorescent product known as fluorescein. This energy-independent reaction allows the measurement of both enzyme activity and cell membrane integrity, which activates and retains the intracellular fluorescent products, respectively. Dead or damaged cells retain some residual esterase activity while leaking the majority of the dye (Joux and Lebaron, 2000). Varying levels of stress or addition of drugs may cause variations to metabolic activity in *M. tuberculosis.* For example, in *Salmonella typhimurium* fluorescent dyes to assess respiratory activity, glucose uptake and DNA synthesis activity were used to analyse the varying metabolic activities in subpopulations of VBNC cells (Morishige *et al.*, 2015). Therefore multiple dyes are available for testing different metabolic characteristics in bacteria.

Fluorescein diacetate (FDA) has the ability to penetrate mycobacteria's hydrophobic cell membrane, where it is rapidly hydrolysed to free fluorescein due to the increased amount of esterase in viable cells. Dead cells would hydrolyse less FDA, therefore viable cells can easily be distinguished based on their incorporation of FDA (Bonecini-Almeida, 2000).

Upon entry into cells, Calcein-AM is converted by intracellular esterases to calcein, a derivative of fluorescein. In *Staphylococcus aureus* the detection of calcein progressively increases over time in live cells, while in cells with compromised membranes, calcein rapidly leaks out. This fluorescent product provides a good measure of metabolic activity and cell viability (Comas and Vives-Rego, 1998).

The metabolic status of *M. tuberculosis* has shown correlation with the maturation of a phagosome to a phagolysosome when infected in mammalian cells containing dextran Texas Red stained lysosomes. Therefore, the absence or presence of colocalization with dextran Texas Red is a dependable marker of metabolically active or non-viable *M. tuberculosis* (Lee *et al*., 2012).

Dextran is resistant to cleavage by most endogenous cellular glycosidases, thus dextran conjugated Texas Red enables long-term markers for live cells. This is preferred over Texas Red, as it is characterised by low solubility in water, which may affect its conjugation to some biomolecules (Lee *et al*., 2012).

The monotetrazolium dye 5-cyano-2,3-ditolyl tetrazolium chloride (CTC) acts as a redox indicator, as bacterial cells producing ATP via the electron transport chain will absorb CTC and further reduce CTC by dehydrogenases or reductases into an insoluble fluorescent formazan product (Stellmach and Severin, 1987). Presumably, injured cells or cells with reduced respiratory activity, such as VBNC bacteria, will produce less formazan product due to decreased CTC reduction. For example, CTC was used as a colorimetric assay for determining susceptibility to the front-line drug pyrazinamide in *M. tuberculosis*. This has shown to be a useful indicator of drug susceptibility as it is active at low pH, a characteristic of clinical isolates (Gillespie, 2002; Kalir *et al*., 2013). The water insoluble nature of CTC allows accumulation of this dye intracellularly without diluting and thus increases the fluorescent intensity and rapidity of the results due to the reduced incubation time needed. This could also be useful for testing other anti-tuberculosis drugs (Li *et al*., 2016).

Studying antimicrobial activity in combination with an oxidative stress assay could potentially be a useful application in *M. tuberculosis*. The hosts' microenvironment has a considerable effect on bacterial metabolism and *M. tuberculosis* has the ability to subvert the immune system through unknown mechanisms to ensure redox balance. More specifically, there is uncertainty regarding the influence of an intracellular redox imbalance on the efficacy of anti-tuberculosis drugs such as

isoniazid and ethionamide, since these drugs are only effective upon reduction of NADH (Vilchèze *et al.*, 2005). The mechanism by which redox homeostasis is maintained in *M. tuberculosis* during varying environmental conditions and how this impacts *M. tuberculosis* physiology is unknown.

2.5.5 Cell cycle determination

Despite *M. tuberculosis* being capable of inducing necrosis, it is known to develop mechanisms resisting host apoptotic death, usually occurring at a lower bacterial load. Annexin V, a calcium-dependent phospholipid binding protein, serves as a marker for apoptotic or necrotic cells (Janko *et al.*, 2013). During the early stages of apoptosis, the membrane impermeable viability dyes PI or 7-aminoactinomycin D (7-AAD) will be excluded, whereas a loss of cell membrane integrity in late apoptotic or necrotic cells allows annexin V binding and staining of PI or 7-AAD (Koopman *et al.*, 1994). At a higher multiplicity of infection in the host, it has been shown that apoptosis rapidly proceeds to necrosis, thus releasing and spreading *M. tuberculosis*. Following macrophage exposure, apoptotic cell death was confirmed by staining with annexin V, while PI positive were necrotic cells. Cells positive for annexin V and PI were apoptotic cells undergoing secondary necrosis (Lee *et al.*, 2012).

Annexin V and PI staining has been exploited to show that RAW264.7 macrophages stimulated with the PE25/PPE41 protein complex is responsible for the induction of host immune cell necrosis (Tundup *et al.*, 2014). In contrast, apoptosis in macrophages was reported to be inhibited due to the manipulation of gene regulation when stained with annexin V and PI, causing *M. tuberculosis* to upregulate the anti-apoptotic gene, *BCL2* (Elliott *et al.*, 2015).

This staining combination could be advantageous to studying *M. tuberculosis,* as *M. tuberculosis* counteracts the protective mechanisms of macrophages by resisting host apoptotic death and promoting nutrient uptake inside granulomas to encourage multiplication (Aguilo *et al.*, 2013; Loeuillet *et al.*, 2006). Additionally it would be valuable to assess the degree of apoptosis induced by anti-tuberculosis agents, however these processes are poorly understood.

2.5.6 Targeting cell surface components

The mycobacterial cell wall is highly complex and substantial changes occur in the cell wall during infection due to interaction with host cells. For this reason response to the *M. bovis* BCG vaccine differs considerably among individuals. Therefore it would be valuable to identify novel cell envelope antigens to provide a more effective and thorough immune defence response against *M. tuberculosis* (Bonecini-Almeida, 2000). This can be achieved by using immunofluorescent techniques, which involves the staining of surface antigens or proteins. This incorporates the binding of antibodies against a target compound or an epitope on a protein, which could capture certain proteins or protein

modifications by conjugation to fluorophores (Tracy *et al*., 2010). Different fluorophores in combination with specific antibodies has been used to investigate the variation and distribution of antigens on the cell envelope of *M. tuberculosis* (Ozanne *et al.*, 1996). Depending on the environmental conditions or physiological state of the cell, binding to the antibody varies (Davidow *et al.,* 2005). These proteins could be identified and functionally verified to determine its effect on growth, survival and interaction with host cells when infected and may offer potential for the development of novel small synthetic antibodies.

Tuberculosis patients appear to express variation in their antigens, which may influence the specificity of antibodies and subsequently affect the evaluation of disease progression (Ozanne *et al.*, 1996; Singh *et al.,* 2005). The tuberculin skin test utilizes purified protein derivative (PPD) for identification of tuberculosis, although PPD is a crude mixture of shared antigens in *M. tuberculosis, M. bovis,* BCG and other environmental mycobacteria (Goletti *et al.*, 2016). Therefore the identification of novel biomarkers using flow cytometry by simultaneously evaluating various immune functions of cells could provide accurate markers to allow for early detection and for discrimination between active and latent *M. tuberculosis.* Additionally, flow cytometric detection of novel mycobacterial surface antigens and their interaction with macrophages could help gain insight regarding the host-pathogen interactions (Bonecini-Almeida, 2000).

2.5.7 Analysis of gene expression

Gene expression can be analysed by flow cytometry using reporter gene assays or protein tags containing endogenously labelled fluorescent proteins, a more non-invasive technique as opposed to staining. Information regarding the transcriptional activity of a promoter or the expression levels of proteins can be revealed by transcriptionally and translationally fusing the reporter gene to the protein of interest, respectively (Sevastsyanovich *et al*., 2009). In *M. tuberculosis,* identification of certain mycobacterial promoters were induced in granulomas but not in macrophages. This allows for determination whether certain genes are selectively expressed in only granulomas or macrophages for understanding progression of disease (Ramakrishnan *et al.*, 2000).

Fluorescence-based methods can also be used for assessing replication upon infection, as adaptation to host immune responses is known to result in phenotypic variation. For example, persister populations have been detected upon internalization of *Salmonella* by macrophages using the fluorescence dilution technique, which was further confirmed by resumption of growth in the absence of antibiotic on agar plates (Helaine *et al.*, 2014). Fluorescence dilution involves dual fluorescent reporters, where a constitutive reporter serves as a marker for viable bacteria and an inducible reporter to measure the extent of bacterial replication (Helaine *et al.*, 2010). The technique is based

on the principle that the inducible fluorescent signal is halved with each cell division, after induction has been stopped. Subsequently, bacterial cells not undergoing replication retain their maximum fluorescence intensity and replication can be monitored, both *in vitro* and *in vivo* in macrophages (Helaine et al., 2010, 2014). The fluorescence dilution technique has also been adapted and applied in *M. tuberculosis,* which detected a subpopulation of slowly replicating bacteria 48 hours after infection of macrophages (Mouton *et al.,* 2016). An alternative strategy incorporated the proportional relationship between the average amount of ribosomes per cell and its growth rate. To measure single-cell growth dynamics in *M. tuberculosis* both *in vitro* and *in vivo*, a fluorescent reporter was designed by cloning a destabilized GFP at the rRNA locus. The wide range of phenotypic heterogeneity that was noticed included a proportion of non-replicating bacteria that produced high levels of fluorescence indicating high levels of protein production (Manina *et al*., 2015).

This could be a likely explanation for the decreased metabolic activity observed within VBNC cells and further proves how physiologically distinct VBNC cells are from exponentially growing cells. This is especially relevant in *M. tuberculosis,* as noncompliance of drug regimens could not only cause multi-drug resistance but may also trigger the VBNC state (Li *et al*., 2014).

2.6 CONCLUSION

The complex interaction of *M. tuberculosis* with the host is still poorly understood. Nonetheless, research shows promise for the analysis of mycobacterial physiology by exploiting flow cytometry to specifically study heterogeneous bacterial populations, identify the different stages of infection and develop probes and immune-based tests that offer greater specificity. This will be advantageous in the hope of improving the current routine tuberculosis tests available. A combination of fluorescent probes that provide information about the physiological state of *M. tuberculosis* should be considered future research and could expand our current knowledge about antibiotic sensitivity, drug resistance and heterogeneity in *M. tuberculosis* at a single-cell level.

CHAPTER 3:

DEVELOPMENT OF A NEXT-GENERATION FLUORESCENCE DILUTION REPORTER PLASMID

3.1 INTRODUCTION

Direct quantification and studying of the replication dynamics of a heterogeneous mycobacterial population at a single cell level is highly valuable for the understanding of adaptation and virulence of *Mycobacterium tuberculosis* within the host or in response to anti-tuberculosis drugs. This is usually achieved through direct colony counts after colony forming unit (CFU) plating. Apart from the lengthy time period needed for growth of *M. tuberculosis,* CFU plating does not yield information about the heterogeneity within the bacterial population. Specifically, it does not reflect the combination of bacterial killing and replication sustained under environmental challenges, and it may not detect viable but non-culturable (VBNC) bacteria.

Studying the heterogeneity at a single cell level in a bacterial population can be accomplished using the newly reported fluorescence dilution (FD) technique, which utilizes 2 fluorescent reporters; a constitutive reporter (GFP) that enables the tracking of all live bacterial cells, and an inducible reporter (TurboFP635) for detecting the measurement of bacterial replication. Developed by Helaine *et al.* for use in *Salmonella,* the FD technique is based on the equal distribution of fluorescent proteins at each cell division, resulting in their fluorescence intensities to be halved (Helaine *et al.*, 2010). In our group, the FD technique has successfully been adapted and optimized for use in both *M. tuberculosis* and *Mycobacterium smegmatis* and allows monitoring of bacteria for up to 5 generations. This approach has been applied to both *in vitro* and in macrophage infection models (Mouton *et al*., 2016), and could potentially also be used in *in vivo* infection models.

The adaptation of the FD system for use in mycobacteria made use of an RNA-based riboswitch. RNA enables recognition of a broad range of regulatory signals with high specificity due to its highly flexible structure and its ability to undergo conformational changes in response to a signal, thereby impacting gene regulation and expression (Henkin, 2008). Additionally, RNA operates in a protein independent manner, thus allowing faster regulatory responses. Riboswitches therefore effectively exploit these factors to regulate gene expression. The development of a riboswitch system involves the main RNA genetic regulatory element or expression platform to regulate gene expression, which is embedded

within the non-coding sequences of some mRNA and upon recognition and binding of its aptamer to a small molecule or ligand, results in a change in protein production encoded by mRNA. Aptamers are able to recognize ligands with high specificity and affinity and a number of natural riboswitches have been utilized to control gene expression (Garst *et al*., 2011; Henkin, 2008). In response to endogenous metabolites, such as amino acids, nucleotide derivatives, coenzymes or ions, natural aptamer domains usually represent off switches by repressing gene expression. This may however lead to a feedback inhibition, whereby a certain metabolite produced by the inducer inhibits the synthesis of the riboswitch-controlled gene product (Henkin, 2008). This also displays the variation in the effects of transcription natural riboswitches may have.

Great effort has been put into creating synthetic riboswitch systems by developing laboratory generated aptamers that operate similarly to natural riboswitches, in a variety of bacteria (Fowler *et al*., 2008; Topp *et al*., 2010; Van Vlack and Seeliger, 2015). Synthetic riboswitches control gene expression in response to an external signal in the form of a ligand by undergoing a conformational change to regulate transcription. They can be engineered to recognize and respond to any cell-permeable, non-toxic molecule capable of interacting with RNA (Lynch *et al*., 2007). Ideally, these systems should not have an effect or target native regulation when induced besides controlling the targeted gene, and allow rapid induction in replicating and non-replicating bacteria (Hatfull and Jacobs, 2014). This enhances the versatility and potential of synthetic riboswitches as gene expression systems in *M. tuberculosis* can be applied to regulate gene expression through silencing (Boldrin *et al*., 2010), overexpress proteins (Van Vlack and Seeliger, 2015), construct novel mycobacterial expression vectors (Mouton *et al.*, 2016), analyse gene expression in macrophage infection models (Seeliger *et al*., 2012), and potentially identify certain populations for sorting.

The riboswitch-based induction system offers advantages over other inducible systems in mycobacteria. One of the earliest described endogenous mycobacterial inducible systems involves the *M. smegmatis* acetamide-inducible acetamidase promoter. This system however displays a high level of basal activity in media containing non-inducing compounds such as glutamate or succinate, despite its functional purpose in conditional mutant construction (Parish *et al*., 1997; Roberts *et al*., 2003). The theophylline riboswitch system has been optimized for use in *M. smegmatis,* displaying high induction and low basal expression. Additionally, this system will be well suited to animal models as the inducer, theophylline, is a Food and Drug Administration (FDA)-approved drug that is well tolerated in mice and guinea pigs (Machtel *et al.*, 2016; Seeliger *et al*., 2012).

The theophylline riboswitch machinery is encoded by a 300 bp DNA segment that incorporates an inducible mycobacterial promoter, a variant of the phsp60 promoter from *Bacillus Calmette-Guérin*

(BCG) and a synthetic RNA aptamer that binds to the ligand, theophylline (Seeliger et al., 2012; Topp et al., 2010) (Fig 3.1). This riboswitch system allows for an easy induction mechanism as no additional exogenous proteins are required for induction, thus it can easily be modified or implemented in different strains or species (Topp *et al*., 2010). Additionally, the effects of theophylline is reversible upon removal of the inducer. The theophylline binding aptamer is fused to a sequence complementary to the 3' region of the aptamer via a short linker sequence (Seeliger *et al*., 2012). Depending on whether the aptamer is in a ligand bound or unbound state, the terminator will destabilize or form a stable loop structure, respectively, leading to the activation or inhibition of gene expression. Thus, the ligand is responsible for initiating the change in the conformation of the complex hairpin loop in the intrinsic terminator, to favour the formation of an anti-terminator structure (Wachsmuth *et al*., 2013).

Here we aimed to apply the synthetic theophylline inducible riboswitch system to develop a next-generation dual fluorescent reporter system that could be applied to explore the heterogeneity of intracellular replication at a single-cell level. This was necessary since the first version of the FD reporter developed by our group made use of a far-red reporter (TurboFP635), which is less commonly used for flow cytometry, due to a limited number of flow cytometers which are equipped to excite and detect this reporter. Our goal was therefore to replace TurboFP635 (Ex/Em 588/635) with a lower wavelength reporter tdTomato (Ex/Em 554/581), since most available flow cytometers are equipped with lasers suitable to excite this reporter; this would allow for improved accessibility and application of this technique.

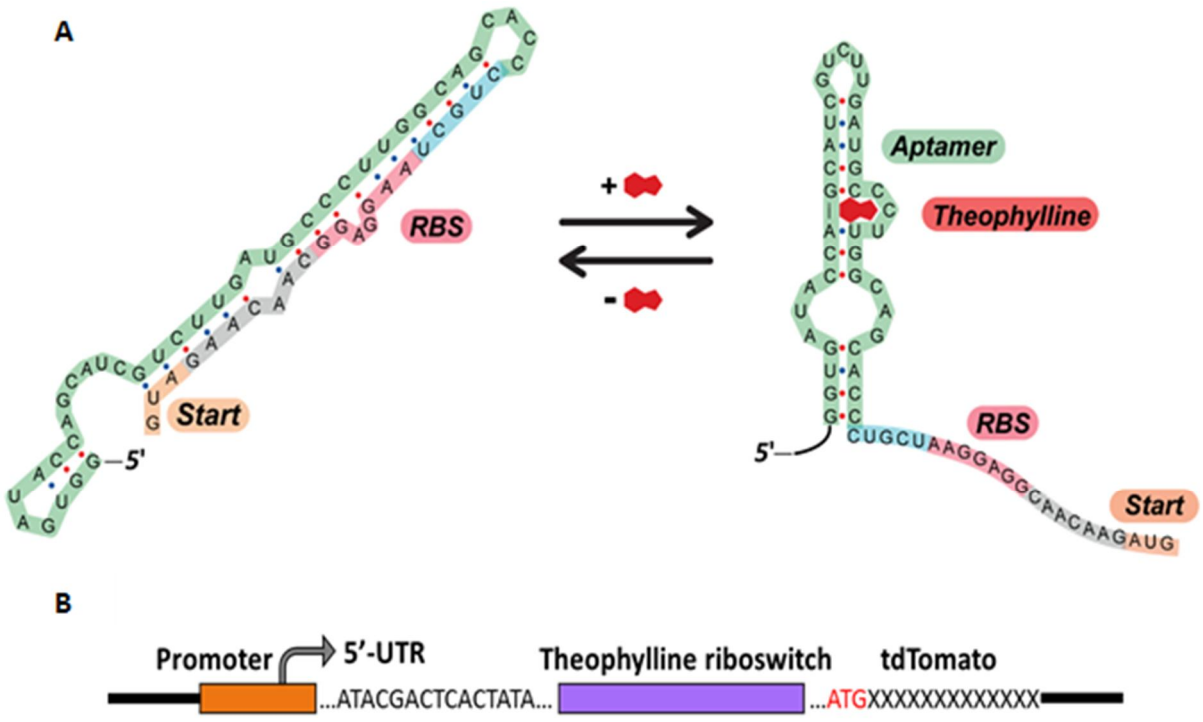

Fig 3.1. The theophylline riboswitch. A) The 3' region of the aptamer (green) fuses to the 5bp linker sequence (cyan) and the complementary ribosome binding site (RBS) sequence (red) in the absence of the ligand, theophylline. The reversible nature of the synthetic inducible theophylline riboswitch adopts a conformation whereby the aptamer is bound to theophylline through the sequestration of the ribosome binding site (RBS), also known as the Shine Dalgarno sequence, thus allowing protein translation. This effect is reversible upon removal of theophylline. (Figure from Seeliger et al., 2012). B) The theophylline inducible promoter transcribes the theophylline riboswitch in the presence of theophylline. The constant sequence (5'-UTR) contains the regulatory elements and is responsible for regulating the expression of the riboswitch and tdTomato, which is immediately downstream of the theophylline riboswitch.

3.2 MATERIALS AND METHODS

3.2.1 Bacterial strains, plasmid DNA and media

The bacterial strains and plasmids used in this study are summarised in Table 3.1. *Escherichia coli* strains and constructs were grown in Luria-Bertani (LB) broth (10 g Bacto tryptone, 5 g Bacto yeast extract, 5 g NaCl), overnight at 37°C, 180 rpm, to mid-log phase (optical density at 600nm [OD_{600nm}] = 0.6) or on LB agar medium (10 g Bacto tryptone, 5 g Bacto yeast extract, 5 g NaCl, 15 g Bacto agar). When required, kanamycin and hygromycin (Thermo Scientific, USA) were added to the cultures at a final concentration of 50 µg/ml and 150 µg/ml, respectively. *Mycobacterium smegmatis* mc^2155 obtained from the American Type Culture Collection (ATCC 700084) and constructs were grown in Middlebrook 7H9 media (Difco Laboratories, USA) supplemented with 10% OADC (oleic acid-albumin-dextrose-catalase supplement) (BD Biosciences, USA), 0.2% (v/v) glycerol and 0.05% (w/v) Tween-80 (7H9-OGT) for 48-72 hours at 37°C, 180 rpm, till OD_{600nm} = 0.8. When required, kanamycin and hygromycin (Thermo Scientific, USA) were added to the cultures, at a final concentration of 25 µg/ml and 50 µg/ml, respectively. Bacterial strains were stored at -80°C in 80% (v/v) glycerol as a cryoprotectant for long term storage.

Table 3.1. Bacterial strains and vectors used in this study

	Relevant characteristics	Size (bp)	Reporter	Excitation wavelength (nm)	Emission wavelength (nm)	Source/ Reference
Bacterial strains						
E. coli DH10B	High transformation efficiency cloning strain	N/A	N/A	N/A	N/A	Invitrogen, USA
M. smegmatis mc^2155	High transformation efficiency cloning strain	N/A	N/A	N/A	N/A	ATCC 700084, USA
Vectors						
pASTA3	Bacterial Expression vector, Hyg^R	7032	tdTomato	554	581	Carroll *et al.*, (2010) Addgene plasmid, #24657
pST5552	Bacterial Expression vector, Kan^R	5103	eGFP	485	520	Seeliger *et al.*, (2012) Addgene plasmid, #36255
pTiGc	Dual fluorescent reporter construct, Kan^R	6531	TurboFP635 GFP	588 485	635 520	Mouton *et al.*, (2016)

3.2.2 Generating a next-generation dual fluorescent reporter

3.2.2.1 Primer design and PCR conditions

All primers utilized in this study were synthesized by Whitehead Scientific (IDT, South Africa) and are listed in Table 3.2. The standard 20 µl PCR reaction was set up utilizing Phusion High Fidelity Taq polymerase (Thermo Scientific, USA) as summarised in Table 3.3. Optimization of the PCR conditions was carried out by gradient PCR by involving a range of annealing temperatures on the Veriti 96-Well Fast Thermo Cycler (Applied Biosciences, USA).

Table 3.2. Primers used to generate the dual fluorescent reporter

	Primers	Primer sequence (5'-3')	Restriction sites	Optimized annealing temperature (°C)*
1st cloning strategy	TomF	AGGAGGGAATTCATGGTGAGTAAG	EcoRI	56
	TomR	ATCGATAAGCTTTTACTTGTACAG	HindIII	
Sequencing primers	Tom1F	AGCATCGTCTTGATGCCCTT	N/A	N/A
	Tom1R	ACGAGGCGGTTCCTGAACTA		
	Tom2F	ACCACCTGTTCCTCGGTCAT		
	Tom2R	GCAGTCGATCGTACGCTAGTT		
	GFP-F	AACTCCGTTGTAGTGCCTGT		
	GFP-R	GCGTTGTGGTCACCTCTAGATT		
2nd cloning strategy	TomFP2	CCAGGAGATATCTCATGGTGAG	EcoRV	55
3rd cloning strategy	TomFP3	ATCGATGATATCATGCATCATCACCAC CACCATGAATTCATGGTGAGTAAGGGC	EcoRV, EcoRI	65

Underlined sequence represents restriction sites, *Tm used in the PCR cycling conditions (See Table 3.3).

The plasmid pASTA3 (Addgene, USA) designed by Tanya Parish (Carroll *et al*., 2010) contains the red fluorescent protein, tdTomato, which was amplified using the primers TomF and TomR to yield a 1455 bp fragment. For confirmation of clones by colony PCR, FastStart Taq DNA polymerase (Roche, Switzerland) using a standard 15 µl PCR reaction (Table 3.3) was utilized. Approximately half a colony was resuspended into a PCR Eppendorf microcentrifuge tube containing the PCR reaction mix. All amplified samples were electrophoretically fractioned on a 1% agarose gel, using Tris-EDTA (TE) buffer (1 M Tris-HCl, 0.5 M EDTA), containing 0.005% ethidium bromide for approximately 2h at 120 V. For determination of the size of the PCR product, the GeneRuler 1kb Plus DNA ladder (Thermo Scientific, USA) was loaded into the first well. Samples were visualized under ultra violet light using the Kodak Digital Science Electrophoresis Documentation and Analysis System 120 (VilberLourmat, France).

Table 3.3. PCR reaction components and cycling conditions

	Phusion High Fidelity Taq	FastStart Taq
Components	Amount (µl)	
Water	13.3	9.15
10X Buffer	4	2.5
25 mM Mg^{2+} buffer	-	1.25
10 mM dNTPs	0.4	0.25
100% DMSO	0.6	-
Taq polymerase	1 U/50 µl	2 U/50 µl
10 µM forward primer	0.5	0.625
10 µM reverse primer	0.5	0.625
DNA	0.5	0.5
Total volume	20	15
PCR cycling conditions		
PCR run (35 cycles)[1]	Time	
98°C	10 min	4 min
98°C[1]	30 sec	30 s
*Tm Table 3.2[1]	30 sec	30 s
72°C[1]	1 min per kb	30 s per kb
72°C	10 min	10 min
4°C	10 min	10 min

3.2.2.2 Cloning

PCR products were purified from 1% agarose gels using the Wizard SV Gel and PCR Clean-Up System kit (Promega, USA) as per manufacturer's instructions. Restriction enzymes were purchased from Roche (Switzerland) and are listed in Table 3.2. The digested pST5552 vector was dephosphorylated using rAPid Alkaline phosphatase (Roche, Switzerland) for the prevention of re-circularization during ligation, as per manufacturer's instructions. eGFP, under control of the theophylline inducible promoter in pST5552, was replaced with tdTomato. To achieve this, restriction enzyme digested tdTomato (1437 bp) was ligated for an hour at room temperature into the digested pST5552 using T4 DNA Ligase (New England Biolabs (NEB), USA) with a vector to insert 1:3 molar ratio. For transformation into *E. coli*, 2 µl of the ligation mix was resuspended with 40 µl *E. coli* DH10B electro-competent cells (See section 3.2.2.3). The mixture was transferred into Gene Pulser/MicroPulser 1 mm electroporation cuvettes (Bio-Rad, USA). Electroporation was done using the following settings: EC2, 2.5 kV (Bio-Rad, USA). Cells were recovered by resuspending with 600 µl Super Optimal Broth (SOC) media (2% Bacto tryptone, 0.5% Bacto yeast extract, 10 mM NaCl, 2.5 mM KCl, 10 mM $MgCl_2$, 10 mM $MgSO_4$, 20 mM glucose) in 1.5 ml Eppendorf tubes and incubated at 37°C, shaking at 180 rpm for 60 min. Cells were plated onto kanamycin LB plates and incubated overnight at 37°C, allowing

transformant selection. Upon verification of the presence of tdTomato by colony PCR (section 3.2.2.1), the recombinant pST5552 plasmid DNA was purified by culturing the remainder of the colony.

Subsequently, GFP under control of the constitutive mycobacterial hsp60 promoter (1200 bp) was excised from pTiGc and ligated into the digested and dephosphorylated recombinant pST5552 vector containing tdTomato. Colonies were screened for the presence of GFP by colony PCR and plasmids were confirmed to have the correct inserts by Sanger sequencing (Central Analytical Facility (CAF), Stellenbosch University). Transformants were then screened for the presence of both tdTomato and GFP by colony PCR and subsequently transformed into *M. smegmatis.* The recombinant pST5552 vector now referred to as pToiGc, contained tdTomato and GFP under expression of an inducible and constitutive promoter, respectively.

For transformation into *M. smegmatis,* 200 ng of pToiGc plasmid DNA was resuspended with 400 µl *M. smegmatis* mc^2155 electro-competent cells (See section 3.2.2.4). The mixture was transferred into Gene Pulser/MicroPulser 1 mm gap electroporation cuvettes (Bio-Rad, USA) and electroporated using the following settings: R10, 2.5 kV, 25 µF and 1000 Ω, as previously described (Snapper *et al*., 1990). Cells were recovered by resuspending with 1 ml LBGTW (LB, 0.5% (w/v) glucose, 0.05% (w/v) tween-80) in 1.5 ml Eppendorf tubes and incubated at 37°C, shaking at 180 rpm for 3 hours. Cells were plated onto LB plates containing 25 µg/ml kanamycin, and incubated at 37°C for 3 days, allowing transformant selection.

3.2.2.3 Preparation of E. coli electro-competent cells

A single colony of *E. coli* DH10B cells grown overnight on LB agar plates was inoculated into a 50 ml starter culture of LB. The starter culture was grown overnight at 37°C, with shaking at 180 rpm. The following day, the starter culture was passaged 1 in 100 into LB media and incubated at 37°C, with shaking at 180 rpm until OD_{600nm} = 0.6. The culture was immediately placed on ice and harvested by centrifugation in pre-chilled 50 ml conical centrifuge tubes (Corning, USA) at 5000 rpm, at 4°C for 10 min. The supernatant was discarded and the pellet was resuspended and washed with the original volume of pre-chilled distilled water and centrifuged as previously mentioned. For the second and third wash step, the pellet was resuspended in half the original volume with distilled water, followed by a fiftieth of the original volume with pre-chilled 10% (v/v) glycerol, respectively. Centrifugation of cells occurred between each wash step. Following the third wash step, the pellet was resuspended in five-hundredth of the original volume with 10% glycerol, aliquoted into 1.5 ml Eppendorf tubes and snap-frozen in liquid nitrogen. Electro-competent *E. coli* cells were stored at -80°C for subsequent use.

3.2.2.4 Preparation of M. smegmatis electro-competent cells

A single colony of *M. smegmatis* mc^2155 cells grown on LB agar plates for three days was inoculated into a 10 ml 7H9-OGT starter culture and grown with shaking at 180 rpm for 3 days at 37°C. The starter culture was passaged 1 in 100 into LBGTW media and incubated overnight at 37°C, shaking at 180 rpm until OD_{600nm} = 0.6. The culture was immediately placed on ice and harvested by centrifugation in pre-chilled 50 ml conical centrifuge tubes (Corning, USA) at 5000 rpm, at 4°C for 10 min. The supernatant was discarded and the pellet was resuspended and washed with the original volume of pre-chilled 10% (v/v) glycerol and centrifuged as previously mentioned. For the second wash step, the pellet was resuspended in half the original volume with 10% glycerol. Following centrifugation, each pellet was resuspended in 1 ml 10% glycerol-10% (w/v) sucrose, aliquoted into 1.5 ml Eppendorf tubes and snap-frozen in liquid nitrogen. Electro-competent *M. smegmatis* cells were stored at -80°C for subsequent use.

3.2.3 Fluorescence screening by theophylline induction

M. smegmatis transformants carrying the pToiGc plasmid were grown in 200 µl 7H9-OGT, with 25 µg/ml kanamycin in Costar 96 well opaque microplates (Corning, USA), sealed with sterilized breathable sealing film (Corning, USA) and incubated for 3 days at 37°C. Fifty microlitres of the cell suspension was subcultured into plates containing 150 µl 7H9-OGT and kanamycin with and without 2 mM theophylline. Plates were sealed with breathable sealing film and incubated overnight at 37°C. *M. smegmatis* wildtype, *M. smegmatis*::pST5552 and *M. smegmatis*::pASTA3 containing theophylline inducible GFP and constitutively expressed tdTomato, respectively, served as single colour controls. Controls were cultured with the appropriate antibiotics overnight at 37°C, shaking at 180 rpm.

Prior to readings, controls were added to the induced and uninduced plates in triplicate and plates were sealed with optically clear film. Fluorescence readings were obtained using the FLUOstar Omega 96-well microplate reader (BMG Labtech, Germany). Optic settings were adjusted using a 485/520 nm and a 544/590 nm filter according to GFP and tdTomato excitation and emission spectra (Table 3.1). The auto-gain adjustment setting was applied to limit background noise, using the GFP and tdTomato single colour controls.

3.3 RESULTS

3.3.1 Rationale

The objective of this work was to improve upon an existing dual fluorescent reporter plasmid that was previously constructed in our lab (Mouton *et al*., 2016). The existing reporter plasmid, pTiGc contains the far red TurboFP635 (Ex/Em: 588/635 nm) reporter. To construct the next-generation reporter plasmid, we replaced TurboFP635 with the red fluorescent reporter tdTomato, which has lower excitation and emission wavelengths; flow cytometers are more frequently equipped with lasers capable of exciting these lower wavelengths, thus making this technique easily accessible. In an attempt to overcome technical difficulties experienced with expression levels of tdTomato from the first cloning strategy, two alternative cloning strategies were developed to improve expression levels, by generating a clone with a shortened and extended 5' region from the riboswitch.

3.3.2 First cloning strategy

Initially, the cloning strategy was designed whereby eGFP in pST5552 was replaced with tdTomato, thus placing it under control of the inducible theophylline riboswitch promoter. Secondly, GFP under control of the constitutive hsp60 promoter was introduced from pTiGc into the resulting construct (Fig 3.2).

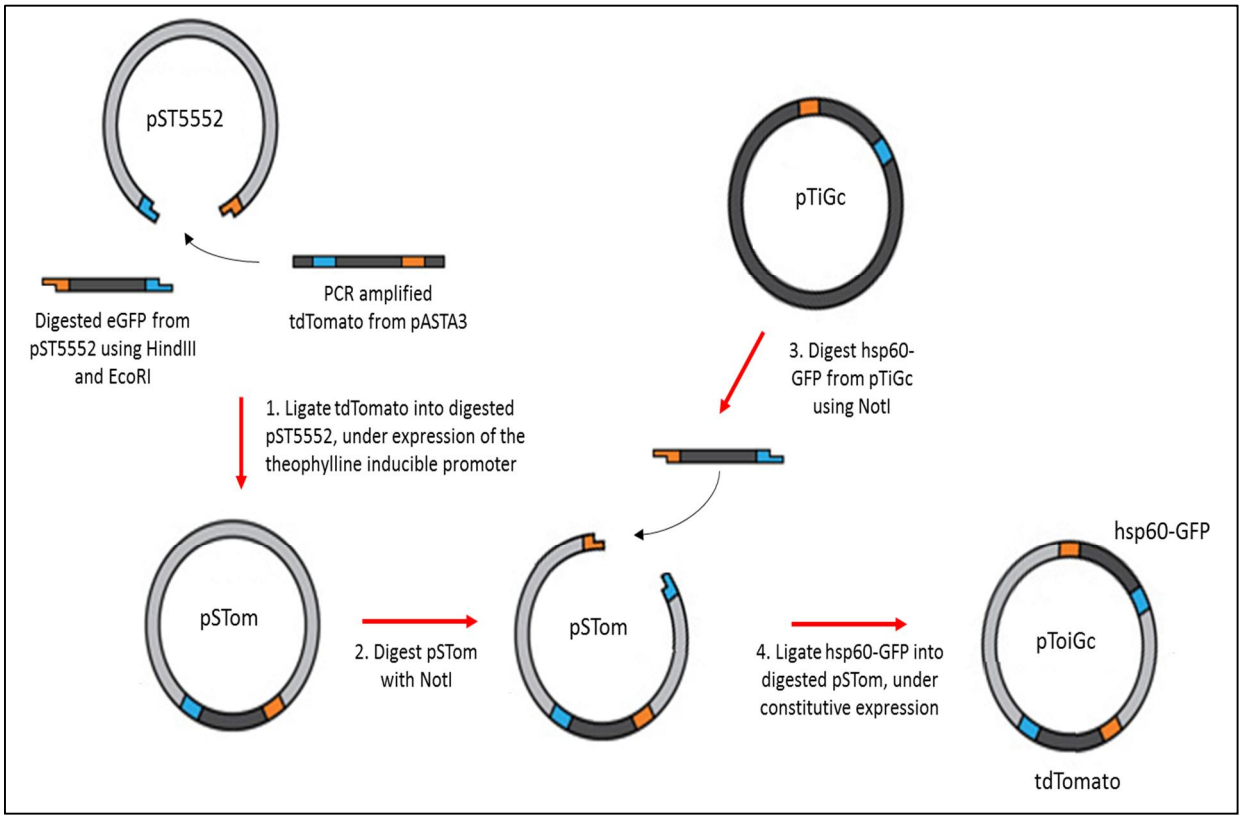

Fig 3.2. Cloning design of the first cloning strategy. pToiGc was constructed by placing tdTomato under inducible expression, and hsp60-GFP under constitutive expression.

The reporter tdTomato was successfully amplified from pASTA3 with the primers TomF and TomR (Table 3.2), as visualised by agarose gel electrophoresis and corresponded to the expected product size of 1455 bp (Fig 3.3).

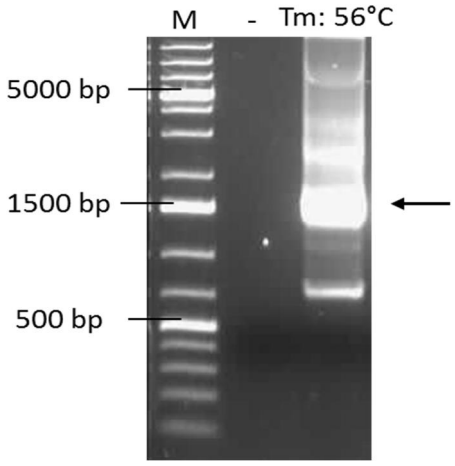

Fig 3.3. Amplification of tdTomato. PCR amplification with TomF and TomR primers yielded a band corresponding to the expected size of 1455 bp (Indicated by the arrow). Samples were electrophoresed on a 1% agarose gel using TAE buffer. M: GeneRuler 1kb Plus DNA ladder, - : Negative control

The resulting PCR fragment of tdTomato was gel purified using the Wizard SV Gel and PCR Clean-up System kit (Promega, USA). tdTomato was subsequently digested using EcoRI and HindIII to yield a 1437 bp fragment, purified and subsequently ligated with the EcoRI/HindIII-digested, dephosphorylated and purified pST5552 (Fig 3.4), to replace GFP with tdTomato.

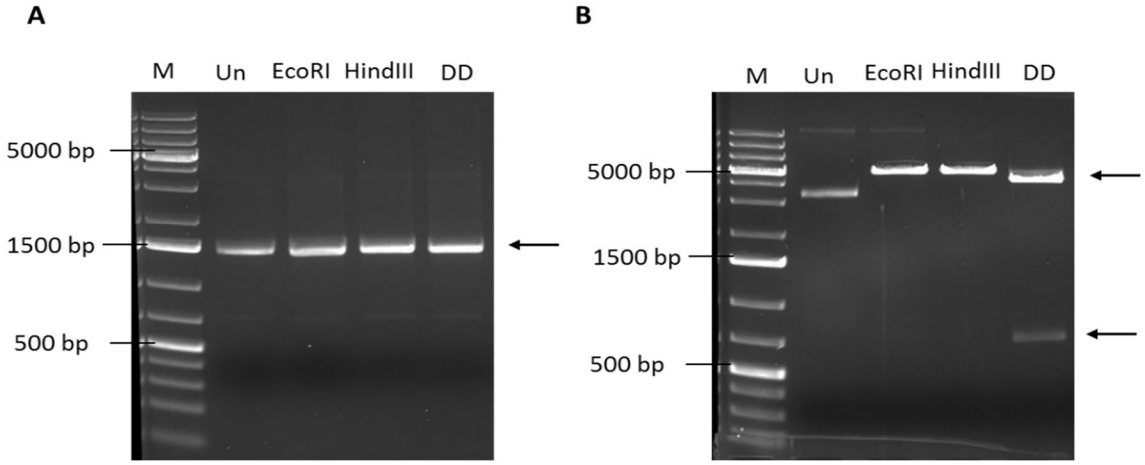

Fig 3.4. Restriction enzyme digestion. A) Digested tdTomato yielded a band corresponding to the expected fragment size of 1437 bp (Indicated by the arrow) and B) Digestion of pST5552 excised the GFP fragment (714 bp, bottom arrow) to yield the cut vector with a predicted size of 4389 bp (Indicated by the top arrow). Samples were electrophoresed on a 1% agarose gel using TAE buffer.
M: GeneRuler 1kb Plus DNA ladder, Un: Undigested control, DD: Double digest

The resulting plasmid, pSTom was transformed into *E. coli* and the presence of the insert (tdTomato) was confirmed by colony PCR (Fig 3.5). Forty-eight colonies were screened and multiple positive clones were identified. Plasmid DNA was purified using the Wizard SV Plus Minipreps DNA Purification system kit (Promega, USA) from two randomly selected positive colonies ($pSTom_{1.5}$ and $pSTom_{1.40}$), and verified using Sanger sequencing at CAF. Sequencing data was analysed using BioEdit Sequence Alignment Editor Software (Ibis Biosciences, USA), confirming that the clones harboured the correct sequence. These clones were retained for further experiments.

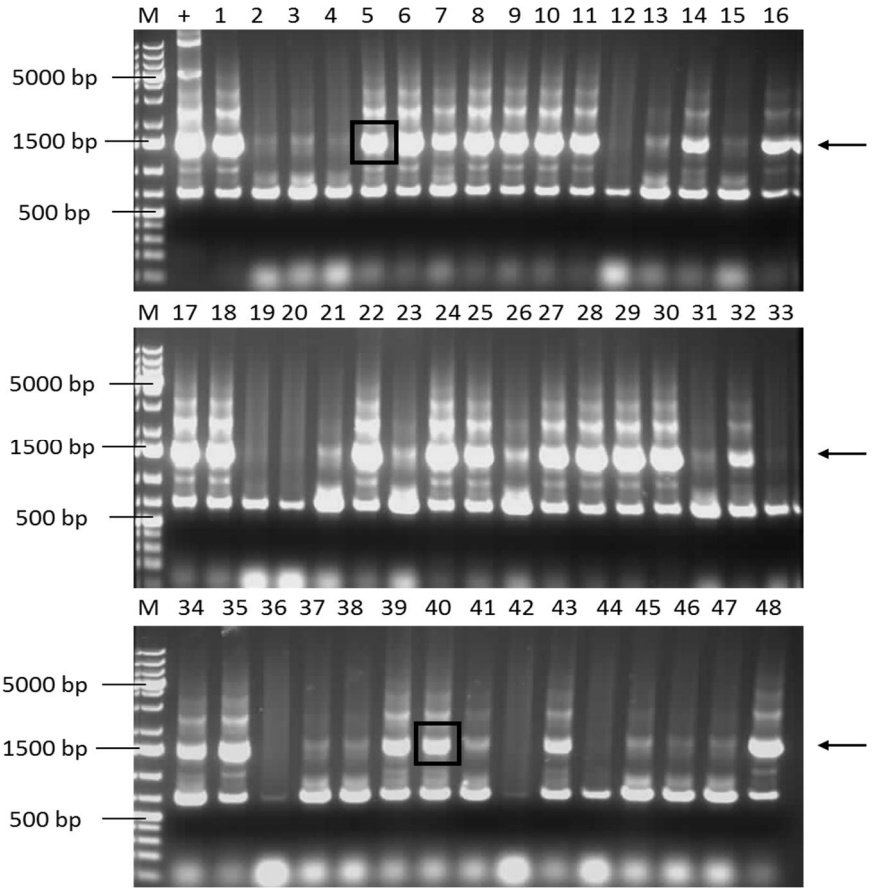

Fig 3.5. Verification of pSTom. Colony PCR result using the first cloning strategy primers (TomF and TomR) indicated that out of the 48 colonies that were screened, 27 colonies contained tdTomato (1437 bp) (Indicated by the arrow). $pSTom_{1.5}$ and $pSTom_{1.40}$ clones (enclosed) were selected for further experiments. Samples were electrophoresed on a 1% agarose gel using TAE buffer. M: GeneRuler 1kb Plus DNA ladder, +: Positive control

The sequence-verified $pSTom_{1.5}$ and $pSTom_{1.40}$ clones were subjected to restriction digestion with NotI and dephosphorylated. Furthermore, hsp60-GFP was excised from pTiGc, resulting in a 1200 bp fragment (Fig 3.6). Following purification, hsp60-GFP was ligated into the digested $pSTom_{1.5}$ and $pSTom_{1.40}$. The ligated DNA was transformed into *E. coli*, resulting in pToiGc with tdTomato under inducible expression (Toi), whilst GFP is constitutively expressed (Gc).

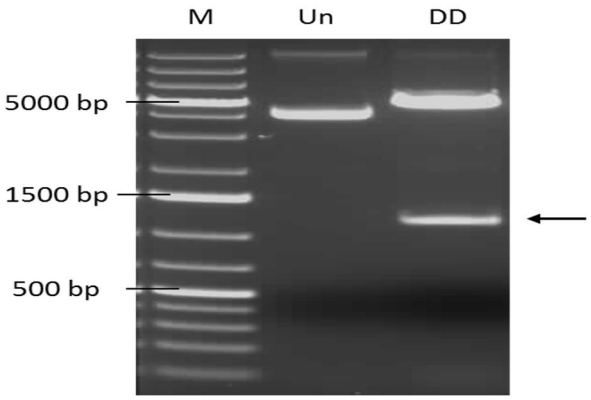

Fig 3.6. Restriction enzyme digestion of pTiGc. hsp60-GFP excised from pTiGc yielded a 1200 bp fragment (Indicated by the arrow). Samples were electrophoresed on a 1% agarose gel using TAE buffer. M: GeneRuler 1kb Plus DNA ladder, Un: Undigested control, DD: Double digest.

The sequencing primers GFP-F and GFP-R (Table 3.2) were used for detection of GFP in pToiGc. Five out of the 19 colonies screened contained the insert (Result not shown). The colony PCR was repeated for two of these colonies (Fig 3.7). Following plasmid purification, both $pToiGc_{11}$ and $pToiGc_{12}$ were confirmed to be correct by Sanger sequencing.

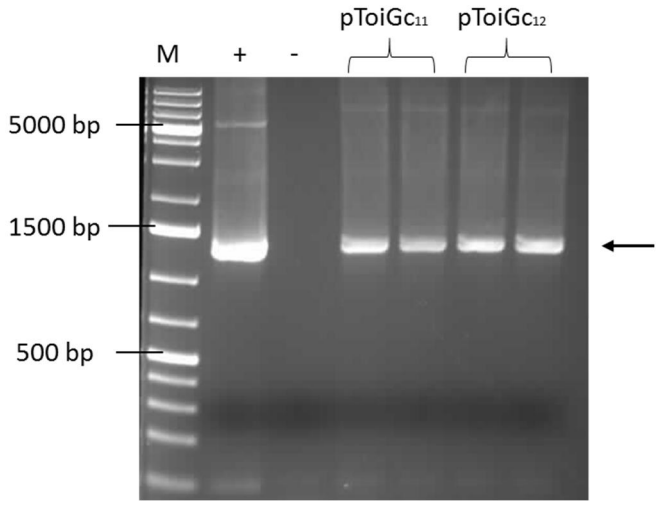

Fig 3.7. Confirmation of the presence of GFP. Colony PCR indicating the presence of GFP (1200 bp) in pToiGc (Indicated by the arrow). Samples were electrophoresed on a 1% agarose gel using TAE buffer. M: GeneRuler 1kb Plus DNA ladder, +: Positive control, - : Negative control

3.3.3 Screening colonies by monitoring basal and induced fluorescence

Single colour controls were first examined to assess baseline and induced expression levels of the selected reporters. Wildtype *M. smegmatis* (WT) was used as a control since bacteria are naturally autofluorescent; this needs to be eliminated as background from both the single colour controls as well as the samples. pST5552 and pASTA3 were used as single colour positive controls for green (GFP) and red (tdTomato) fluorescence, respectively (Fig 3.8). pST5552 was also used as an induction control. Fluorescence was measured using the excitation/emission filter for green and red fluorescence at 485/520 and 544/590, respectively. All controls were monitored in triplicate at OD_{600} = 1, and yielded high expression for either GFP or tdTomato, which confirmed effective expression and detection of our fluorescent reporters. We then assessed fluorescence and induction thereof in *M. smegmatis* transformed with $pToiGc_{11}$ and $pToiGc_{12}$. By exposing bacterial cells to 2 mM theophylline for 4 hours (≈ 1 doubling time) at 37°C, the production of tdTomato was induced. Previously, in similar conditions in our lab, *M. smegmatis*::pTiGc in the presence of 2 mM theophylline demonstrated an approximately 100 fold increase in red fluorescence, thus demonstrating the functionality of the riboswitch (unpublished data). Following subtraction of the autofluorescence from all samples, the fold change was calculated based on the ratio of relative fluorescence units (RFU) between samples with and without theophylline. The RFU values from the single colour controls were used as determinants for expression in our clones.

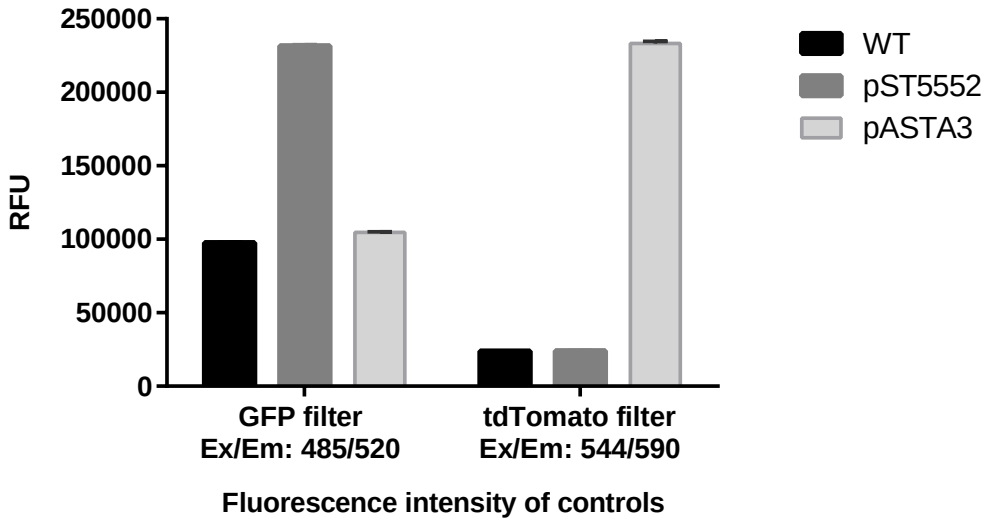

Fig 3.8. Testing of single colour controls. High green and red fluorescence signals were yielded for pST5552 (Ex/Em: 485/520) and pASTA3 (Ex/Em: 554/581), respectively. The WT sample displays autofluorescence, which was subtracted from controls and samples. All data are presented as means of triplicate replications with standard deviation. RFU: Relative fluorescence units, WT: Wildtype.

Twenty-four *M. smegmatis* colonies carrying pToiGc$_{11}$ and pToiGc$_{12}$ were screened for fluorescence (Fig 3.9). Only 25% and 12.5% of the pToiGc$_{11}$ and pToiGc$_{12}$ colonies respectively fluoresced both green and red. Furthermore, the highest fold increase in red fluorescence observed was 3 fold, which is substantially less than expected based on previous results. Readings were repeated at 24 and 48 hours, but with no improvement (data not shown). False positives were excluded from analysis, as these clones gave the impression of high expression, as their RFU values were negative in the presence and absence of theophylline, due to expression below that of the background.

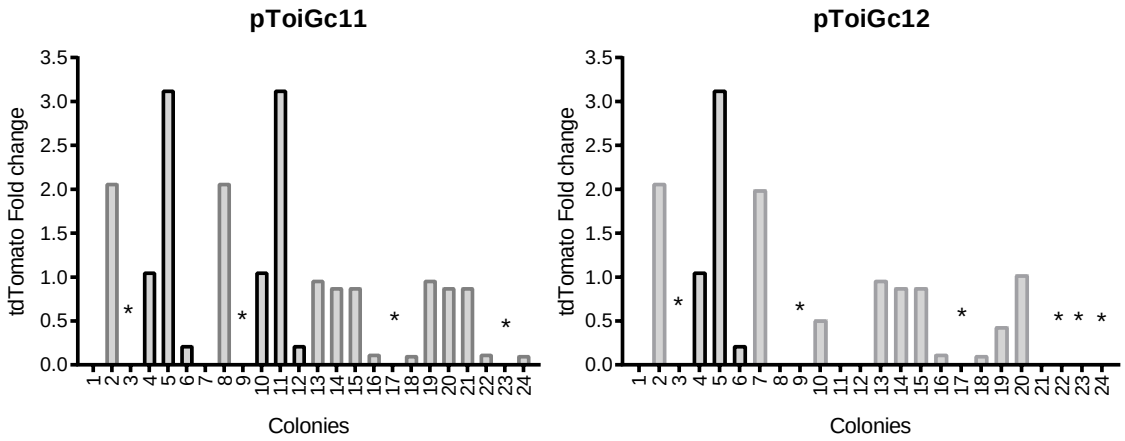

Fig 3.9. Fold change of tdTomato expression in pToiGc$_{11}$ and pToiGc$_{12}$. Twenty-four colonies were tested for expression of GFP and tdTomato, four hours post induction. False positives were excluded from all the graphs and are indicated by the *. Bars outlined in black represent clones expressing both tdTomato and GFP, whilst bars outlined in grey represent clones expressing only tdTomato.

To address the possibility of clone-specific problems, an additional 3 clones previously confirmed by colony PCR (pToiGc$_{7}$, pToiGc$_{10}$ and pToiGc$_{13}$) were transformed into *M. smegmatis* to test expression of GFP and tdTomato. Twenty-four colonies were screened for each clone, none of which displayed tdTomato fluorescence values above that of the WT (result not shown). A repeated attempt at cloning GFP into pSTom with direct transformation into *M. smegmatis* also did not yield clones with the expected inducible fluorescence (data not shown).

We next opted to repeat the cloning procedure from the start, using the same cloning design strategy. However, in this instance, we assessed basal and inducible red fluorescence following generation of the pSTom construct (before introducing the GFP). Twenty-four colonies were screened from each of 6 PCR-positive clones. Once again, very low fold-induction values were observed (data not shown). We additionally tested longer growth times, but this also did not yield improved fluorescence induction (data not shown). Finally, we recovered DNA from 2 colonies from *M. smegmatis* to send for sequencing; this confirmed that no unexpected mutations had been introduced into the modified Hsp60 promoter or riboswitch region.

3.3.4 Alternative cloning strategies

Despite screening multiple clones and colonies, multiple cloning attempts and extended incubation times, we were unable to obtain dual green and red fluorescent clones with inducible red fluorescence as expected. We hypothesized that the lack of red fluorescence induction seen in the first cloning strategy was either due to the theophylline binding site being blocked by complex folding or that the first part of the sequence may not have been able to properly unfold, leading to a blockage in the ribosome binding site/start codon. We therefore designed two alternative cloning strategies (Fig 3.10). The first of these generated a clone with a shortened 5' region, to lessen the potential blockage or misfolding of the sequence ahead of the theophylline binding site. The second alternative strategy incorporated a linker sequence for extension of the 5' region. We utilised a 6x His tag to act as a linker sequence and a marker for Western blot for detection of tdTomato protein production if no expression was observed.

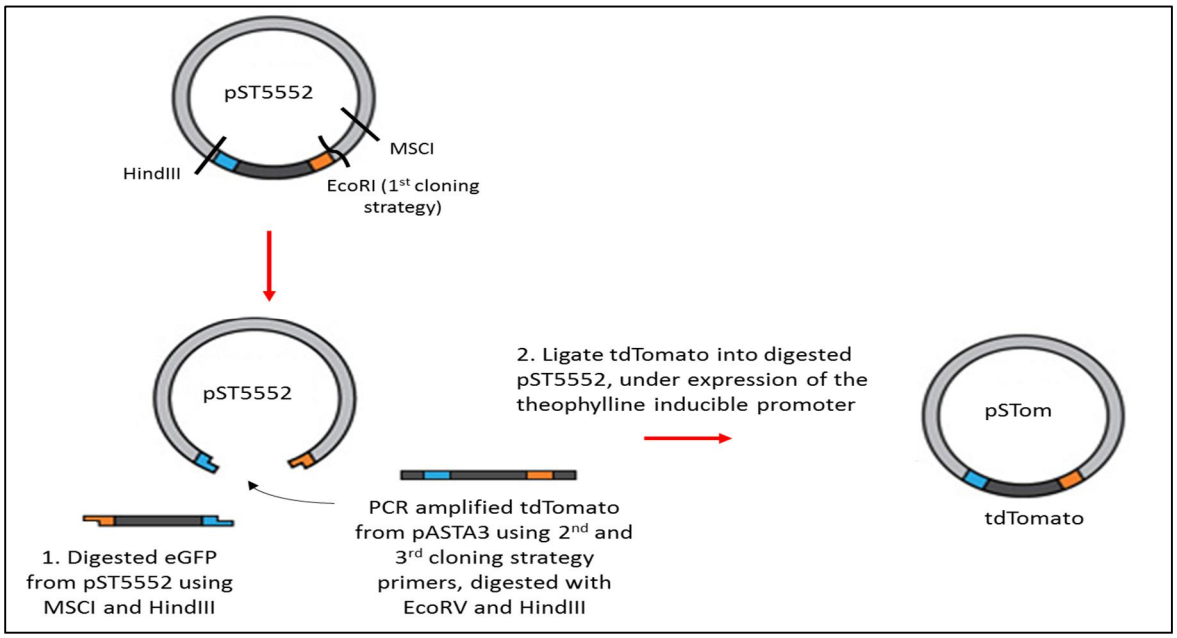

Fig 3.10. Cloning design for both alternative cloning strategies. The second and third cloning strategy generated a clone with a shortened 5' region and a clone containing a linker sequence, respectively. pSTom was constructed by placing tdTomato under inducible expression.

Cloning was carried out as previously described (See section 3.3.2) to produce $pSTom_2$ and $pSTom_3$. These were generated using the second and third cloning strategy primers, TomFP2 and TomFP3, respectively (Table 3.2). TomFP2 was designed to generate the shortened 5' region, whereas TomFP3 introduced a linker sequence. The reverse primer from the first cloning strategy (TomR) was used for both alternative cloning methods (Fig 3.11).

DNA of two colonies from each clone, as confirmed by colony PCR (result not shown) was transformed into *M. smegmatis* and screened for fluorescence. Twenty-four colonies for each clone ($pSTom_{2.6}$, $pSTom_{2.10}$, $pSTom_{3.8}$ and $pSTom_{3.12}$) were screened. However the maximum fold increase for $pSTom_2$ and $pSTom_3$ was 4.73 and 2.94, respectively (Fig 3. 12). The Hsp60 promoter, riboswitch and tdTomato regions were sequenced, this revealed no polymorphisms.

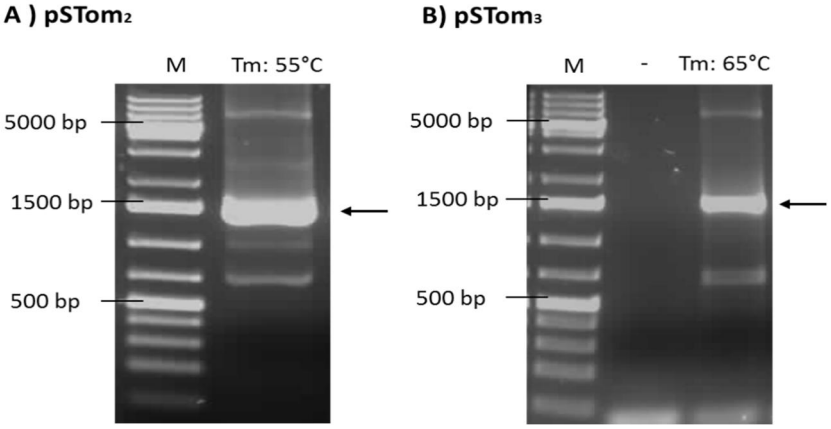

Fig 3.11. Amplification of tdTomato. A) The primers TomFP2 and TomR were used to amplify tdTomato with a truncated 5' region, yielding a 1457 bp product (Indicated by the arrow) and B) TomFP3 and TomR were used to amplify the 1482 bp product (Indicated by the arrow) of tdTomato containing the 6xHis tag linker sequence. Samples were electrophoresed on a 1% agarose gel using TAE buffer.
M: GeneRuler 1kb Plus DNA ladder, - : Negative control.

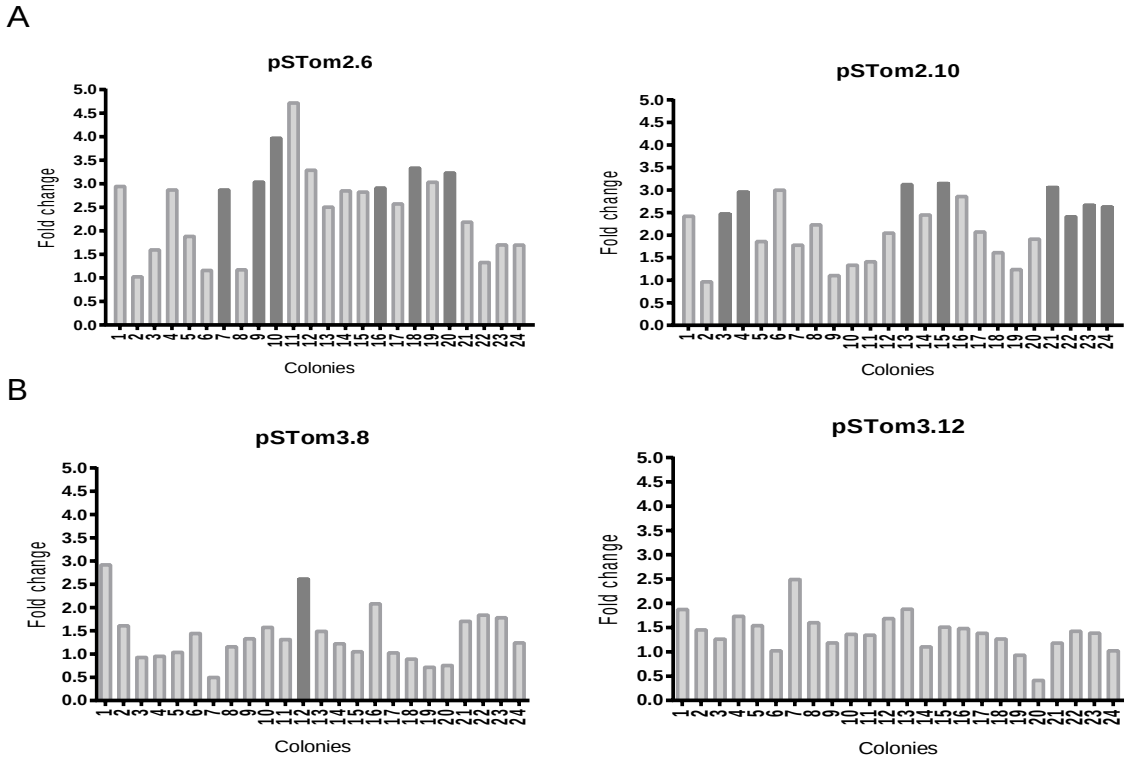

Fig 3.11. Fold change of tdTomato for $pSTom_{2.6}$, $pSTom_{2.10}$, $pSTom_{3.8}$ and $pSTom_{3.12}$. Twenty-four colonies were screened for each clone 4 hours post theophylline induction using the A) second and B) third cloning design strategies. Dark grey bars represent clones containing basal fluorescence below average.

3.4 DISCUSSION

To improve the accessibility of applying the theophylline riboswitch specifically to applications for mycobacteria, the existing riboswitch was adapted by replacing the far-red inducible reporter (TurboFP635) with tdTomato, a lower wavelength reporter. Since most standard flow cytometers are suited with lasers for exciting lower wavelengths, tdTomato would improve the application of pToiGc.

The development of the next-generation reporter system pTioGc involved the replacement of TurboFP635 within the existing reporter system, with tdTomato. Production of pToiGc was achieved by the excision of eGFP in pST5552 for the incorporation of tdTomato under control of the riboswitch-based theophylline inducible promoter to produce the plasmid pSTom (Fig 3.5). Following this, hsp60-GFP was introduced into the plasmid to generate pToiGc (Fig 3.7). TurboFP635 could not directly be replaced with tdTomato in pTiGc since the hsp60 promoter contained the MSCI site needed for digestion of TurboFP635.

3.4.1 Fluorescent reporter proteins

The development of fluorescent proteins has grown over the years and provides an extensive array of tools for understanding protein function, monitoring protein-protein interactions and tracking and quantifying bacterial cells (Olenych *et al*., 2007).

The approximate brightness of a fluorescent protein is determined by a combination of its maturation time, the ability of the chromophore to absorb light (extinction coefficient) and to fluoresce by re-emitting photons (quantum yield). Naturally, fluorescent proteins are mostly monomeric. Tandem dimerization is known to enhance brightness (Carroll *et al*., 2010). Native dsRed forms tetramers, which may form toxic aggregates. Additionally, green intermediates are formed during dsRed's slow maturation time (Table 3.4), therefore making it an unsuitable reporter (Müller and Davey, 2009). These problems were overcome by generating a monomeric mutant derivative of dsRed through multiple rounds of directed mutagenesis, these include mCherry, mPlum, tdTomato and TurboFP635 (Shaner *et al*., 2004). These fluorescent reporters have been expressed using mycobacterial promoters (Carroll *et al*., 2010). tdTomato is a result of the fusion of two copies of the dTomato gene with a 12 bp linker, and functionally acts as a monomeric protein. The tandem dimer structure enhances its brightness and also plays a role in its low aggregation (Shaner *et al*., 2004). Additionally, it is a highly photostable protein, comparable to the monomers mCherry and mKO_K.

Table 3.4. Properties of orange-red fluorescent reporters

Fluorescent protein	Ex/Em (nm)	Oligomerization	Maturation time at 37°C	Relative brightness[a] (M^{-1} cm^{-1})	Reference
GFP	485/520	Monomer	10 min	48	Shaner *et al.*, 2004
DsRed	558/583	Tetramer	10 h	59	Shaner *et al.*, 2004
tdTomato	554/581	Tandem dimer	60 min	95	Shaner *et al.*, 2004
TurboFP635	588/635	Dimer	20 min	70	Shaner *et al.*, 2004
mCherry	587/610	Monomer	15 min	50	Shaner *et al.*, 2004
mPlum	590/649	Monomer	1.25 h	12	Shaner *et al.*, 2004
mKO_2	551/563	Monomer	1.2 h	39.6	Sun *et al.*, 2009
mOrange	548/562	Monomer	2.5 h	49	Shaner *et al.*, 2004

[a]Brightness of a fully mature protein (% of eGFP) = $\frac{\text{extinction coefficient x quantum yield}}{1000}$ (Shaner *et al.*, 2004).

3.4.2 Determining induction of pToiGc

Having confirmed the regulation of gene expression in *M. smegmatis* and *M. tuberculosis* suggests that the inducible regulatory machinery of the theophylline riboswitch are suitable in both bacteria (Mouton *et al.*, 2016; Seeliger *et al.*, 2012). However, problems relating to promoter and codon usage, ligand permeability and protein folding could still occur, especially when transferring the inducible regulatory machinery across species. For example, due to a limited amount of mycobacterial promoters being recognized by the transcriptional machinery in *E. coli,* many genes cannot be expressed in *E. coli* (Topp *et al.*, 2010). For this reason, verifying induction of fluorescence in *E. coli* was not possible. Therefore, following confirmation of clones in all three cloning strategies, they were transformed into *M. smegmatis* for testing of expression of tdTomato.

Confirmation of expression of the positive controls was important as this indicated the functioning of the fluorescent proteins required for construction of the riboswitch system (Fig 3.8). As observed previously, background fluorescence due to autofluorescence was evident. This is typical of bacteria, since specifically 488 nm excitation is known to excite inherent cellular components, such as NADPH and proteins containing aromatic amino acids. This varies in different bacteria and is also influenced by the biological and physiological conditions of the cells (Monici, 2005). Therefore a true fluorescence value is achieved by subtracting the fluorescence reading obtained from WT bacteria (autofluorescence) from single colour controls and samples.

To validate the functionality of the riboswitch, addition of 2 mM theophylline to the existing reporter plasmid (pTiGc) approximately showed a 100 fold increase in fluorescence intensity. Synthetic riboswitches should be photostable and bright in comparison to the autofluorescence of the sample. Low background expression should be observed in the absence of the ligand through gene expression, whilst displaying high gene expression in the presence of the ligand due to well conserved translational machinery. Additionally, it is important that the selected riboswitch functions similarly and effectively *in vivo* and *in vitro.* These criteria have been met in the existing FD reporter constructed from pST5552 (Mouton *et al*., 2016).

The inducible acetamidase gene in *M. smegmatis* has displayed that induction by acetamide is dependent on media (Parish *et al.*, 1997). In contrast, the media (7H9-OGT) used in our study for culturing of *M. smegmatis* has not been associated with reduced or lack of theophylline induction and is not expected to have an effect on the quantum yield or absorption spectra of our fluorescent proteins.

Despite numerous cloning attempts which involved screening 11 clones, 266 colonies in total, allowed for longer growth of *M. smegmatis* and extended induction with theophylline, we were unable to obtain dual green and red fluorescent clones with inducible red fluorescence as expected. The most effective fold induction that was observed was 9.8 for pSTom in the first cloning strategy (result not shown); whilst this fold increase will allow for applications for genetic screening, this will not allow tracking of more than 2 bacterial replications, and was thus not a suitable candidate for our reporter.

We hypothesize that problems with pTioGc or pSTom therefore is a result of molecular recognition and folding of the aptamer in response to theophylline, or incorrect translation or folding of tdTomato. A point mutation (C27A) in the theophylline aptamer region has been shown to decrease the affinity for theophylline by 10 fold, whilst increasing the affinity and restoration of full activity for a theophylline derivative, 3-methylxanthine (Desai and Gallivan, 2004). This indicates how easily the specificity for theophylline could change with a single base pair mutation, thus sequencing of the entire riboswitch region and tdTomato was essential to rule out possible mutations contributing to the lack of expression. However, intact sequencing was observed for both clones, thus it is unlikely that this explains why tdTomato displayed limited expression. This also indicated that expression was not dependent on the presence of an intact sequence.

Gene expression is regulated post-transcriptionally by involving base pairing between the aptamer and the expression domain in the absence of theophylline (Seeliger *et al*., 2012). If these base pairing interactions are too strongly or weakly bound, may cause the switch to be repressed or leaky,

respectively (Lynch and Gallivan, 2009). In addition, in the ligand binding state, a stronger RBS is indicative of a more stable secondary structure to enable high expression (Lynch and Gallivan, 2009).

The limited red fluorescence induction seen in the first cloning strategy may have been either due to a blockage in the theophylline binding site or in the ribosome binding site/start codon as a result of complex folding or the inability of the aptamer sequence to properly unfold. Therefore, the second and third cloning design strategies were employed to improve expression by creating a clone with a shortened 5' region and a clone with an extended 5' region to prevent potential misfolding or blockage of the aptamer or RBS sequence. Two clones and 24 colonies were screened for each alternative cloning design strategy (Fig 3.12), although we were unable to obtain clones with inducible red fluorescence as expected.

3.4.3 Aspects to consider for improving expression

In trying to generate a reporter to replace TurboFP635, our results indicate that despite tdTomato having 2 intrinsic fluorophores and being regarded as one of the brightest red fluorescent proteins (Rizzo *et al*., 2009; Shaner *et al*., 2004), we were unable to obtain a clone with inducible expression of tdTomato. A broad range of fluorescent proteins are available, their success depends on their level of brightness and oligomerization. The expression of these reporters needs to be considered for use in bacteria to consider autofluorescence, and their nature of folding into alternative plasmids or promoters. There is however limited regulated gene expression systems available for mycobacteria.

3.4.3.1 Folding

Proper folding of the riboswitch region as well as the reporter gene is essential for gene expression. Interference with folding commonly occurs in the formation of the intrinsic transcription terminator in synthetic riboswitches, as this controls whether transcription terminates or controls the formation of the destabilized terminator to ensure that translation of the downstream reporter gene is sequestered.

Transcriptional terminators should be placed in the 5' and 3' UTR regions from the expression cassette for the prevention of transcriptional read-throughs that could be caused by other promoters within the plasmid. The initial bases transcribed by the native promoter (15-30 bp) in *M. smegmatis* is usually added in the 5'-UTR sequence (Topp *et al*., 2010). It is possible that expression of the gene of interest may be affected by the regulatory elements located within the 5'-UTR.

It has been observed that reduction in gene expression and fluorescence intensity occurs when secondary structure elements, such as riboswitch elements, are inserted into the 5'-UTR of GFP (Fowler *et al*., 2008). Replacement of a construct displaying high expression levels in the 5'-UTR

sequence with the 5'-UTR of a leaky construct results in constructs to behave leaky, with high basal fluorescence (Lynch *et al.*, 2007). In the absence of the ligand, translation is minimized by the pairing of the RBS, and upon ligand binding, causes the RNA to unpair the RBS. Thus, sequences of the reporter gene complementary to the RBS will display minimal protein translation in the absence of the ligand, as the 30S subunit of the ribosome binds preferably to single-stranded RNA (de Smit and van Duin, 1990; Lynch *et al.*, 2007).

Folding of tdTomato may interfere with the riboswitch mechanism, therefore alternative fluorescent reporters could be tested. In silico analyses using web-based programs such as mFold can be exploited to structurally predict folding and to determine the stability of the RNA conformation between the ligand bound and unbound states. Kinetic barriers between these 2 states should be low to ensure the proper functioning of the riboswitch. Additionally, Lynch *et al.,* used mFold to show that a few conserved or semi-conserved motifs were complementary to the theophylline aptamer (Lynch *et al.*, 2007). It has been shown that altering the sequence between the theophylline aptamer and the RBS has an effect on the function and expression of the riboswitch and the downstream reporter gene, respectively. The pairing of these regions by forming a secondary structure near the RBS has shown to reduce translation of downstream RNA, and is essential for functioning of the riboswitch (de Smit and van Duin, 1990). The tertiary structure of the riboswitch should be correctly folded prior to ligand binding as this may influence the affinity of the ligand binding site. mFold predictions (Zuker, 2003) for the first cloning strategy displayed a probability of the aptamer being blocked by complementary motifs. In all predictions, bases between the aptamer and RBS were paired, suggesting that translation would be inhibited in the absence of theophylline.

Sequences upstream of the inducible promoter may fold prior to transcription of downstream sequences, this could result in the destabilization of the hairpin loop before synthesis of the hairpin loop, or folding of the aptamer region could occur before translation of the expression domain (Garst *et al.*, 2011).

3.4.3.2 Linkers

Linker sequences have shown to have an effect on the folding, to increase protein production. Their design is crucial, to avoid formation of secondary structures as this has shown to limit the flexibility of the protein. Despite structural similarities between synthetic theophylline riboswitch constructs tested by Wachsmuth *et al.*, a longer linker sequence in the terminator loop was shown to create a too stable terminator, resulting in theophylline independent repression of the riboswitch, thereby displaying constitutive expression of the reporter gene. Weakening of the terminator hairpin by removal of 2 bp from the linker sequence displayed constructs that did not respond to theophylline

due to the permanent destabilized structure of the terminator (Wachsmuth *et al*., 2015). During transcription, if the linker sequence forms base pairs with the aptamer, this is likely to interfere with the ligand biding properties. The structural shift initiated by ligand binding may result in a structural shift downstream, thus affecting gene expression by impacting folding in the transcription terminator or the initiation of translation. Successful riboswitches should have high affinity for the ligand, followed by the ligand-dependant structural shift. The same riboswitch may also display differential response in regulating different genes (Henkin, 2008).

3.4.3.3 Large-scale screening

Flow cytometry based screens offer a rapid approach for generating synthetic theophylline riboswitches that display high gene expression. This is achieved by screening clones containing randomized sequences between the aptamer and RBS region (Lynch *et al*., 2007; Lynch and Gallivan, 2009). The regulatory parameters of riboswitches could also be altered by mutagenesis as this could alter the flexibility in the structural and functional components of the riboswitch, which could yield varying expression results (Berens and Suess, 2015). The cloning strategies presented here could be compared and adapted to those structures, which would further provide understanding of the mechanisms of riboswitches.

3.5 CONCLUSION

The development of a riboswitch displaying tight regulation to activate or repress gene expression in response to a ligand using riboswitches offers valuable applications with great diversity. This can provide sensitive screens for rapid changes in environmental conditions, cellular metabolites, bacterial metabolism or response to drugs. The existing riboswitch has indicated that the regulatory elements of the theophylline riboswitch functional in *M. smegmatis* and *M. tuberculosis,* therefore it would be valuable for adaption and incorporation of a riboswitch containing an alternative inducible reporter to enhance the diversity in applications for mycobacteria.

CHAPTER 4:

CHARACTERIZATION OF DIFFERENTIALLY REPLICATING *M. SMEGMATIS* UPON MACROPHAGE INFECTION

4.1 INTRODUCTION

Emerging data highlights the more heterogeneous nature of mycobacterial populations than previously thought (Hendon-Dunn *et al*., 2016; Manina *et al*., 2015; Mouton *et al*., 2016). Exposure to specific circumstances may promote heterogeneity as an advantageous survival mechanism for *Mycobacterium smegmatis.* For example, viable but non-replicating (VBNR) bacteria exhibits heterogeneity and can include a subpopulation of persistent bacteria, defined as bacteria in a reversible phenotypically drug tolerant state without acquiring antibiotic resistance-conferring mutations (Balaban *et al*., 2013; Walter *et al*., 2015). This phenomenon has also been detected in other bacteria (Helaine and Kugelberg, 2014; Prax and Bertram, 2014), and in *Escherichia coli* at a single-cell level in real time using microfluidics systems (Gefen *et al*., 2008). In response to prolonged antibiotic treatment for the complete sterilization of *M. tuberculosis*, persisters may arise and are proposed to exist in a non- or slowly-replicating state, referred to as viable but non-replicating (VBNR) (Manina *et al.,* 2015). These populations contribute to the persistence and recurrence of infection with *M. tuberculosis,* therefore the understanding of these populations and their replication dynamics is essential. However, this understanding is limited by the available tools, due to the difficulty in identifying and isolating the various physiological and replication states of mycobacteria.

Differentially replicating bacterial populations comprise of a spectrum of actively replicating to non- or minimally replicating bacteria, and have been detected using fluorescence dilution (FD) reporters in combination with flow cytometry. Helaine *et al.* reported that a significant amount of *Salmonella* do not undergo replication, but enter into a VBNR state both *in vitro* and *in vivo,* in macrophages (Helaine *et al*., 2010). A similar approach was adapted for mycobacteria.

FD using the dual-reporter plasmid constructed by Mouton *et al.* detects the overall live bacterial population with a constitutive reporter GFP, while bacterial replication is based on dilution of the inducible reporter TurboFP635 (Fig 4.1). When applying FD to study *M. smegmatis* replication dynamics upon macrophage infection, the majority of bacteria were found to exist in a VBNR state.

Unexpectedly, a subpopulation of more rapidly replicating *M. smegmatis* was observed (Mouton *et al.*, 2016).

M. smegmatis is often used a surrogate for studying *Mycobacterium tuberculosis,* although certain aspects of its behaviour and adaptation in macrophages are not fully understood. Reports have indicated that *M. smegmatis* does not readily survive the environment within macrophages, and would only be expected to undergo minimal replication (Kuehnel *et al*., 2001; Prakash *et al.,* 2010). Understanding the nature of this apparently replicating population is important to meaningfully extrapolate conclusions to *M. tuberculosis.*

One question that arose was whether the replicating *M. smegmatis* population was perhaps replicating extracellularly. To provide an understanding of whether the slowly replicating population occurs inside or outside the macrophage, the FD technique in combination with a fluorescently labelled mycobacterial specific antibody was be applied to enable single-cell analysis of this population using flow cytometry.

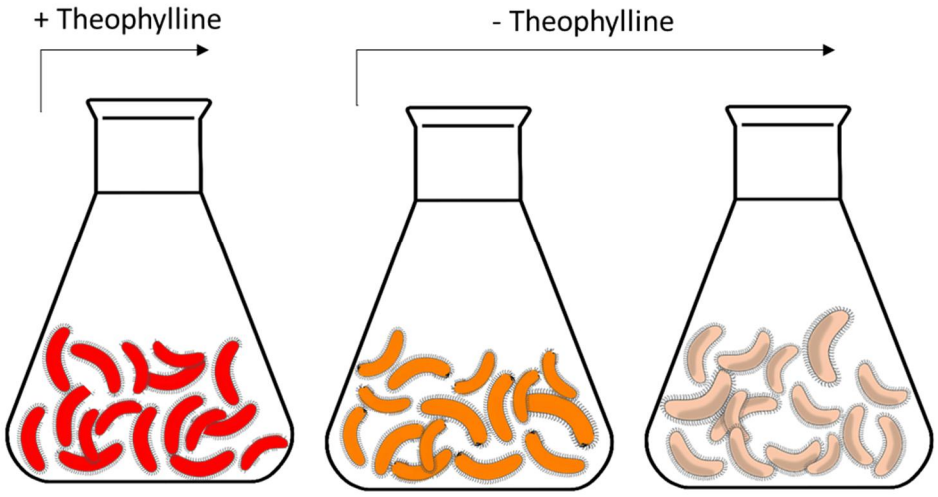

Fig 4.1. Measurement of bacterial replication using fluorescence dilution. Following removal of the inducer, theophylline, dilution of red fluorescence occurs upon bacterial replication.

4.2 MATERIALS AND METHODS

4.2.1 Bacterial strains and media

Table 4.1. Bacterial strains and vectors used in this study

	Relevant characteristics	Size (bp)	Reporter (ex/em)	Source/ Reference
Bacterial strains				
M. smegmatis mc^2155	High transformation efficiency cloning strain	N/A	N/A	ATCC, 700084
M. tuberculosis (Δ*leuD* Δ*panCD*)	Double leucine and pantothenate auxotroph	N/A	N/A	Sampson *et al*., (2004)
Vectors				
pTiGc	Dual fluorescent reporter construct, Kan^R	6531	TurboFP635 (588/635) GFP (408/509)	Mouton *et al*., 2016
pST5552	Bacterial Expression vector, Kan^R	5103	eGFP (408/509)	Addgene, USA #36255 (Seeliger et al., 2012)
pSTCHARGE	Bacterial Expression vector, Kan^R	5094	TurboFP635 (588/635)	Mouton *et al*., 2016

The bacterial strains and plasmids used in this study are summarised in Table 4.1. Middlebrook 7H9 media (Difco Laboratories, USA) supplemented with 10% OADC (oleic acid-albumin-dextrose-catalase supplement) (BD Biosciences, USA), 0.2% (v/v) glycerol and 0.05% (w/v) Tween-80 (7H9-OGT) was used as a growth medium for *Mycobacterium smegmatis,* obtained from the American Type Culture Collection (ATCC 700084) and was cultured for 48-72 hours at 37°C, 180 rpm, till OD_{600nm} = 0.8. An attenuated strain of *M. tuberculosis* H37Rv (Δ*leuD* Δ*panCD*) was constructed as previously reported (Sampson *et al*., 2004) and cultured in 7H9-OGT supplemented with 50 µg/ml leucine and 24 µg/ml pantothenate for 3 weeks at 37°C, shaking at 180 rpm, until OD_{600nm} = 0.8. When required, kanamycin (Thermo Scientific, USA) was added to the cultures, at a final concentration of 25 µg/ml. For colony forming unit (CFU) determination *M. smegmatis* was grown on Luria-Bertani (LB) agar (10 g Bacto tryptone, 5 g Bacto yeast extract, 5 g NaCl, 7.5 g Agar) at 37°C.

4.2.2 Preparation of the conjugated antibody

The rabbit anti-*M. tuberculosis* IgG polyclonal antibody ab905 (1 mg/ml) (Abcam, USA) was used as a surface-binding antibody for mycobacteria. To allow detection of the antibody, it was conjugated with the Alexa Fluor 405-labelled goat anti-rabbit Fab fragment (200 µg Fab fragment/ml) using the Zenon

rabbit IgG labelling kit (ThermoScientific, USA). The Zenon labelling reagent is composed of a fluorophore-bound Fab fragment, which has high affinity for binding of the Fc region of the antibody to form a labelling complex. One labelling is defined as the amount of Zenon labelling reagent to conjugate 1 µg antibody with a 3:1 Fab to antibody molar ratio, as suggested by the kit (Fig 4.2).

To determine optimal binding of the conjugate to *M. smegmatis,* the antibody concentration was titered using the 3:1 ratio. A master mix of the conjugated antibody was prepared using a 6:1 ratio by adding 10 µl of the Alexa Fluor 405 conjugated Fab fragment per 1 µg of antibody. The mixture was incubated for 5 min at room temperature, followed by neutralizing the excess or unbound Fab fragment by addition of 10 µl non-specific IgG blocking reagent (5 mg/ml) per 1 µg of antibody.

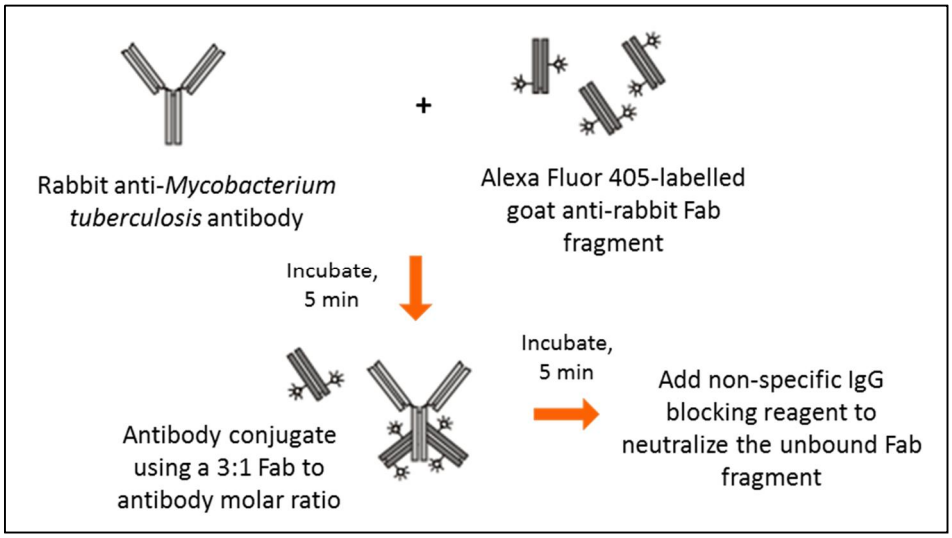

Fig 4.2. Formation of the antibody conjugate. An anti-*M. tuberculosis* antibody was conjugated to an Alexa Fluor 405 Fab fragment using the Zenon labelling kit. A 3:1 Fab to antibody ratio was used, as suggested by the kit.

4.2.3 Labelling *M. smegmatis* with the conjugate

To prepare *in vitro* cultured bacteria for labelling, wildtype *M. smegmatis* was used and theophylline induced pST5552 and pSTCHARGE was used as single colour unlabelled controls. *M. smegmatis* grown overnight from stock in 50 ml tubes at 37°C, 180 rpm was sonicated in an in an ultrasonic waterbath (UC-1D, Zeus Automation, South Africa) at 37 kHz for 12 min at room temperature. The bacterial culture was filtered using a 40 µm cell strainer (Corning, USA), whereby a 1 ml aliquot was transferred and pelleted in 2 ml microcentrifuge screw cap tubes (Corning, USA) for 7 min at 14 000 rpm and adjusted to an OD_{600nm} = 1 (≈ $1x10^8$ bacteria/ml) by resuspending in PBS. The culture was further diluted to $1x10^3$ bacteria/ml to represent a similar amount of bacteria expected per well in the macrophage infection. Samples were prepared by pelleting 500 µl aliquots for 7 min at 14 000 rpm.

Non-lysed macrophages were pelleted for 10 min at 1 100 rpm to prevent bursting or lysis of the macrophage.

Following preparation of the conjugate mastermix, bacteria were labelled by resuspending the cell pellet together with the conjugate and incubated in the dark for 30 min at room temperature. Cells were washed with 500 µl PBS, pelleted for 7 min at 14 000 rpm and fixed for 30 min with 4% formaldehyde, as previously mentioned. Similarly, non-lysed macrophages were fixed using the same conditions, but wash steps were carried out with a lower centrifugation speed (1 100 rpm for 10 min). Samples were transferred and filtered into flow cytometric tubes containing cell strainer caps and analysed on the LSRFortessa. Statistical analysis was performed using GraphPad Prism software (version 7.01) for Windows (GraphPad software, USA).

4.2.4 Mammalian cell culture

4.2.4.1 Preparing a starter culture

Culturing of the macrophage cell line, RAW 264.7 (ATCC TIB-71) was carried out using D10 media, which consists of Dulbecco's Modified Eagle's Medium (DMEM) (Sigma Aldrich, USA), supplemented with 10% heat-inactivated fetal bovine serum (FBS) (Sigma Aldrich, USA). A -80°C stock of RAW cells, cryopreserved in DMSO, was rapidly thawed at 37°C, then slowly added to 10 ml D10 media in a 50 ml conical centrifuge tube (Corning, USA) and centrifuged for 5 min at 1 600 rpm. The cells were thoroughly resuspended in 6 ml D10 to prevent clumping and were transferred to a 25 cm^2 tissue culture flask containing a vented cap (Sigma Aldrich, USA) and incubated at 37°C in 5% CO_2 until 80% confluent.

Cells were viewed under a microscope for detection of confluency and adherence. Splitting of cells was carried out by replacing the D10 media, followed by gently dislodging the cells from the base of the flask using a cell scraper. Cells were thoroughly resuspended using a 10 ml serological pipette and subcultured at a ratio of 1:6 with a final volume of 12 ml D10 media in a 75 cm^2 tissue culture flask containing a vented cap (Sigma Aldrich, USA) and incubated at 37°C in 5% CO_2 until 80% confluent. Cells were passaged every 2-3 days or upon reaching 80% confluency.

4.2.4.2 Macrophage infection

To prepare cells for infection, the D10 media was replaced, cells scraped and thoroughly resuspended in 5 ml D10. An aliquot of cells was mixed with Trypan blue using a 1:5 ratio to assess cell viability. This cell impermeable dye cannot penetrate healthy cells and these will therefore appear white, whilst dead or damaged cells stain blue. A coverslip was placed on a hemocytometer and the chambers filled with 10 µl of the cell suspension. Live, unstained cells were counted on the 5 by 5 grid of the

hemocytometer, and multiplied by the 1:5 dilution factor and hemocytometer conversion factor to calculate the amount of live cells/ml. Cells were diluted and seeded in 24 well plates consisting of 400 µl at a final concentration of $5x10^5$ cells/well. For adherence of the cells, the plates were incubated overnight at 37°C in 5% CO_2. *M. smegmatis* wildtype (WT) and single colour controls; pST5552 plus 2 mM theophylline (pT), pSTCHARGE pT, pTiGc pT and pTiGc minus theophylline (mT) were grown up overnight in 10 ml 7H9 with the required antibiotic at 37°C, shaking at 180 rpm.

The following day, inspection of the macrophage monolayers under a microscope was performed to confirm adherence and the media replaced with 300 µl fresh D10 media at the corner of each well to prevent cell disruption. Preparation of *M. smegmatis* strains for infection involved straining of the culture using a 40 µm cell strainer (Corning, USA), followed by sonication as previously described. A 2 ml bacterial culture aliquot was pelleted for 10 min at 14 000 rpm and resuspended in D10 media (supplemented with 1 mM theophylline where necessary) to ensure OD_{600nm} = 1. *M. smegmatis* strains were added to the monolayers at a multiplicity of infection (MOI) of 5 bacteria per macrophage (5:1) in D10 media supplemented with 1 mM theophylline where required, and the plates incubated for 3 hours at 37°C in 5% CO_2.

Following the bacterial uptake period, cells were washed with 300 µl PBS and the media replaced with 400 µl D10 containing 100 U/ml penicillin-streptomycin. Plates were incubated for an hour at 37°C in 5% CO_2 to kill extracellular bacteria.

Cells were washed thrice with 300 µl PBS and replacement of 400 µl D10 media to cells that were maintained to later time points. To ensure dilution of the fluorescent signal occurred after macrophage uptake, the addition of 1 mM theophylline was excluded following the penicillin-streptomycin treatment, this was regarded as the 0h time point. *M. smegmatis*::pTiGc with 1 mM theophylline was added to wells without macrophages for *in vitro* controls. Recovery of bacteria for CFU determination and flow cytometry involved lysing the macrophages with 500 µl distilled sterile water. For the 24h time point, macrophages were treated with penicillin-streptomycin, followed by 3 PBS washes as described above, replicating previous experimental conditions (Mouton *et al.*, 2016). For bacterial enumeration, serial dilutions of bacteria were plated onto LB-agar plates in triplicate and incubated for 3 days at 37°C.

To harvest infected, non-lysed macrophages for staining prior to flow cytometry, cells were resuspended in 500 µl PBS to loosen macrophages, without lysing them. Macrophages were confirmed loosened as visualized under a microscope. Selected samples were labelled with the antibody conjugate, as mentioned in section 4.2.3.

4.2.5 Flow cytometric sample preparation and acquisition

Bacteria that were cultured *in vitro,* or recovered from macrophages were transferred to 1.5 ml microcentrifuge tubes (Eppendorf, USA), pelleted for 7 min at 14 000 rpm and fixed with 4% formaldehyde for 30 min in the dark. Cells were washed with 800 µl PBS and pelleted for 5 min at 14 000 rpm, followed by resuspending the pellet in 500 µl PBS and filtering into a flow cytometric tube containing a filter cap (Corning, USA).

The LSRFortessa flow cytometer (Becton Dickinson, USA) was used for sample analysis. This instrument allows detection up to 18 colours with the use of 4 lasers; a blue (488 nm, 50 mW solid state), a red (640 nm, 40 mW HeNe), a violet (405 nm, 50 mW solid state) and a green laser (561 nm, 50 mW). The forward scatter (FSC) signals were detected by the photodiode detector whilst side scatter (SSC) was detected by the photomultiplier tube (PMT). Both detectors detected light generated by the blue laser with a 488/10 bandpass filter (Table 4.2).

The workspace previously set up by Dr. Jomien Mouton was used for analysis of samples. To set up compensation, an unstained control and theophylline induced pST5552 and pSTCHARGE single colour controls were used for endogenous green and red fluorescence, using filters for detecting GFP and TurboFP635, respectively. Additionally, *in vitro* cultured WT was labelled with the antibody conjugate for incorporation of Alexa Fluor 405 for compensation. In acquisition mode signals were acquired using logarithmic scaling. SSC and FSC settings were adjusted to ensure the bacterial population shifted to the middle of the plot. A gate was applied to the bacterial population in a FSC vs. SSC plot, whereby 30 000 events were captured using the bacterial stopping gate for all samples. BD FACSDiva Software version 8.0.1 generated raw data, which was subsequently processed and analysed using FlowJo software version 10.0.8 (Tree Star Inc., USA).

Table 4.2. LSRFortessa laser configuration

Channel	Filter	Laser	Fluorochrome
FSC	488/10	Blue	N/A
SSC	488/10	Blue	N/A
FL 1	450/50	Violet	Alexa Fluor 405
FL2	488/10	Blue	N/A
FL3	530/30	Green	GFP
FL4	610/20	Red	TurboFP635

4.3 RESULTS

4.3.1 Rationale

The fluorescence dilution technique has shown to be an accurate quantitative measure of mycobacterial replication. It has been previously observed that *M. smegmatis* recovered from macrophages 24h post infection includes a subpopulation with a reduced TurboFP635 fluorescent signal, consistent with replicating bacteria (Mouton *et al*., 2016).

In order to determine whether the apparently replicating population occurred intracellularly or extracellularly of the macrophage, we developed a method exploiting an anti-*M. tuberculosis* antibody in combination with flow cytometric analysis of the infected macrophages. In this approach, extracellular bacteria would be expected to stain positively with the anti-mycobacterial antibody. In contrast, in the absence of membrane permeabilization, the antibody would not be able to access bacteria inside macrophages, and these would therefore not be expected to stain. This was detected by an Alexa Fluor 405-labelled Fab fragment using the Zenon rabbit IgG labelling kit. Detecting this population involved reproducing the experiment to observe the replicating *M. smegmatis* population, optimizing the antibody conjugate for optimal binding to *M. smegmatis,* and applying the optimized antibody conjugate to *M. smegmatis*-infected macrophage samples.

4.3.2 Reproduction of previous experimental conditions and results

Samples were analysed on the LSR Fortessa using the optimized FACSDiva workspace and as expected from previous results (Mouton *et al*., 2016), we confirmed that addition of 2 mM theophylline induced robust expression of TurboFP635, with no expression of TurboFP635 in the absence of theophylline. Green fluorescence remained unchanged in the presence of the inducer, indicative of constitutive GFP production. A similar level of induction was seen for intracellular controls, further suggesting the stability of these fluorescent reporters (Fig 4.3).

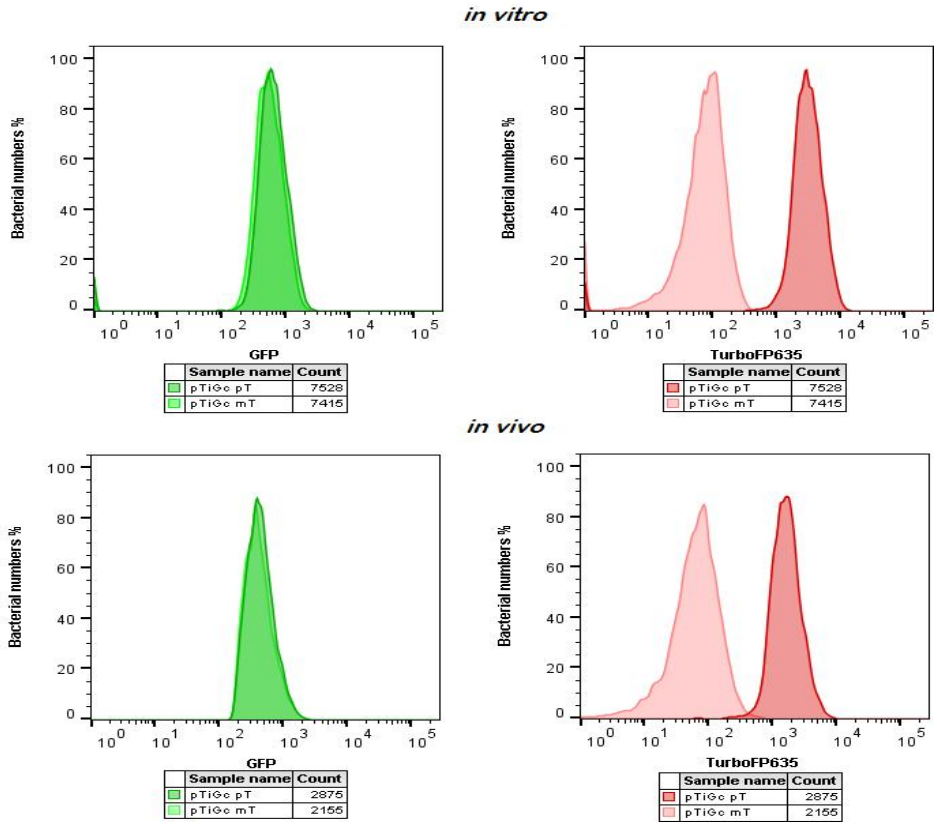

Fig 4.3. Confirmation of induction. In M. smegmatis::pTiGc GFP displayed constitutive expression and TurboFP635 was expressed only upon induction with 2 mM theophylline, both *in vitro* and intracellularly. M. smegmatis::pTiGc was induced overnight with 2 mM theophylline and intracellular M. smegmatis::pTiGc was harvested from macrophages at 0h. pT: plus theophylline, mT: minus theophylline.

We next wished to confirm the previous experimental results showing the presence of a sub-population of replicating *M. smegmatis* upon macrophage infection. As before, the dual-reporter plasmid was used to determine replication dynamics of *M. smegmatis*::pTiGc during infection of murine macrophages over the course of 24 hours (Mouton *et al*., 2016). Following antibiotic treatment with penicillin-streptomycin (to kill non-phagocytosed bacteria), theophylline was removed from the culture. This results in the decrease of the far-red fluorescent signal at each bacterial division as additional TurboFP635 would not be synthesized following removal of the inducer. *M. smegmatis*::pTiGc was recovered from lysed macrophages for analysis by colony forming unit (CFU) determination and flow cytometry.

Consistent with previous experiments, a relatively homogeneous population was seen in intracellular bacteria at 0h and 3h (Fig 4.4), whereas the intracellular bacteria displayed a more heterogeneous distribution at 24h. As previously reported, a subpopulation of more rapidly replicating bacteria was apparent. CFU data (which measures the summative population replication), displayed a decrease in intracellular bacteria numbers over 24h, whilst *in vitro* bacteria increased, as expected.

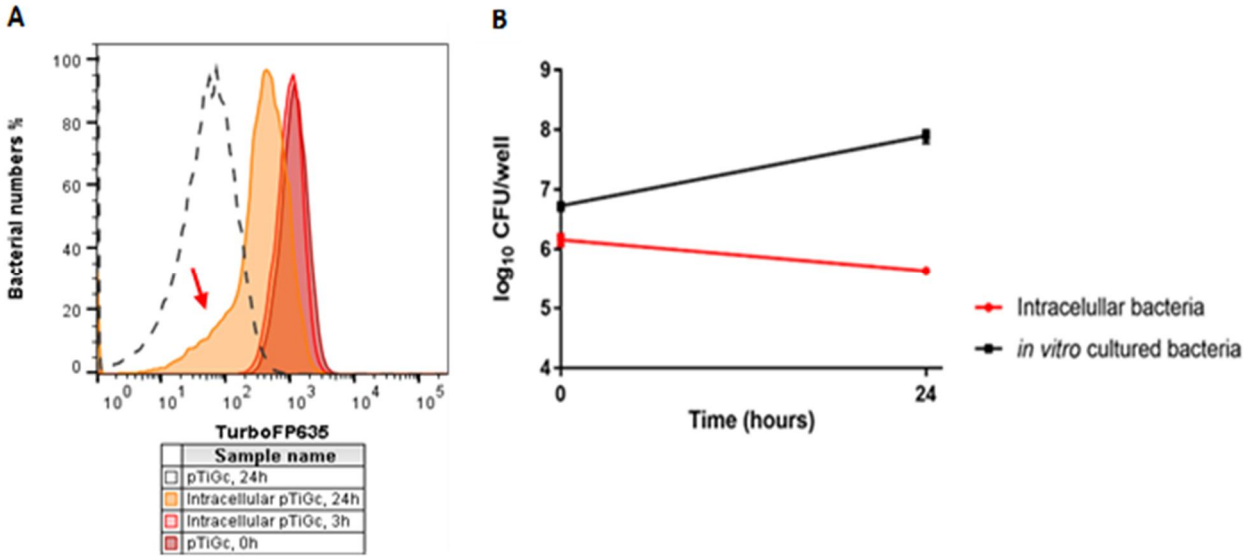

Fig 4.4. Population-wide and summative *M. smegmatis* replication dynamics upon macrophage infection. A) Fluorescence dilution which allows visualization of population-wide replication dynamics, indicated heterogeneous replication at 24h for the intracellular bacteria, with a small subpopulation of rapidly replicating bacteria (Indicated by the arrow). This was in contrast to the homogenous population seen intracellularly at 0h and 3h. B) CFU determination which measures the summative bacterial replication, indicated an overall reduction in *M. smegmatis* CFU following macrophage infection, in comparison to actively replicating in vitro bacteria at 24h.

4.3.3 Determination of the optimal antibody binding to *M. smegmatis*

We initially used labelling conditions as suggested by the manufacturer (Fig 4.5), but undertook two subsequent optimization steps for optimal labelling of *M. smegmatis.* Firstly, the optimal conjugated antibody to bacteria ratio needed to be determined. Secondly, the optimal antibody to fluorophore ratio needed to be determined.

4.3.3.1 Titering antibody:*M. smegmatis* ratios

For initial experiments, we utilised the 3:1 molar ratio of Fab:Antibody (as suggested by the manufacturer), to generate the conjugated antibody (i.e. the Alexa Fluor 405-labelled anti-mycobacterial antibody). The 3:1 conjugated antibody was then used to label *in vitro*-cultured *M. smegmatis* (Fig 4.5).

Varying amounts of conjugate (0.5 μg, 1 μg, 2 μg) were mixed with $1x10^6$ bacteria and incubated, washed and prepared as described (section 4.2.3) for flow cytometric analysis (Fig 4.6, top panel).

A large overlap was noticed when samples were overlayed with the unlabelled bacteria, suggesting that a large proportion of the bacteria were unstained (Fig 4.6, top panel). However, increasing amounts of conjugated antibody resulted in a larger stained proportion, and samples labelled with 2 μg antibody showed the most binding (31.8%).

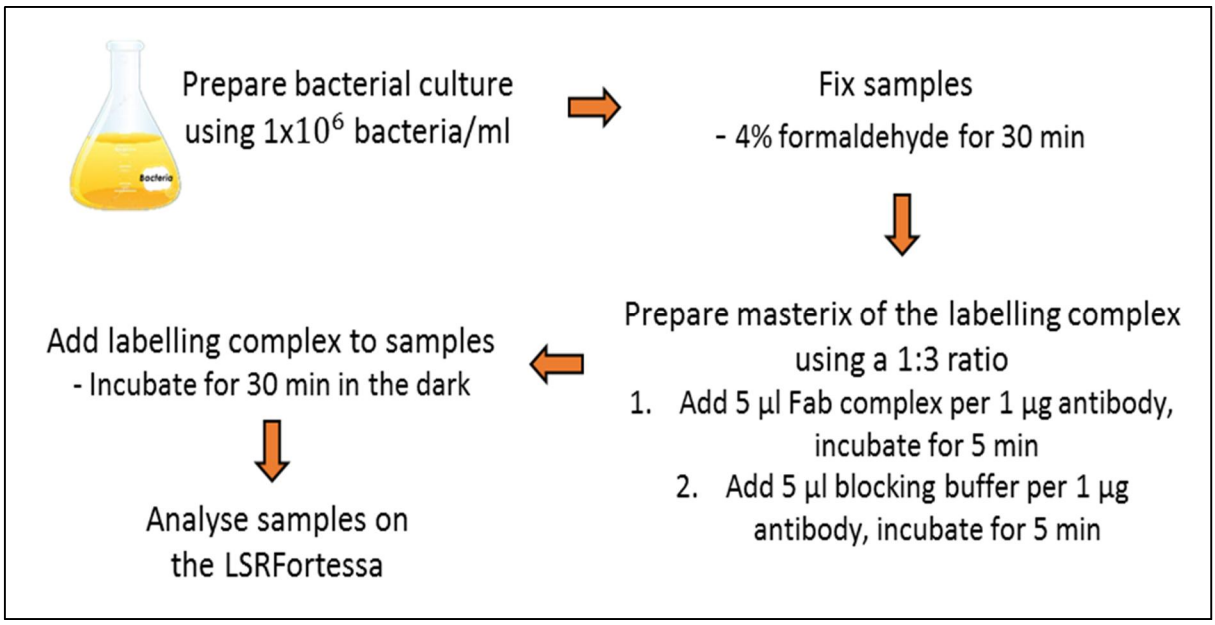

Fig 4.5. Workflow for preparing samples with the labelling complex as suggested by the Zenon Labelling kit.

Having demonstrated that increasing amounts of antibody with a fixed amount of bacteria increased the proportion of labelled bacteria, titering of the antibody conjugate was applied to decreasing amounts of WT bacteria as the majority of the $1x10^6$ bacteria previously overlapped with the unlabelled bacterial population. Bacteria were fixed, stained, followed by an additional fixation step to secure binding of the labelling complex. Antibody binding improved at $1x10^4$ and $1x10^3$ bacteria using 2 µg antibody (Fig 4.6). Proportionally, less binding of the 2 µg antibody occurred as the amount of bacteria increased. The ratio of 2 µg antibody to $1x10^3$ bacteria gave optimal staining, and was used for subsequent experiments.

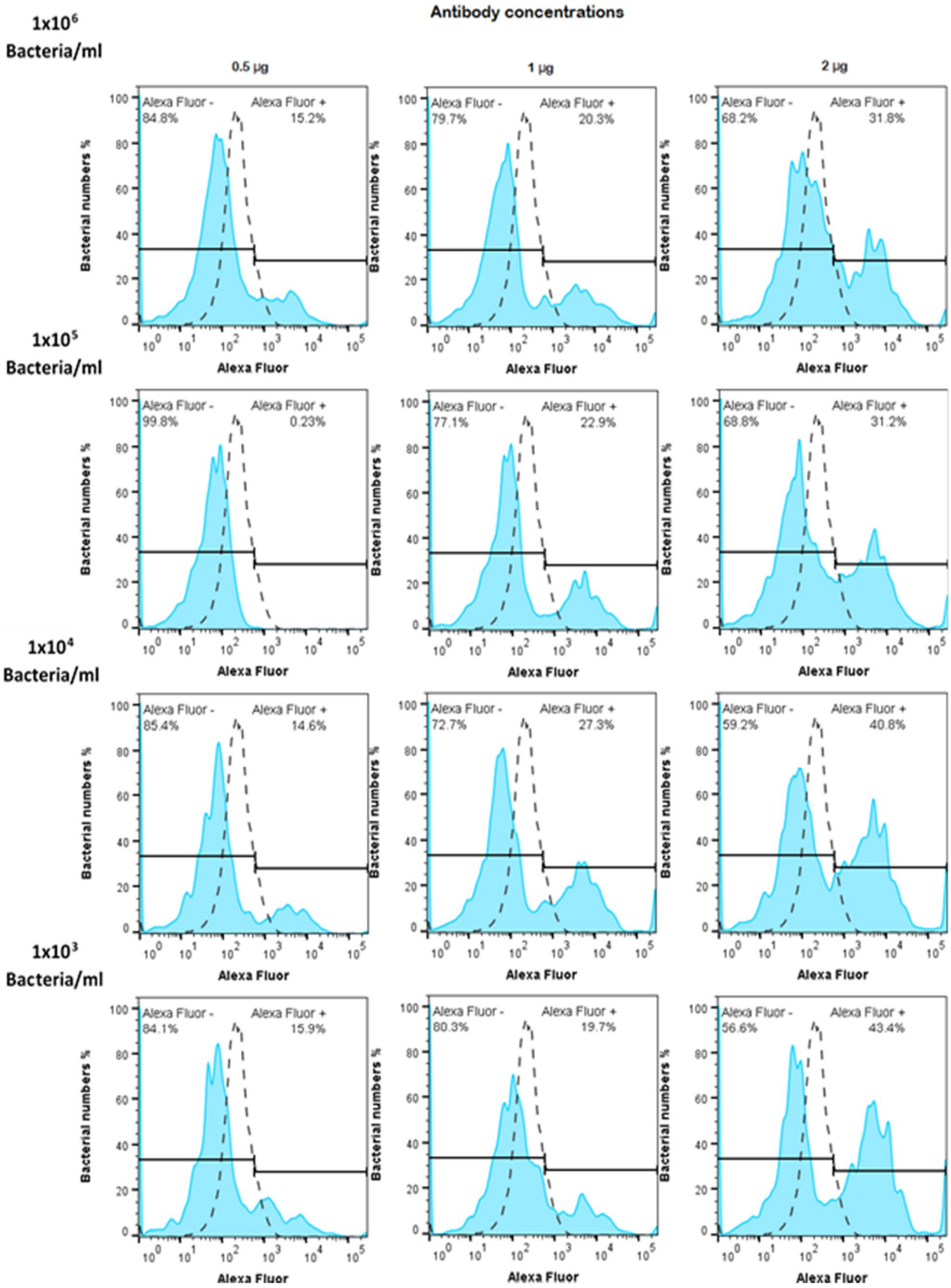

Fig 4.6. Increasing ratios of antibody:bacteria improved labelling. Binding improved using 2 µg antibody as the amount of bacteria decreased. The dotted line represents unlabelled *M. smegmatis*::pTiGc. Optimal staining occurred using 2 µg antibody, using the 3:1 conjugate labelling ratio.

4.3.3.2 Fixing methods

Initially, samples were prepared by fixing the bacteria, labelling with the antibody conjugate, (as suggested by manufacturer) followed by an additional fixation step. To determine whether the additional fixation step had an effect on binding, we compared the fix-labelling-fix method in comparison to labelling then fixing (Fig 4.7). The additional fixation step could alter binding sites for the antibody conjugate as this may change the outer cell surface of the bacteria, thus affecting cross-linking with the antibody. The distinction between unlabelled and labelled bacteria was clearer using the labelling-fix method, with more discrete peaks and more binding at the higher fluorescence regions. The labelling-fix method was thus adopted for subsequent experiments.

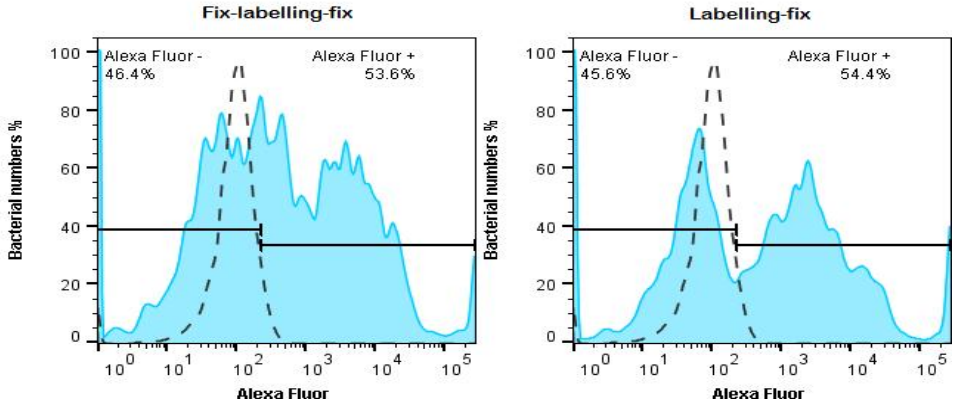

Fig 4.7. Comparison between fixation methods. The labelling-fix method displayed improved distinction between labelled and unlabelled bacteria, in comparison to the fix-labelling-fix method. Optimal staining occurred using 2 µg antibody to $1x10^3$ bacteria, using the 3:1 conjugate labelling ratio.

4.3.3.3 Optimizing the antibody to fluorophore ratio

Binding appeared near-saturated at 2 µg, with little increase from 2 µg to 4 µg in comparison to the larger increase from 1 µg to 2 µg, suggesting no additional antibody could be bound (Fig 4.8). We speculated that this could be as a result of insufficient conjugation of the antibody, therefore the

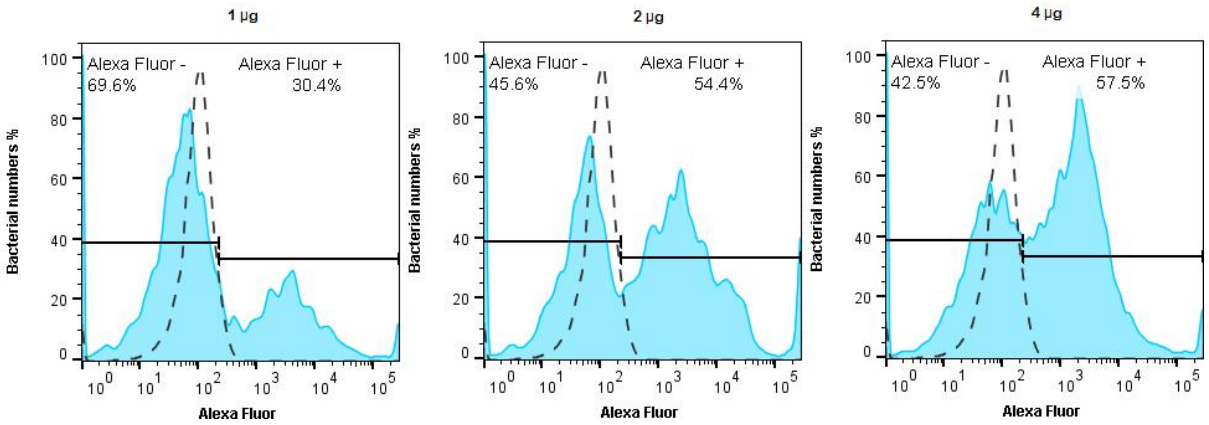

Fig 4.8. Saturation of binding at 2 µg. $1x10^3$ bacteria were labelled with varying amounts of antibody, using the labelling-fix method. The mean fluorescence intensity (MFI) of the Alexa Fluor 405 positively labelled population was 3234, 3206 and 2063 for 1 µg, 2 µg and 4 µg antibody, respectively.

antibody to Fab complex ratio was increased to a 6:1 ratio (1 µg antibody per 10 µl Fab complex) (Fig 4.9) to enhance conjugation of the antibody to the Alexa-Fluor Fab fragments and to enhance the fluorescence intensity.

The majority of WT (90.7%) was bound by the antibody conjugate using 2 µg antibody. Additionally, a 3-fold increase in the mean fluorescence intensity (MFI) of Alexa Fluor 405 was noticed when using the 6:1 ratio for 2 µg antibody, in comparison to the 3:1 ratio (Fig 4.8).

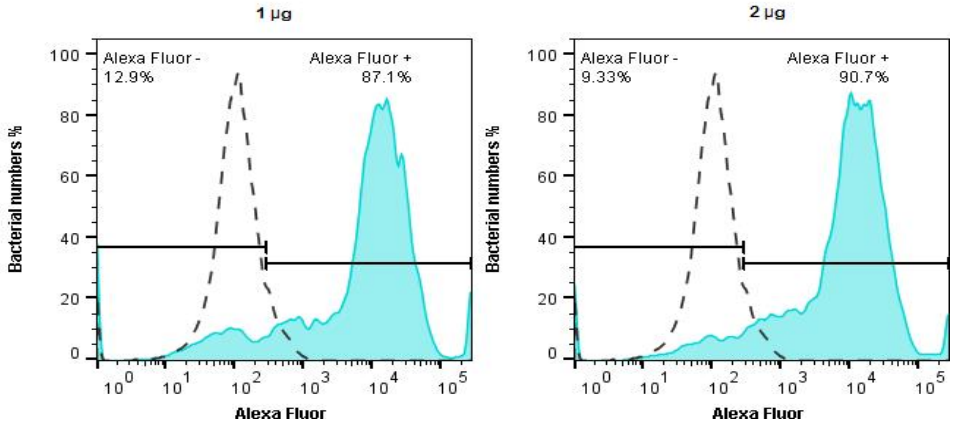

Fig 4.9. Fluorescence was enhanced and binding improved using the 6:1 ratio. Optimal binding occurred using 2 µg antibody to 1x10^3 bacteria. The mean fluorescence intensity (MFI) using the geometric mean of the Alexa Fluor 405 positively labelled population was 10 150 and 9260 for 1 µg and 2 µg antibody, respectively.

We next confirmed that similar results would be obtained with *M. smegmatis*::pTiGc, which was to be used in the subsequent macrophage infection experiments. We applied labelling of 1, 2 and 3 ug antibody (6:1 Fab:antibody conjugation ratio) to 1x10^3 bacteria, using *M. smegmatis*::pTiGc. Here the highest proportion of labelled bacteria was detected with 3 ug antibody (Fig 4.10), which was therefore applied to the macrophage infection experiments. It is inconclusive why *M.* smegmatis::pTiGc was differently labelled than the wildtype. The optimized workflow is illustrated in figure 4.11.

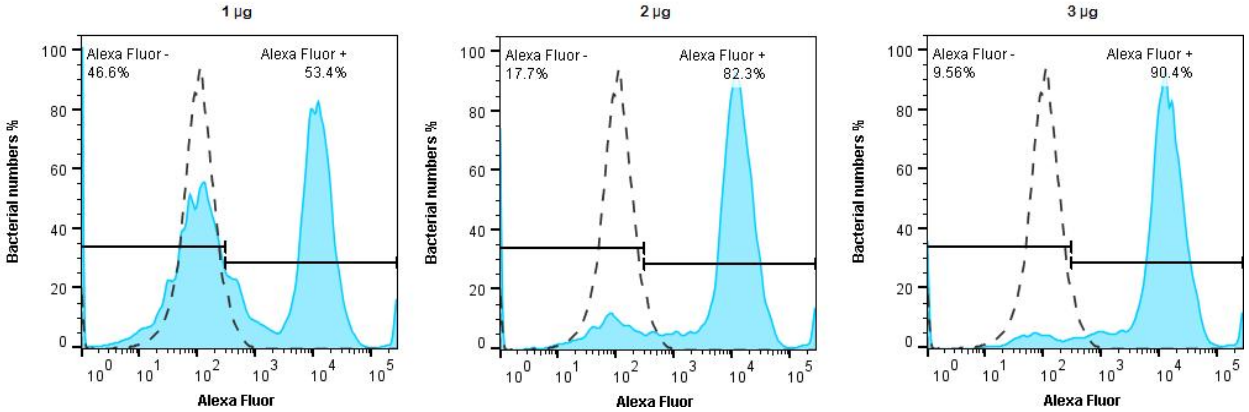

Fig 4.10. *M. smegmatis*::pTiGc displayed optimal binding to the antibody conjugate using 3 µg antibody. The 3:1 conjugate labelling ratio was used to label 1x10^3 bacteria. The mean fluorescence intensity (MFI) using the geometric mean of the Alexa Fluor 405 positively labelled population was 7118, 10 546 and 11 657 for 1 µg, 2 µg and 3 µg antibody, respectively.

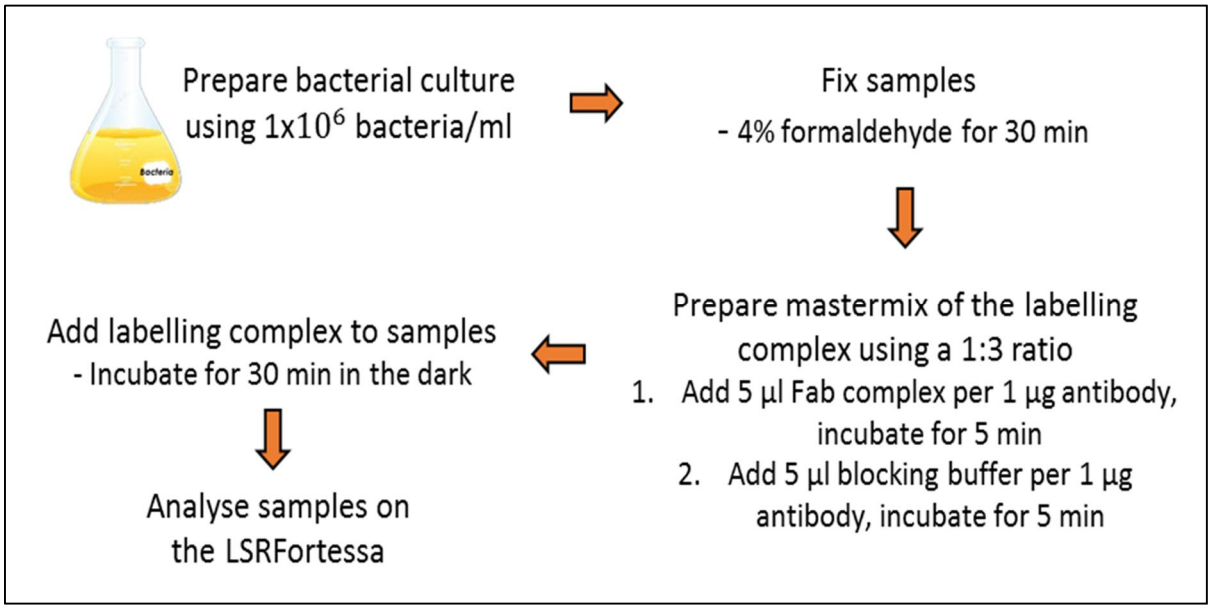

Fig 4.11. Optimized workflow for labelling bacteria with the antibody conjugate.

4.3.4 Applying the optimized antibody conjugate to *M. smegmatis*-infected macrophages

For incorporation of Alexa Fluor 405 into the flow cytometric analysis, the workflow had to be slightly adapted to set up compensation. The analysis strategy is exemplified in Figure 4.12. First, bacteria were selected based on their FSC/SSC properties (Fig 4.12, A). Live cells were then selected by gating on positive GFP fluorescence (Fig 4.12, B). Thereafter, an additional gate was set to capture the majority (>95%) of live cells, but to exclude those with an Alexa Fluor 405 signal > 10^5 (Fig 4.12, C) (this unexpectedly high signal was likely an artefact from macrophage debris or background fluorescence, which effectively is a blue-negative population (data not shown)).

Next, the low red and high red fluorescence intensity populations were gated (Fig 4.12, D). The low red range was determined by overlaying intracellular *M. smegmatis*::pTiGc with *in vitro M. smegmatis*::pTiGc at 24h, which was previously shown to be the point at which only background red fluorescence was detectable after >6 bacterial generations. The shift in red fluorescence of intracellular *M. smegmatis*::pTiGc was a measure of bacterial replication.

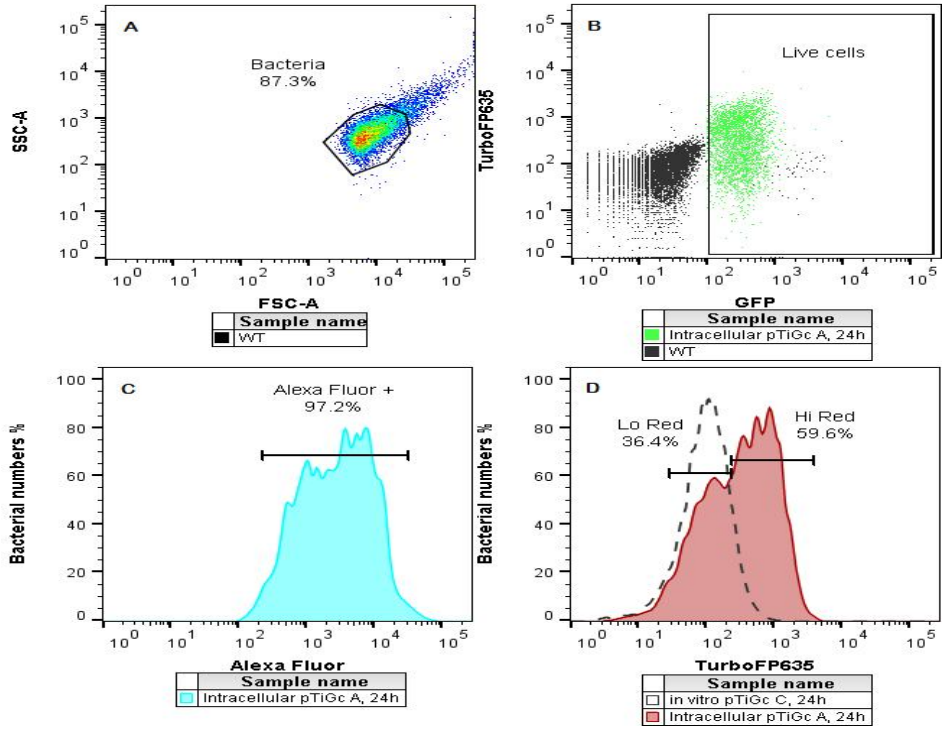

Fig 4.12. Gating strategy. A) The total bacterial population was captured by applying a gate in a FSC vs. SSC plot. B) Within the bacterial population, a rectangular gate was set up to select all live bacteria, determined by positive green fluorescence when overlayed with WT. C) Selecting on the live bacteria for blue fluorescence in a histogram plot, a range tool was used to select the majority of bacteria, but excluding an artefactually high blue fluorescent population. D) Selecting on the live bacteria positive for blue fluorescence in a histogram plot, the range tool was used to select for Lo and Hi red population, based on the overlap of *in vitro* pTiGc. The blue fluorescence MFI was calculated from the Lo and Hi red populations.

To determine whether the replicating *M. smegmatis* observed at 24h occurred intracellularly or extracellular of the macrophage, the optimized antibody conjugate was applied to both lysed and non-lysed *M. smegmatis*-infected macrophages (Fig 4.13).

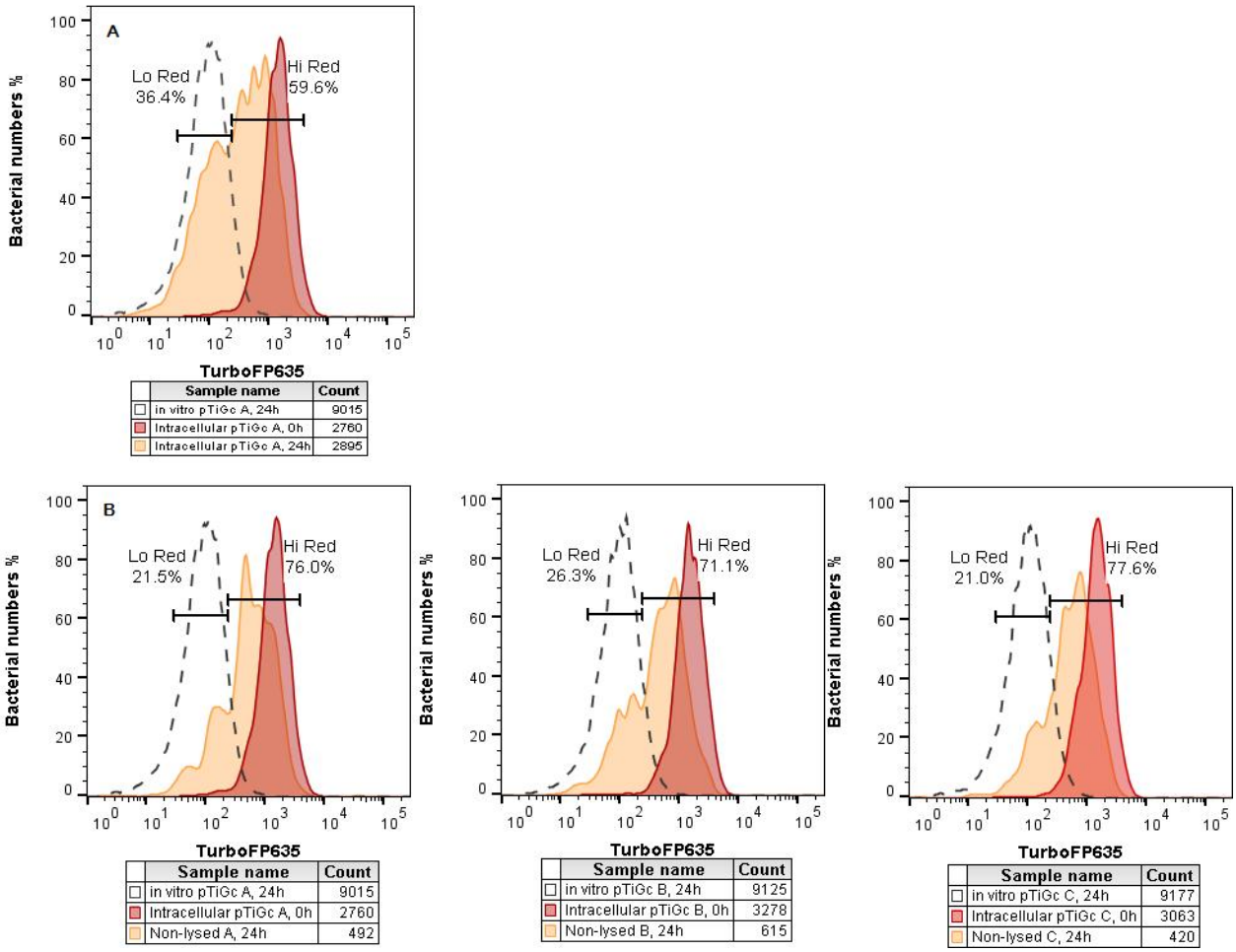

Fig 4.13. The heterogeneous bacterial population at 24h in lysed and non-lysed macrophages. A heterogeneous population, including replicating bacteria were identified in *M. smegmatis*::pTiGc-infected macrophages at 24h. The plots above represent bacteria recovered from A) lysed macrophages and B) non-lysed macrophages (the latter in triplicate), after labelling with the Alexa Fluor 405-conjugated anti-mycobacterial antibody.

Populations identified at 24h showed heterogeneous red fluorescence (including replicating bacteria) in both lysed and non-lysed macrophages, as expected (Fig 4.13). The blue MFI was then determined for both the Lo Red (replicating) and Hi red (non- or slowly-replicating) bacterial subsets. For the lysed macrophages, we would predict that a similar mean blue fluorescence intensity would be observed for all bacteria, since the lysis prior to staining would expose all bacteria equally to the antibody. For the non-lysed macrophages, if the bacteria are extracellular, they would be expected to show a higher mean blue fluorescence intensity than intracellular bacteria, since the latter should not be accessible to the antibody (Fig 4.14).

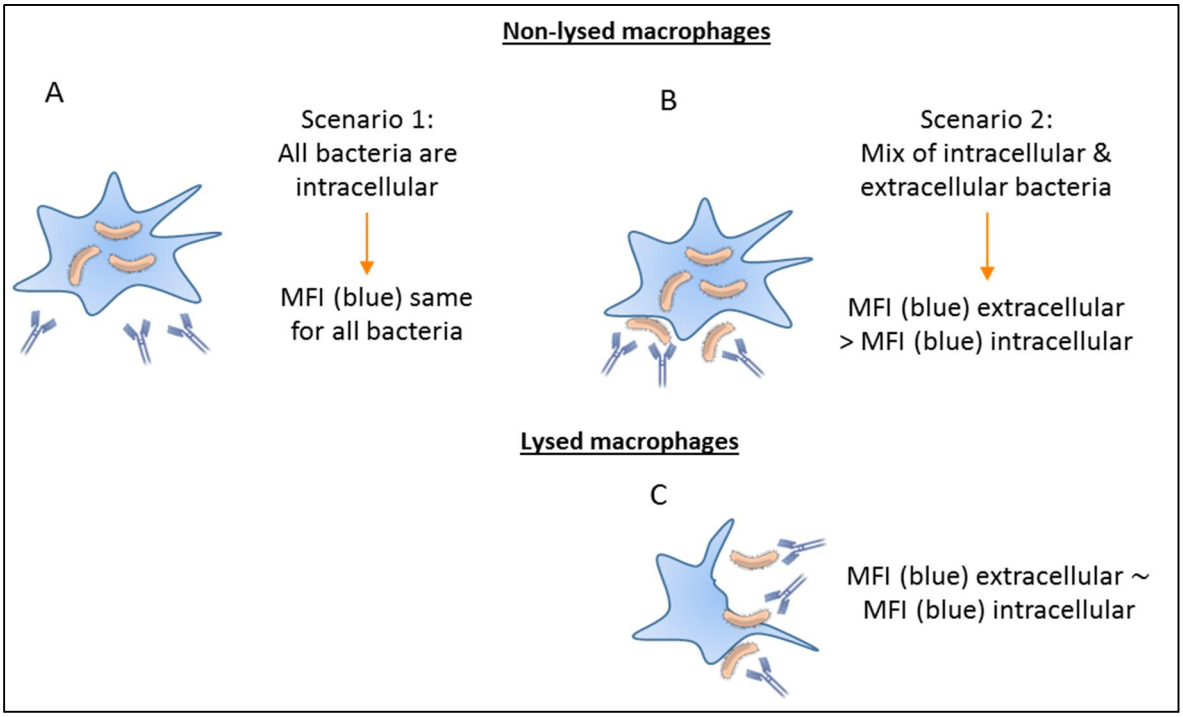

Fig 4.14. Possible scenarios for labelling with the antibody conjugate. The blue mean florescence intensity (MFI) was calculated for the Lo red subset, representative of replicating bacteria. Labelling may differ in non-lysed macrophages depending on the A) absence or B) presence of extracellular *M. smegmatis*. C) Labelling to both extracellular and intracellular bacteria would occur in lysed macrophages irrespective of the absence or presence of extracellular *M. smegmatis*, resulting in similar MFI values.

When the blue MFI of the Hi Red and Lo Red populations recovered from the non-lysed bacteria was compared, a trend towards a higher MFI in the Lo Red (replicating) population than in the Hi Red population (Table 4.3) was noticed. However, this was not statistically significant. Furthermore, upon closer analysis, we observed that the MFI values for both of these populations were both very similar to the MFI of bacteria from the lysed macrophages, and relatively high in comparison to unlabelled (i.e. no antibody) bacteria recovered from macrophages. The lower MFI values for unlabelled *M. smegmatis*::pTiGc recovered from macrophages at 24h suggests that the macrophages may have been compromised during harvesting, thus allowing access of the antibody to intracellular bacteria. Therefore based on these results it is not possible to conclusively determine whether the replicating bacteria are intracellular or extracellular of the macrophage. Further optimisation of the harvesting protocol will be the subject of further work.

Table 4.3. Mean fluorescence intensity of Alexa Fluor 405 for the live bacteria

	Lysed macrophages A, 24h	Non-lysed A, 24h	Non-lysed B, 24h	Non-lysed C, 24h	Unlabelled lysed, 24h
Hi Red	2968	2917	2372	2221	575
Lo Red	2381	3924	3055	2341	337

4.3.5 Testing antibody binding on an attenuated strain of *M. tuberculosis*

We also wished to test whether the anti-mycobacterial antibody would be a useful marker for *M. tuberculosis.* To determine whether lack of binding was attributed to less specificity for *M. smegmatis*, binding was compared using *M. tuberculosis*. As 2 µg of antibody showed high binding in *M. smegmatis*, this concentration was applied to *M. tuberculosis* using $1x10^6$ fixed bacteria (Fig 4.15).

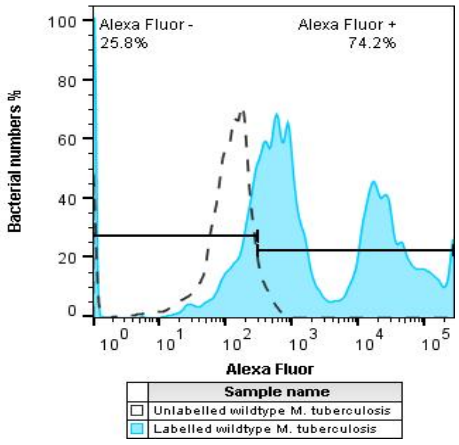

Fig 4.15. Labelling *M. tuberculosis* with the antibody conjugate. *M. tuberculosis* appeared to contain a higher binding affinity than *M. smegmatis* with 2 µg antibody to $1x10^6$ bacteria, using the 3:1 conjugate labelling ratio and the fixed-labelling-fix method.

A high proportion (74.2%) of *M. tuberculosis* was labelled with the antibody conjugate and displayed a greater MFI (4556), suggesting that the conjugated antibody may be useful beyond this study, allowing *M. tuberculosis* to specifically be tracked. For example, *M. tuberculosis* could specifically be identified when recovered from sputum samples, followed by enumeration of live and dead *M. tuberculosis* when stained with SYTO9 and PI.

4.4 DISCUSSION

To explore a previous finding of apparently replicating *M. smegmatis* in a macrophage infection model (Mouton *et al*., 2016), it was important to determine whether these bacteria were intra- or extracellular, as reports have indicated that *M. smegmatis* does not readily survive the environment within macrophages (Kuehnel *et al*., 2001; Prakash *et al*., 2010). It will be valuable to understand the behaviour and adaptation of the replicating *M. smegmatis* and whether these results can be reliably extrapolated to *M. tuberculosis.*

4.4.1 Replication dynamics of infected *M. smegmatis* reveals population heterogeneity

There was previously a lack of a reliable method for the detection of replicating mycobacteria at a single cell level in macrophages. Detection of survival would be achieved through CFU enumeration. CFU of bacteria recovered from lysed macrophages displayed a decrease in replication in comparison to *in vitro* bacteria (Fig 4.4). However, these results would not account for the differential growth rate suggested by the heterogeneous population.

The FD technique developed by Helaine *et al.* for observing replication dynamics in *Salmonella* has provided a remarkable tool for analysis of bacterial replication at a single-cell level (Helaine *et al*., 2010). Characterizing intracellular *M. smegmatis* growth in macrophages has revealed heterogeneity using the dual-reporter plasmid. This study reproduced previous results showing that there is a shift of a homogenous, normally distributed non- or slowly replicating intracellular population at 0h and 3h post infection toward a heterogeneous population at 24h (Fig 4.4). This indicated a subpopulation of relatively rapidly replicating bacteria as detected by the decrease in the TurboFP653 signal. Combining FD with a fluorescently labelled mycobacterial specific antibody should allow the determination of whether the rapidly replicating bacterial population was replicating intracellularly or extracellularly, using flow cytometry.

4.4.2 Optimization of binding of the labelling complex

The anti-*Mycobacterium tuberculosis* antibody used in this study is a polyclonal IgG antibody produced from purified protein derivative (PPD) from *M. tuberculosis.* PPD, also known as tuberculin's, contains a mixture of antigens of varying chemical composition in Mycobacterium species. Therefore this antibody was raised to react to multiple epitopes on PPD (Daniel and Janicki, 1978; Lin *et al*., 2009).

As would be expected, decreasing the relative bacterial amount resulted in more labelling by the antibody. A high level of binding was observed when using 2 µg antibody with $1x10^3$ bacteria (Fig 4.6).

However binding decreased when comparing samples with the additional fixation step. Fixing the bacteria prior to labelling may have altered the epitope accessibility, as formaldehyde crosslinks amino acids in a peptide chain and may cause a conformational change in the antigens, thus being unrecognizable by the antibody (Saper, 2009). A fixation step was necessary following binding of the labelling complex to prevent loss of bound antibody conjugates during the wash steps.

4.4.3 Adaptation to host environment

It has been reported that *M. smegmatis* is unable to survive and grow within macrophages (Kuehnel *et al*., 2001; Prakash *et al*., 2010). Contrastingly, another study reported that although upon uptake the majority of *M. smegmatis* is killed within 4 hours, this was followed unexpectedly by intracellular growth (Anes *et al*., 2006). We therefore wanted to determine whether our results agreed with the latter.

The difference in the replicative nature between *in vitro* and bacteria recovered from lysed macrophages after 24h (Fig 4.13) could be indicative of adaptation by intracellular bacteria, enabling them to survive the intracellular environment. It is likely that bacteria within the same macrophage could have varying replication rates, which is an indication of varying levels of adaptation that selected bacteria undergo, despite being a genetically homogenous bacterial population and experiencing uniform environmental conditions. Microscopy of macrophages infected with *Salmonella* have shown variation in cell division between and within macrophages (Helaine *et al*., 2010). The cell-to-cell variation in *M. tuberculosis* allows progression of infection by evading host immune responses.

The slow growth of *M. tuberculosis* has been thought of as an adaptive mechanism, allowing it to persist in the host without displaying clinical symptoms (Barry *et al*., 2009). This characteristic has also been associated to decreasing the effectiveness of antituberculosis drugs as replication associated functioning is usually targeted by antibiotics, and increased expression of efflux pumps actively export rifampicin and isoniazid (Adams *et al.*, 2011). During antibiotic stress in sputum, upregulation of genes involved in drug efflux and stress response occurs, while decreased replication, production of ribosomal proteins, expression of DNA gyrase and topoisomerase occurred to enable survival (Walter *et al*., 2015). *M. tuberculosis* adaptation has previously been identified in real-time *in vitro* and mouse infection models using microfluidics and time-lapse fluorescence microscopy during a range of stresses (Manina *et al.*, 2015). *M. tuberculosis* can block the maturation of phagosomes by inhibiting phagosome acidification and fusion with lysosomes (Clemens and Horwitz, 1995) to facilitate their survival, this has also shown to occur in *M. smegmatis* (Anes *et al*., 2006).

The mechanisms underlying adaptation in response to the host environment are complex and need to be further explored, especially using single-cell approaches. This could shed light to whether the formation of the heterogeneous population at 24h was a result of damage inflicted by the macrophages or due to initiating and developing an adaptive response within the macrophage intracellular environment. However, it has to first be determined whether this is a true intracellular replicating population of *M. smegmatis*, and not an extracellular population. Despite *M. smegmatis* being non-pathogenic, it most likely expresses certain pathogenic mechanisms to ensure its survival and replication intracellularly, therefore it was valuable to determine whether the rapidly replicating bacteria were extracellular or intracellular of the macrophage. To address this, we exploited an anti-mycobacterial antibody in conjunction with the FD reporter and flow cytometry.

In this experimental setup, we assumed that the antibody would not gain access to intracellular bacteria for non-lysed macrophages, therefore only extracellular bacteria would stain if these were present, and would thus display a higher blue MFI than intracellular bacteria. For lysed macrophages, all bacteria would equally be exposed to the antibody, thus a similar blue MFI would be observed for all bacteria (Fig 4.14). This would allow us to determine where the apparently replicating population was located.

The greater MFI for the Lo red (replicating) population could be attributed to the increased labelling of the antibody conjugate to the lower bacterial numbers in non-lysed samples (Table 4.3). The antibody may not be saturated for this amount of bacteria, therefore would display a greater MFI than lysed macrophages. Although the MFI values for the Lo red population was higher for the non-lysed macrophages than the lysed macrophages, it was not statistically significant ($p=0.254$). Similarly, no significant difference was seen for the Hi red population ($p=0.159$), calculated using a t-test on GraphPad Prism. However, the lower MFI values for unlabelled (no antibody) *M. smegmatis*::pTiGc recovered from macrophages in comparison to the MFI of the Lo red population from non-lysed macrophages at 24h suggests that the macrophages may have been compromised during harvesting, therefore the results are inconclusive as this allowed access of the antibody to intracellular bacteria.

Intracellular growth of *M. smegmatis*::pTiGc has been identified by confocal microscopy and also displayed no extracellular bacteria (Mouton *et al.*, 2016). Imaging flow cytometry which simultaneously rapidly analyses microscopy images using flow cytometry has extensively analysed the relationship between phagosome maturation and the survival of *M. tuberculosis.* This technique has also identified intracellular replication of the virulent H37Rv and avirulent H37Ra *M. tuberculosis* strains (Johansson *et al*., 2015).

Due to the antibody being raised against PPD in *M. tuberculosis,* some of the PPD antigens will likely be more specific to *M. tuberculosis*, though it contains many antigens cross-reactive in other Mycobacterium species. *M. tuberculosis* displayed high binding to the antibody (Fig 4.15), this could be potentially useful for applying this method to *M. tuberculosis*::pTiGc-infected macrophages.

4.4.4 Limitations

Ideally, this experiment would need to be repeated to yield a clear understanding whether the replicating *M. smegmatis* is intracellular or extracellular, and an optimised protocol for harvesting intact mycobacteria would need to be developed. Despite centrifugation of non-lysed macrophages at a lower speed (1100 rpm), thorough pipetting to loosen the adhered macrophages may have damaged them.

4.4.5 Future work

- To ensure the macrophages remain intact, the macrophage harvesting protocol with controls will need to be optimized.
- Investigate *in situ* staining by labelling extracellular bacteria with the antibody in tissue culture plates to overcome any lysis problems upon harvesting.
- Combine antibody labelling of *M. smegmatis*-infected macrophages with confocal microscopy to localise the bacteria.
- Optimize the antibody labelling for *M. tuberculosis.*
- Apply the optimized antibody labelling for *M. tuberculosis* in combination with other methods, such as the FD reporter or staining with SYTO9 and PI for enumeration of *M. tuberculosis.*

4.5 CONCLUSION

The population of latent bacteria and persisters are difficult to characterize due to their non- or slowly-replicating nature. This creates complexity in identifying and isolating them and has left us with limited knowledge or understanding of this population. Their understanding is especially important due to the rise in drug-resistant mycobacteria and the need for a reliable approach is required. The use of techniques such as FD in combination with a mycobacterial specific antibody will allow the identification of a heterogeneous mycobacterial population at a single cell level. Additionally, a second inducible promoter could be incorporated into the current system, either for extending the amount of detectable generations to 10 as employed in *Salmonella* (Helaine *et al.*, 2010), or for the analysis of metabolic activity within each cell. This could aid in understanding mechanisms contributing to adaptation to the host environment. Using a single-cell approach, these populations can be sorted using FACS, and could contribute to the understanding of reactivation. Additionally, this technique could be adapted and applied to other host cell types.

CHAPTER 5:

APPLICATION OF FLOW CYTOMETRIC METHODS FOR MYCOBACTERIAL VIABILITY DISCRIMINATION AND CELL ENUMERATION

5.1 INTRODUCTION

Viability of bacteria was previously viewed as being synonymous with the ability to form colonies on solid growth media, however many viable bacteria display limited culturability due to cell damage or environmental stressors. Bacteria in this state are thought to still be viable and therefore the use of fluorescent stains to determine the viability of *Mycobacterium tuberculosis* is of great importance. Cell viability indicators include enzymes involved in substrate uptake and cleavage, the degree of energy production and the integrity of the cell wall and cell membrane (Sträuber and Müller, 2010).

The BacLight Live/Dead Bacterial Viability and Counting kit has been exploited in a range of bacterial species for diverse applications, including disinfection experiments (Berney *et al*., 2006), environmental sciences (Hernlem and Ravva, 2007; Hoefel *et al*., 2003) and food and industrial biotechnology (Bunthof *et al*., 2001). The kit is comprised of two fluorescent dyes; SYTO9, a cyanine dye is a membrane permeable dye and is able to enter both live and dead cells, and the membrane impermeant dicationic dye PI enters dead cells and cells with compromised cell walls (Fig 5.1). Following cell entry, these dyes both bind to nucleic acid. Cells stained in this way can then be monitored by plate-based fluorescence readings, fluorescence microscopy or by flow cytometry.

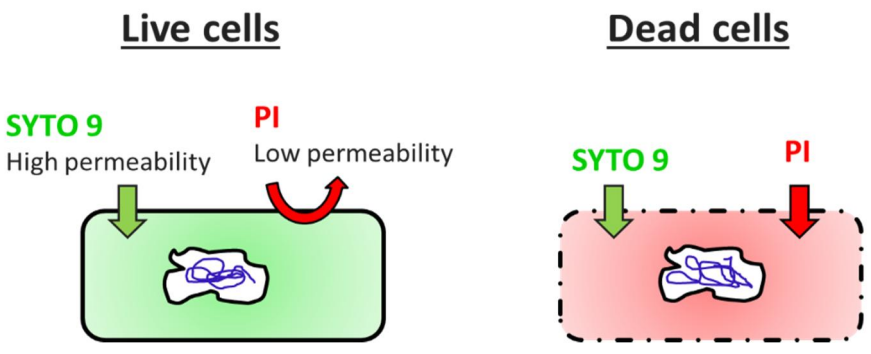

Fig 5.1. Staining of SYTO9 and PI. SYTO9 permeates both live and dead cells due to its high permeability, whereas PI penetrates cells with compromised cell walls. Both dyes bind to bacterial nucleic acid.

In *M. tuberculosis,* the BacLight kit has been applied for the discrimination of live, dead and injured cells in combination with treatment with ethidium monoazide (Soejima *et al*., 2009), the viability of *M. tuberculosis* following recovery from various sputum decontamination methods (Burdz *et al*., 2003), and assessing the viability of cryopreserved clinical samples using different preservation methods and media (Shu *et al*., 2012), although no known studies have utilized this as a counting method, with exception to the attempt by Burdz *et al*., (2003). These studies have not reported on optimisation of the staining protocol for mycobacteria. Furthermore, there have been no reports of this kit having been exploited for rapid mycobacterial counting. In this study, we set out to optimise the staining protocol, as well as to assess whether this kit might be utilised as a rapid and reliable method for the discrimination of live and dead cells within a heterogeneous population and for growth-independent mycobacterial counting.

5.2 MATERIALS AND METHODS

5.2.1 Bacterial strains, media and plasmids

Mycobacterium smegmatis mc^{2}155 (ATCC, 700084) wildtype (WT) was grown in Middlebrook 7H9 media (Difco Laboratories, USA) supplemented with 10% OADC (oleic acid-albumin-dextrose-catalase supplement) (BD Biosciences, USA), 0.2% (v/v) glycerol and 0.05% (w/v) Tween-80 (7H9-OGT) for 48-72 hours at 37°C, shaking at 180 rpm, until OD_{600nm} = 0.8.

An attenuated strain of *Mycobacterium tuberculosis* H37Rv (Δ*leuD* Δ*panCD*) was constructed as previously reported (Sampson *et al*., 2004) and cultured in 7H9-OGT supplemented with 50 µg/ml leucine and 24 µg/ml pantothenate for 3 weeks at 37°C, shaking at 180 rpm, until OD_{600nm} = 0.8. Stocks were stored at -80°C for long term storage. For colony forming unit (CFU) determination *M. smegmatis* was grown on Luria-Bertani (LB) agar (10 g Bacto tryptone, 5 g Bacto yeast extract, 5 g NaCl, 7.5 g Agar) at 37°C, and *M. tuberculosis* on Middlebrook 7H10 agar (Difco Laboratories, USA) supplemented with 10% OADC, 1% (v/v) glycerol, 50 µg/ml leucine and 24 µg/ml pantothenate at 37°C.

For the minimum inhibitory concentration (MIC) determination *M. smegmatis*:pCHERRY expressing the red fluorescent reporter mCherry was cultured as above, in the presence of 50 µg/ml hygromycin.

5.2.2 Preparation of bacterial samples for flow cytometry

5.2.2.1 Preparation of live and dead bacterial suspensions

M. smegmatis was cultured overnight from stocks in 7H9-OGT at 37°C, shaking at 180 rpm, until OD_{600nm} = 1.0. To minimize clumping, bacterial cultures were sonicated in an ultrasonic waterbath (UC-1D, Zeus Automation, South Africa) at 37 kHz for 12 min at room temperature and strained using a 40 µm cell strainer (Corning, USA). Cultures were transferred and pelleted in 2 ml microcentrifuge screw cap tubes (Corning, USA) at 14 000 rpm for 10 min and resuspended in 1.5 ml phosphate buffered saline (PBS). Thereafter, two batches of cells were simultaneously prepared, namely live and dead cells. The live cells were incubated at room temperature for 60 min and the dead cells were heat-killed at 95°C for 60 min in a heating block, with a brief vortex every 15 min. The live and dead cells were harvested by centrifugation at 14 000 rpm for 10 min and the pellet resuspended in 1.5 ml PBS. Following a second centrifugation step as described above, the live and dead cells were fixed in 4% formaldehyde for 30 min in the dark and washed with PBS to yield a final concentration of OD_{600nm} = 1 (corresponding to $1x10^8$ bacteria/ml). An aliquot of 100 µl of live and heat-killed cells were plated in

triplicate on LB agar plates, across 3 serial dilutions and incubated for 3 days at 37°C before quantifying the CFU/ml.

5.2.2.2 Staining of samples

Samples were stained using the BacLight Live/Dead Bacterial Viability and Counting kit, and staining was conducted with some modifications of the manufacturer's protocol. Ten microliters of fixed bacterial cells ($1x10^6$ bacteria) containing known proportions of live and dead bacteria were transferred to 1.5 ml Eppendorf centrifuge tubes containing 1 mM ethylenediaminetetraacetic acid (EDTA) (not part of the manufacturer's protocol) in a final volume of 1 ml PBS to increase uptake of the dyes. The LIVE/DEAD BacLight Bacterial Viability and Counting kit (Invitrogen, USA) supplies two fluorescent dyes, 3.34 mM SYTO9 and 30 mM PI and a calibrated suspension of 6 µm non-florescent microsphere reference beads for quantification of samples. Samples were dual-stained sequentially with 3 µl of SYTO9 for 45 min and 1.5 ml of PI for 15 min in the dark. Thereafter, 10 µl of the reference beads were sonicated for 10 min and added to selected samples. Samples were transferred to 5 ml Falcon flow cytometry tubes via cell strainer caps (Corning, USA) before analysis.

5.2.3 Flow cytometric acquisition

The BD FACS Canto II (Becton Dickinson Biosciences, USA) configured with an 8 colour, 3 laser system; a blue (air-cooled, 488 nm, 20 mW solid state), a red (633 nm, 17 mW HeNe) and a violet laser (405 nm, 30 mW solid state) was used for all sample analysis. Two types of signal detectors are used: the photodiode and photomultiplier tube (PMT). The former detects the stronger FSC signals, which is generated by light from the 488/10 bandpass filter of the blue laser, whereas the latter is more sensitive to detect the weaker signals from SSC as well as all the fluorescence channels. A bandpass filter allows light at a certain wavelength to pass through, while reflecting light above or below the set wavelength. A short (SP) and long pass (LP) filter allows light to pass below and above a specified wavelength, respectively. Multiple fixed wavelength lasers are used for excitation optics, whereas the octagon and two trigon detector arrays are used to transmit the emission signals. The octagon comprises of 5 PMT detectors and detects light from the 488 nm blue laser (FL1 channel). The trigons are comprised of 2 PMTs each and detect light from the 633 nm red (FL2 channel) and 405 nm violet (FL3 channel) laser (Table 4.1). BD Cytometer setup and Tracking beads (BD Biosciences, USA) were run before each experiment to define the baseline fluorescence for each laser to ensure the efficiency of fluorescence in each detector.

The total bacterial population can be detected with the laser emitting at 488 nm, whilst green and red fluorescence from the stained bacteria was collected in the FL1 and FL2 channels, using filters for detecting GFP and PI, respectively (Table 4.1). In acquisition mode signals were acquired using

logarithmic scaling. SSC and FSC settings were adjusted to ensure the bacterial population shifted to the middle of the plot. A gate around the total bacterial population was set up and a second gate for the bead population. To minimize electronic noise, compensation was set up using single-colour controls in a SYTO9 vs. PI plot. The voltage settings were adjusted for each dye to ensure the SYTO9 stained live cells appeared in the lower right quadrant and the PI stained dead cells in the upper left quadrant. Using the bacterial stopping gate, 30 000 events were captured for all samples. BD FACSDiva Software version 8.0.1 generated raw data, which was subsequently processed and analysed using FLowJo software version 10.0.8 (Tree Star Inc., USA).

Table 5.1. FACS Canto II laser configuration

Channel	Filter	Laser	Fluorochrome
FSC	488/10	Blue	N/A
SSC	488/10	Blue	N/A
FL 1	510/50	Violet	N/A
FL2	530/30	Blue	SYTO9
FL3	610/10	Orange-red	PI

5.2.4 Sample preparation for transmission electron microscopy (TEM)

Live and heat-killed cells were prepared as described in section 5.2.2.1 Before fixation, a 1 ml aliquot of live, heat-killed and live cells containing 1 mM EDTA were pelleted at 14 000 rpm for 10 min and preserved with 500 µl of 2.5% gluteraldehyde fixative. Samples were sent for TEM analysis at the National Health Laboratory Service (NHLS) located at Tygerberg hospital. Samples were prepared and images captured by Mrs. Nolan Muller (Practice number: 5200296).

Samples were embedded in resin by resuspending cells in 3% osmium tetraoxide (w/v) for 1h. Cells were rinsed with distilled water and stained with 10% uranyl acetate (w/v) for 15 min, followed by dehydration by treating twice with 70% ethanol for 10 min, followed by 96% ethanol for 20 min. A second staining step using 10% uranyl nitrate for 20 min was performed, followed by three dehydration steps with 100% alcohol for 15, 20 and 30 min. Cells were incubated in Spurr's resin for 60 min, embedded in gelatine capsules and polymerized at 60°C for 24h. From the resin blocks, 200 nm sections were cut on a Leica UC7 ultramicrotome (Leica Microsystems, Germany) using a glass knife. Sections were placed onto a glass slide by stretching with chloroform vapour. Samples were analysed using a JEOL JEM-1011 (JEOL Ltd, Japan) Transmission Electron Microscope with an acceleration voltage of 80 kV.

5.2.5 Staining of *M. smegmatis* recovered from mock sputum

The mock sputum was prepared by dissolving 1% (w/v) methyl cellulose in 1 litre 50 °C distilled water. Following cooling of the solution, an emulsified egg was added and stirred into the solution until evenly suspended, and autoclaved for 20 min at 121 °C. Live and heat-killed bacterial suspensions were prepared as described in section 5.2.2.1, thereafter 500 µl of each bacterial suspension was added to 5 ml of mock sputum and thoroughly vortexed.

Treatment of the spiked mock sputum was performed by addition of 5 ml N-acetyl L-cystein (NALC) (0.5% w/v NALC, 2.7% w/v sodium citrate tribasic dehydrate) solution to the spiked mock sputum, followed by thoroughly vortexing. The spiked mock sputum and NALC mixture was incubated at room temperature for 15 min while agitating gently. Ten millilitres of PBS was added to this mixture and pelleted at 4 000 rpm for 15 min, followed by resuspending the pellet in 2 ml PBS. These samples were fixed in 4% formaldehyde for 30 min and stained with SYTO9 and PI as described in section 5.2.2.2.

5.2.6 Determination of the minimum inhibitory concentration (MIC)

M. smegmatis::pCHERRY (Ex/Em: 587/610 nm) was used to determine the MICs of rifampicin (RIF) and isoniazid (INH) using the broth microdilution method. The MIC is defined as the lowest antibiotic concentration that will inhibit (>90%) bacterial growth. Prior to use, the bacterial culture was sonicated, as previously (Section 5.2.2.1), and filtered using a cell strainer. Each microtitre well was inoculated with 100 µl of bacteria with a final concentration of OD_{600nm} = 0.01. RIF and INH were serially diluted ranging from concentrations of 1.25 – 20 µg/ml to yield a final volume of 200 µl per well. *M. smegmatis* WT, *M. smegmatis*::pCHERRY and 7H9-OGT culture media with either RIF or INH were used as controls. All controls and samples were added in triplicate to a black clear bottom 96-well plate (Corning, USA).

Readings were taken spectrophotometrically with a FLUOstar Omega 96-well microplate reader (BMG Labtech, Germany) for fluorescence and OD measurements at 600 nm at 0, 4 and 24h following addition of each antibiotic. Optic settings were adjusted using a 580/620 nm filter suited for exciting mCherry. The auto-gain adjustment setting was applied to the *M.* smegmatis::pCherry positive control to limit background noise. Plates were incubated at 37°C.

5.3 RESULTS

5.3.1 Rationale

The BacLight Live/Dead Bacterial Viability and Counting kit has been tested on *Escherichia coli* and *Staphylococcus aureus,* demonstrating that organism specific differences affects the level of uptake and staining ability of the dyes in different bacteria (Fig 5.2). Thorough optimization was thus needed for the discrimination between live and dead *M. smegmatis* bacterial cells.

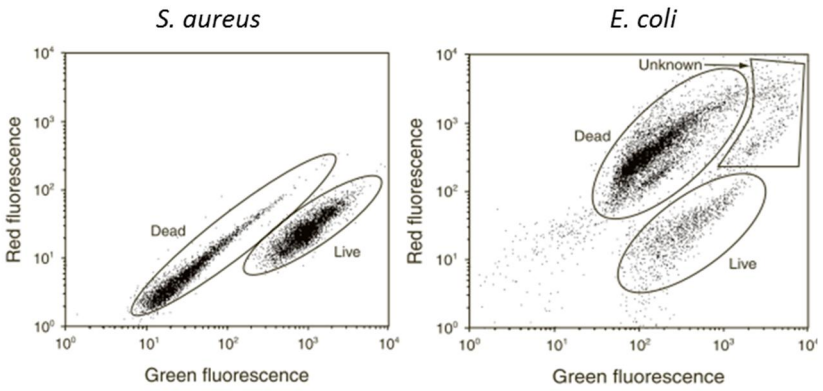

Fig 5.2. Organism specific differences contribute to the variation in staining. *S. auereus* and *E. coli* were stained with SYTO9 and PI, as depicted in the manufacturer's manual.

5.3.2 Optimization of the BacLight Live/Dead Bacterial Viability and Counting kit

Initially, the protocol was followed as suggested by the manufacturer (Invitrogen, USA) (Fig 5.3). To maintain bacterial numbers, a greater amount of bacterial cells was used (OD_{600nm}= 1.4) for sample preparation. An equal amount of SYTO9 and PI (1.5 µl) as suggested by the kit was applied to the live and dead cells, respectively. Initially 70% absolute ethanol was used as a killing method. This, however, resulted in cell lysis as detected by a large proportion of cell debris (Fig 5.4), and thus limited differentiation between the live and dead bacterial populations was observed. Thorough optimization was needed to improve staining and provide a clearer distinction between live and dead cells.

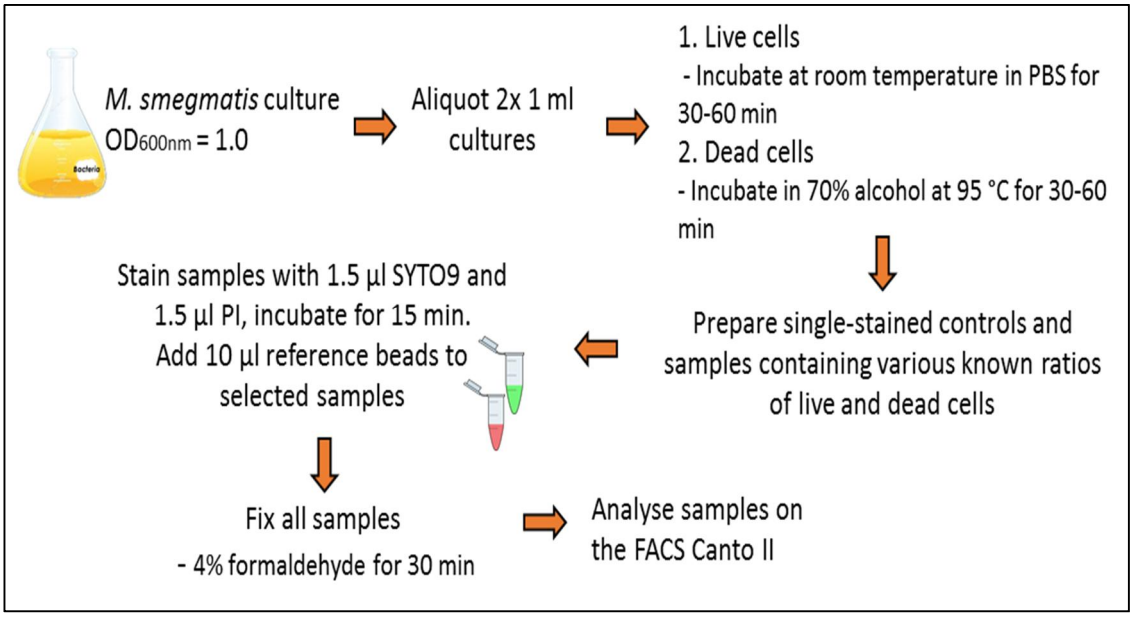

Fig 5.3. Workflow for the BacLight Live/Dead Bacterial Viability and Counting kit. Samples were originally prepared as per manufacturer's protocol.

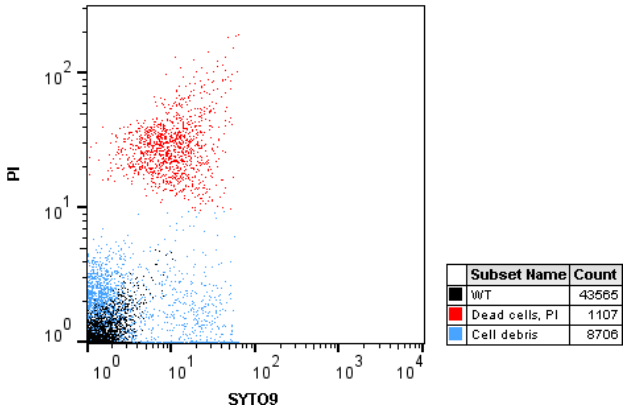

Fig 5.4. Using 70% ethanol as a killing method resulted in a large proportion of cell debris. The tightly grouped unstained WT population can be seen in the unstained quadrant of a SYTO9 vs. PI plot, and overlayed with the cell debris from a PI-stained dead sample. Bacteria were stained with 1.5 µl SYTO9 and 1.5 µl PI for 15 min.

5.3.2.1 Testing killing methods

Cell lysis induced by 70% ethanol treatment interfered with analysis by increasing the noise as the cell debris pooled in the quadrant of the unstained population in a SYTO9 vs. PI plot. We therefore investigated heat-killing at 95°C as an alternative to treatment with 70% ethanol for 30 and 60 min. In contrast to treatment with 70% ethanol, no cell lysis was evident upon heat-killing for 30 min, and much higher bacterial numbers were recovered (Fig 5.5). We therefore opted to use heat-killing for subsequent optimization experiments.

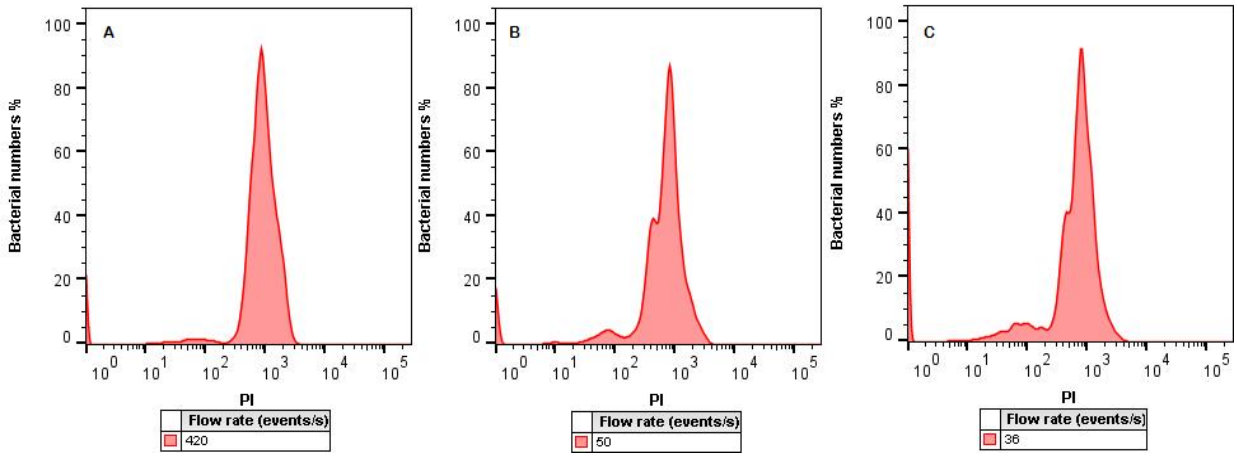

Fig 5.5. Testing killing methods A) Bacterial numbers, as indicated by the sample flow rate improved when using heat-killing at 95°C for 30 min as a killing method, in comparison to treatment with 70% ethanol for B) 30 min and C) 60 min. Bacteria were stained with 1.5 µl PI for 15 min.

We next performed dual-staining of cells incubated at 95°C for 30 min. This revealed that a proportion of the cells were stained with SYTO9 (Fig 5.6). This led us to believe 30 min was insufficient to effect complete killing. This was supported by the fact that some viable bacteria were recovered on solid agar. We therefore tested a longer incubation period of 60 min. Results from plating revealed no CFU at 60 min of heat-killing at 95°C. In agreement with this, flow cytometry of dual-stained samples showed only dead cells. Heat-killing at 95°C for 60 min was therefore used for all further optimization experiments (Fig 4.6).

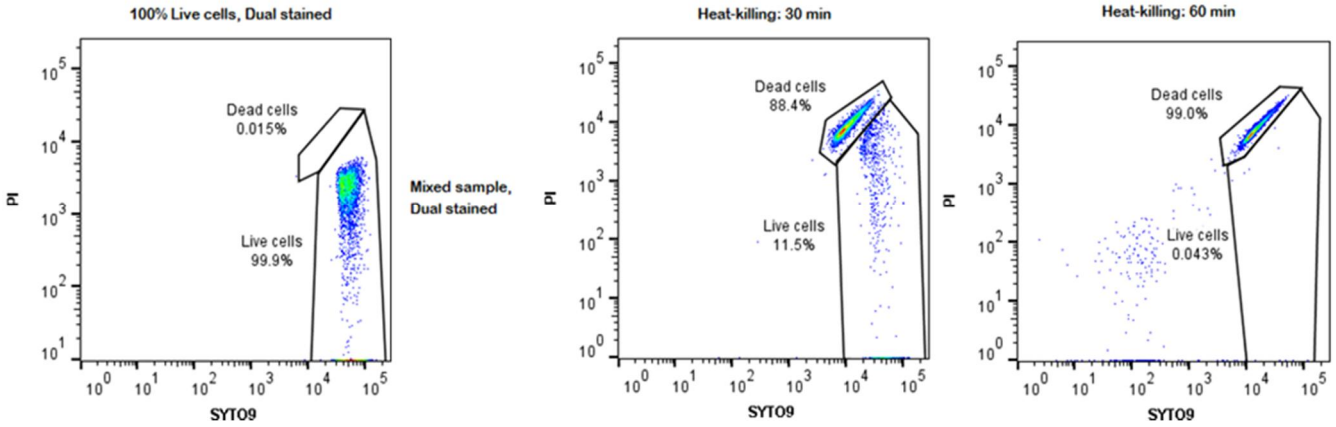

Fig 5.6. Testing heat-killing. Dual-stained *M. smegmatis* heat-killed for 30 and 60 min, displayed 88.4% and 99% of the bacterial cells as dead, respectively. Dual-stained live cells is depicted as a control sample. Bacteria were stained with 1.5 µl SYTO9 and 1.5 µl PI for 15 min.

5.3.2.2 Setting up the FACS Canto II

Voltage settings are unique for each application and bacterial species and therefore needed to be thoroughly optimized for use in *M. smegmatis*. The FSC and SSC voltage settings were defined using an unstained sample for positioning of the bacterial and bead population within the display plot.

SYTO9 and PI voltage settings were adjusted using single stained samples. An unstained sample of *M. smegmatis* confirmed that the PMT voltage settings were appropriately set by displaying the unstained population in the lower left quadrant of a PI vs. SYTO9 plot (Fig 5.7). This is essential as it limits the background noise and is an indication that the settings used for each fluorophore is correct. Having adjusted the voltage settings for the single-stained and unstained cells, these settings were then applied to set up compensation. The compensation values are used by the flow cytometer to calculate and correct the spectral overlap of each colour in the specified detectors to enable distinction in dual-stained samples.

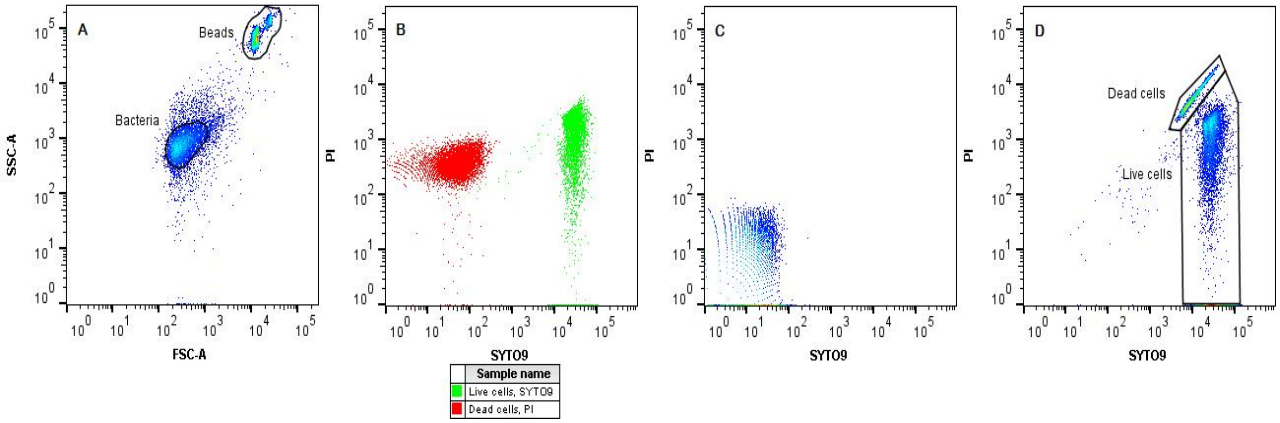

Fig 5.7. Workflow of data analysis. A) A tight gate was applied to the bacterial population in a FSC vs. SSC plot for analysis of this population as a group and a second gate was applied to the bead population for enumeration of the live and dead bacteria. B) Voltage settings for single-stained controls were adjusted to ensure high green and red fluorescence for SYTO9 and PI, respectively, and for setting up compensation. C) Voltage settings adjusted from the SYTO9-stained live cells and PI-stained dead cells ensured that the unstained *M. smegmatis* was situated in the lower left quadrant of a PI vs. SYTO9 plot. D) Selecting on the gated bacterial population, in a SYTO9 vs. PI plot, a gate was applied to the live and dead bacterial population. Bacteria were untreated or stained with 1.5 µl SYTO9 and/or 1.5 µl PI for 15 min.

5.3.2.3 Optimizing incubation times and order of addition for SYTO9 and PI

SYTO9 passively diffuses through the cell wall and due to the thick cell wall of *M. smegmatis*, entry into the cell followed by binding to the nucleic acid would possibly take longer than bacterial cells with less thick cell walls. As suggested by the kit, PI has a higher binding affinity than SYTO9, therefore it was decided to first test incubation of SYTO9 for 15, 30 and 45 min, followed by staining with PI for a further 15 min using 1.5 µl of both fluorophores (Fig 5.8).

Sequential addition of SYTO9, followed by PI resulted in better discrimination of the live and dead populations in mixed samples (50:50 live:dead) (Fig 4.8). Furthermore, extended incubation with SYTO9 (45 min) resulted in tighter grouping of live and dead populations. Incorporation of the 45 min

incubation step with SYTO9 and counterstaining with PI for 15 min was used in all subsequent experiments.

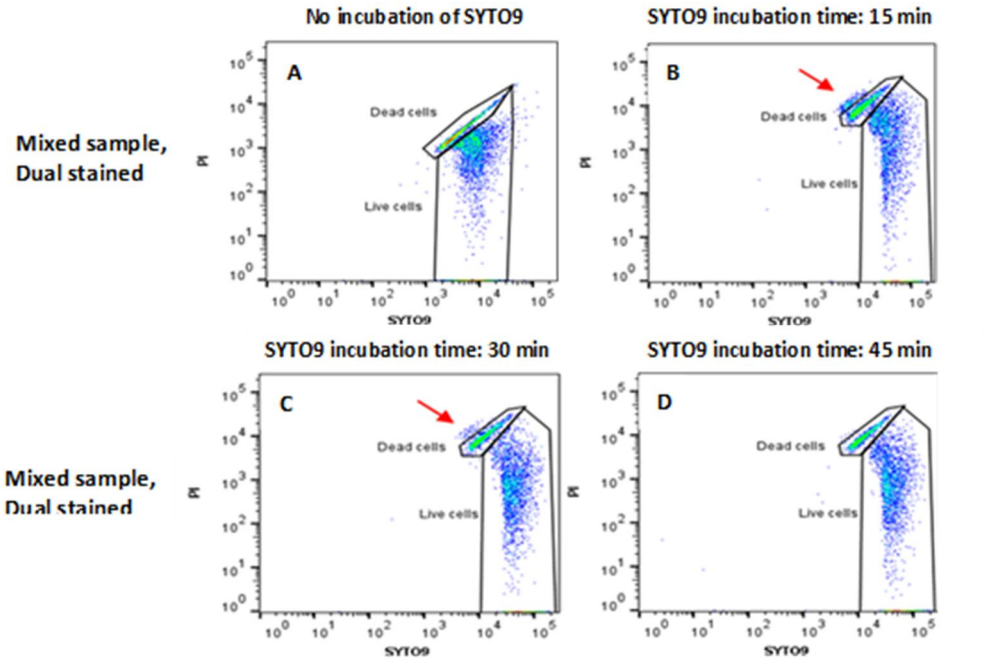

Fig 5.8. Modifications to the protocol by lengthening the incubation time for SYTO9 improved binding. Simultaneous incubation with both SYTO9 and PI for 15 min resulted in the overlap of the live and dead population in mixed samples (Experiment independently done). Therefore, mixed samples were incubated with SYTO9 for B) 15, C) 30 and D) 45 min, followed by counterstaining with PI for 15 min. Improvement with tighter grouping and binding was seen at 45 min, with a decrease in the non-specifically bound population (indicated by the red arrow).

5.3.2.4 Fixing of samples

The manufacturer's protocol suggested that following staining, samples should be fixed with 4% formaldehyde for 30 min. In our hands however, this led to low bacterial numbers being acquired in comparison to an unfixed sample (Fig 5.9). We speculate that the lack of a visible pellet in fixed samples indicated bacterial loss during the wash steps.

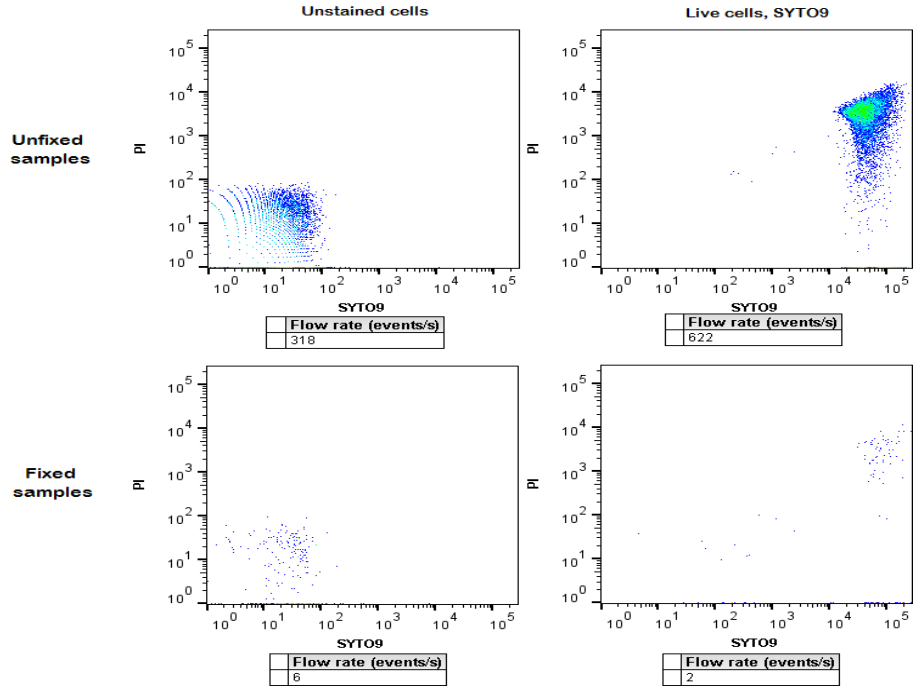

Fig 5.9. Fixing stained samples affected bacterial numbers. Comparison in the bacterial numbers for unstained and single-stained live cells with SYTO9 between an unfixed and fixed sample with 4% formaldehyde. Limited bacterial numbers can be seen in the fixed samples. Bacteria were untreated or stained with 1.5 µl SYTO9 for 45 min.

We subsequently decided to batch-fix samples in larger volumes (10 ml) before staining, which improved the bacterial event rate (Fig 5.10). Ten microliters of the batch-fixed cells (corresponding to $1x10^6$ CFU) was then added to samples containing PBS, followed by staining with 1.5 µl SYTO9 or PI for 15 min. Batch fixing yielded more consistent results and was incorporated in all subsequent experiments.

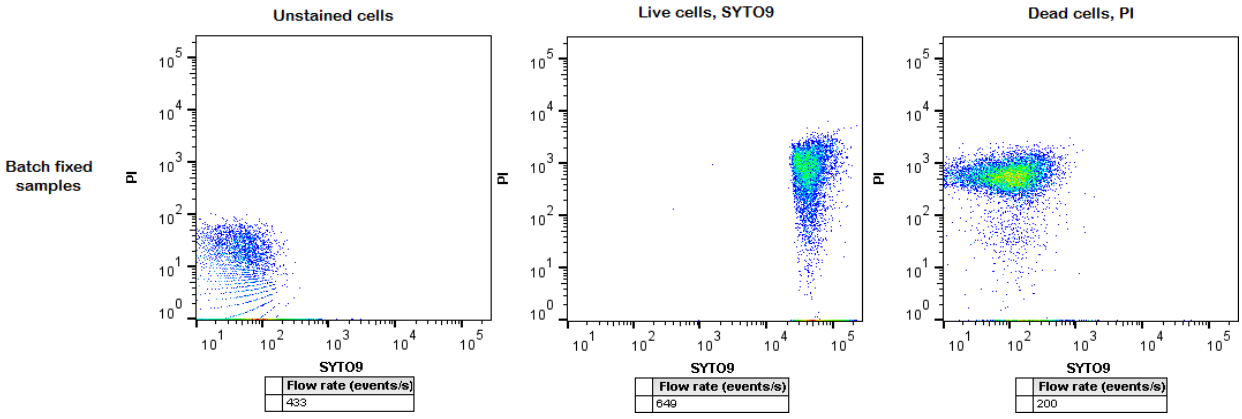

Fig 5.10. Batch fixing samples improved bacterial numbers. Bacteria were untreated or singly-stained with 1.5 µl SYTO9 for 45 min, and 1.5 µl PI for 15 min, and results were comparable to the flow rate of unfixed samples (Fig 5.9).

5.3.2.5 Addition of EDTA

It has been shown in gram negative bacteria that the addition of EDTA enhances the uptake of permeable dyes (Sträuber and Müller, 2010), although this has not been reported in *M. tuberculosis,* to our knowledge. We therefore wished to test whether the inclusion of EDTA in the staining protocol might improve the discrimination of live and dead populations. Indeed, the addition of 1 mM EDTA to dual-stained live cells and mixed samples resulted in the tighter grouping of the live population and was thus added to all subsequent optimization experiments (Fig 5.11). This suggested that the addition of EDTA in *M. smegmatis* increased the uptake of SYTO9.

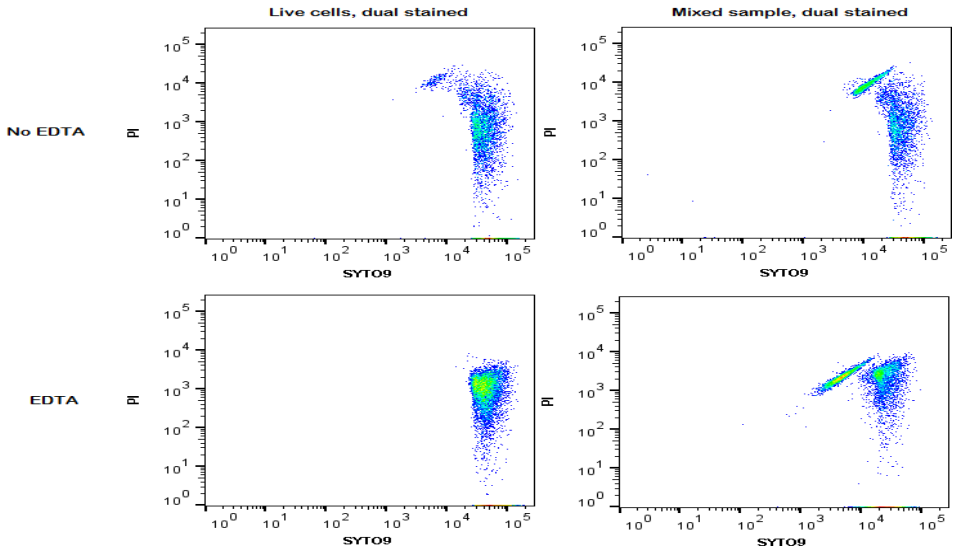

Fig 5.11. The addition of 1 mM EDTA improved grouping of live cells. Tighter grouping was seen for the live population with the addition of 1 mM EDTA for dual-stained live cells and mixed samples. Fixed bacteria were stained with 1.5 µl SYTO9 for 45 min, followed by staining with 1.5 µl PI for 15 min.

5.3.2.6 Optimizing dye ratios

Thus far, we had used dye amounts and ratios as suggested by the manufacturer. We reasoned that varying the amounts and ratios of the dyes may improve our ability to distinguish between live and dead cells. Therefore, a matrix was set up using mixed samples to determine the optimal combination of dye ratios to distinguish between live and dead cell (Fig 5.12).

These results demonstrated that the amounts and ratios of the dyes impacted on the ability to distinguish the live and dead populations. The amounts SYTO9:PI 3:1.5 µl and 3:3 µl showed the best separation between the live and dead populations. The former ratio was used for all subsequent experiments as this yielded the best separation using the least amount of dyes.

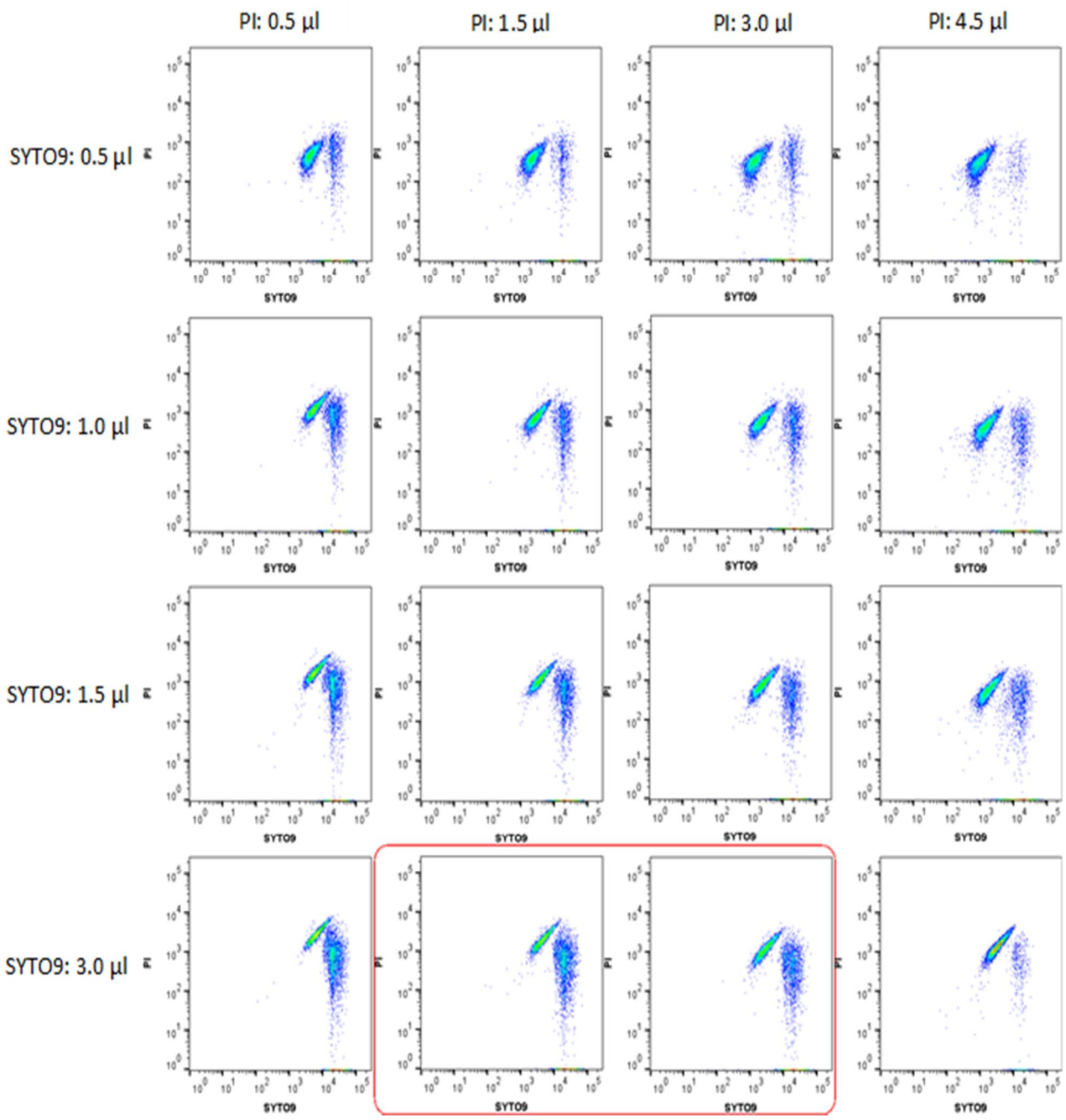

Fig 5.12. Optimizing dye ratios. To improve the separation between live and dead populations, a matrix was set up with increasing ratios of SYTO9 and PI in mixed samples. Compensation was set up using the highest ratio of SYTO9 and the lowest ratio of PI. The best separation was seen using SYTO9:PI amounts 3:1.5 µl and 3:3 µl (enclosed). Fixed bacteria were stained with 1.5 µl SYTO9 for 45 min, followed by staining with 1.5 µl PI for 15 min, treated with 1 mM EDTA.

5.3.2.7 Analysis of samples at 24 hours

We next wished to determine the feasibility of storing samples prior to analysis, which would particularly be useful in the case of clinical samples. We therefore retained samples prepared from the matrix (Fig 5.12), and analysed these at 24h (Fig 5.13), using the above mentioned settings. In all

samples, the bacterial number remained the same and the fluorescent signal did not decrease over time. However, the live population in all dual-stained mixed samples appeared to have shifted upwards at 24h, alongside the dead population. However, the dead cell population was not altered over time and did not shift. This corresponded with grouping and positioning of PI single-stained dead cells (Fig 5.14). In contrast, at 24h the SYTO9 single-stained live population also appeared to shift upwards as the SYTO9 concentration increased. This suggests that the intracellular SYTO9 concentration could be enhanced due to excess SYTO9 in the samples being taken up by the cell.

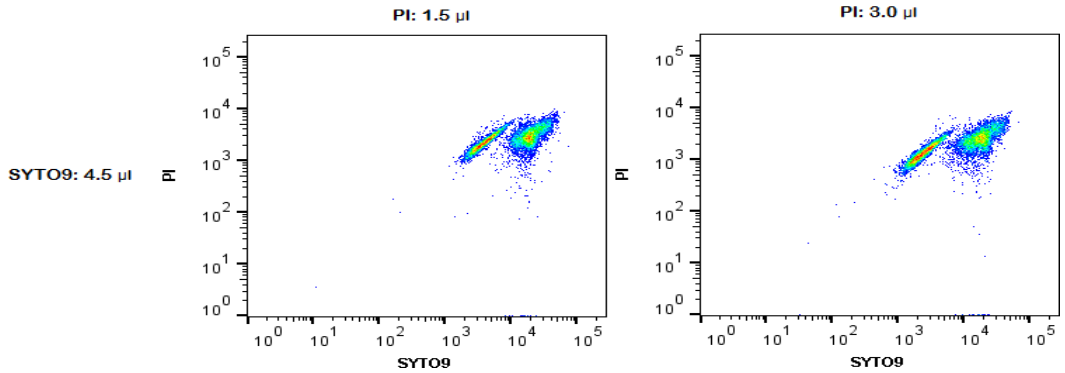

Fig 5.13. Samples were analysed 24h post preparation. Mixed samples displaying the best separation between live and dead populations from the matrix (Fig 5.12) showed an upward shift in the live cell population at 24h.

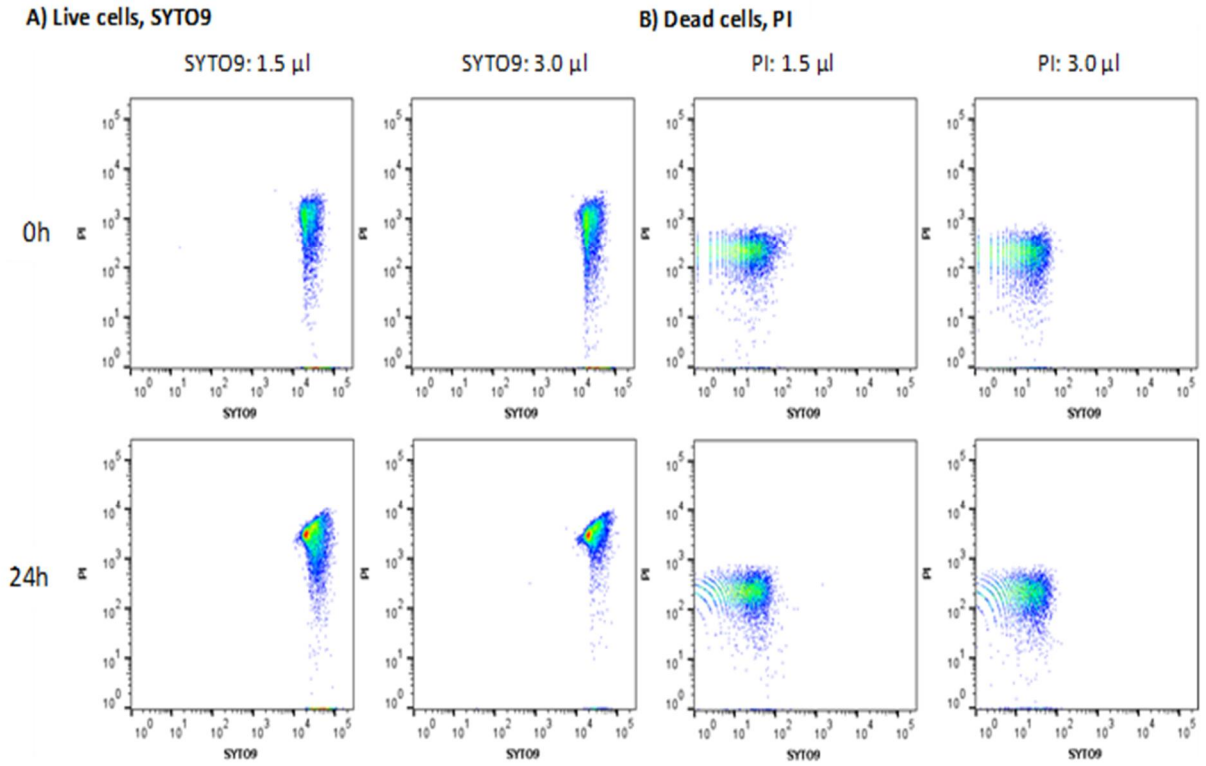

Fig 5.14. Single-stained controls were compared at 0h and 24h post preparation. A) An upward shift was seen in the live cell population at 24 h at the increasing SYTO9 concentration. B) Contrastingly, the dead cell population displayed no change over 24 h, irrespective of the PI concentration. Fixed bacteria were singly-stained with 1.5 µl SYTO9 for 45 min, or 1.5 µl PI for 15 min, treated with 1 mM EDTA.

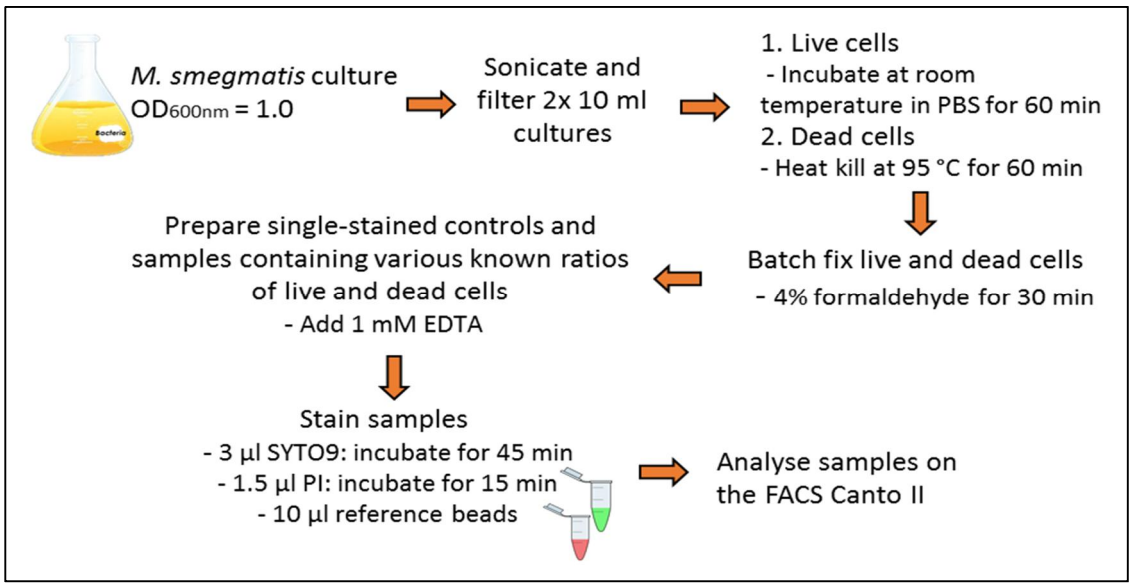

Fig 5.15. Optimized workflow for sample preparation with the BacLight Live/Dead Bacterial Viability and Counting kit.

5.3.3 Enumeration of mixed suspensions of live and heat-killed bacteria

Having established an optimised staining protocol (Fig 5.15) able to reliably distinguish live and dead *M. smegmatis* populations, we next wished to determine whether this method could be used to rapidly and accurately enumerate these bacteria. To do this, we utilized the microsphere beads supplied with the kit as a reference. These counts were compared to values obtained from CFU data. Each bead is 6 µm in diameter and is thus easily distinguishable from *M. smegmatis* (4 µm length) on a FSC vs. SSC plot (Fig 5.16). A single bead represents 10^6 events/ml when added to samples and this is taken into account when calculating the amount of bacteria/ml.

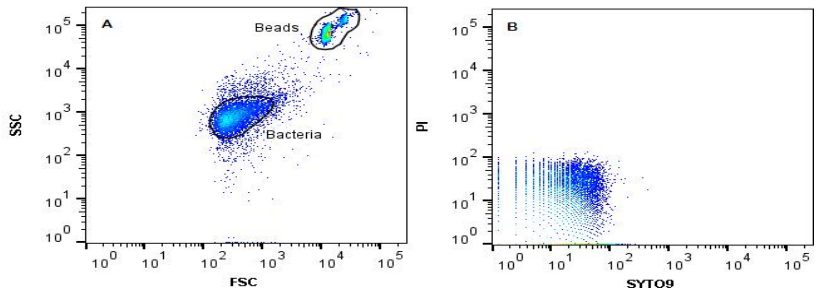

Fig 5.16. Identification of the bead population. A) The bacterial and bead population could easily be distinguished and was separately gated for in a FSC vs. SSC plot. B) The bead population is non-fluorescent and is thus displayed as unstained in a SYTO9 vs. PI plot.

Varying known ratios of live and dead cells were added to each sample, which was prepared using the optimized settings as described above (Fig 5.17). Using the bacterial stopping gate, 30 000 events were captured for each sample. This ensures that our population of interest is recorded, to yield an accurate

amount of cells for analysis. Additionally, this also limits potential cell debris in the samples from being captured as an event. The varying ratios of live and dead cells were accurately displayed as percentages when analysed in FlowJo. Bacteria/ml was calculated for live and dead cells within each sample using the following calculation: $\text{Bacteria/ml} = \frac{\text{Number of events in bacteria region} \times \text{dilution factors}}{\text{Number of events in bead region} \times 10^{-6}}$

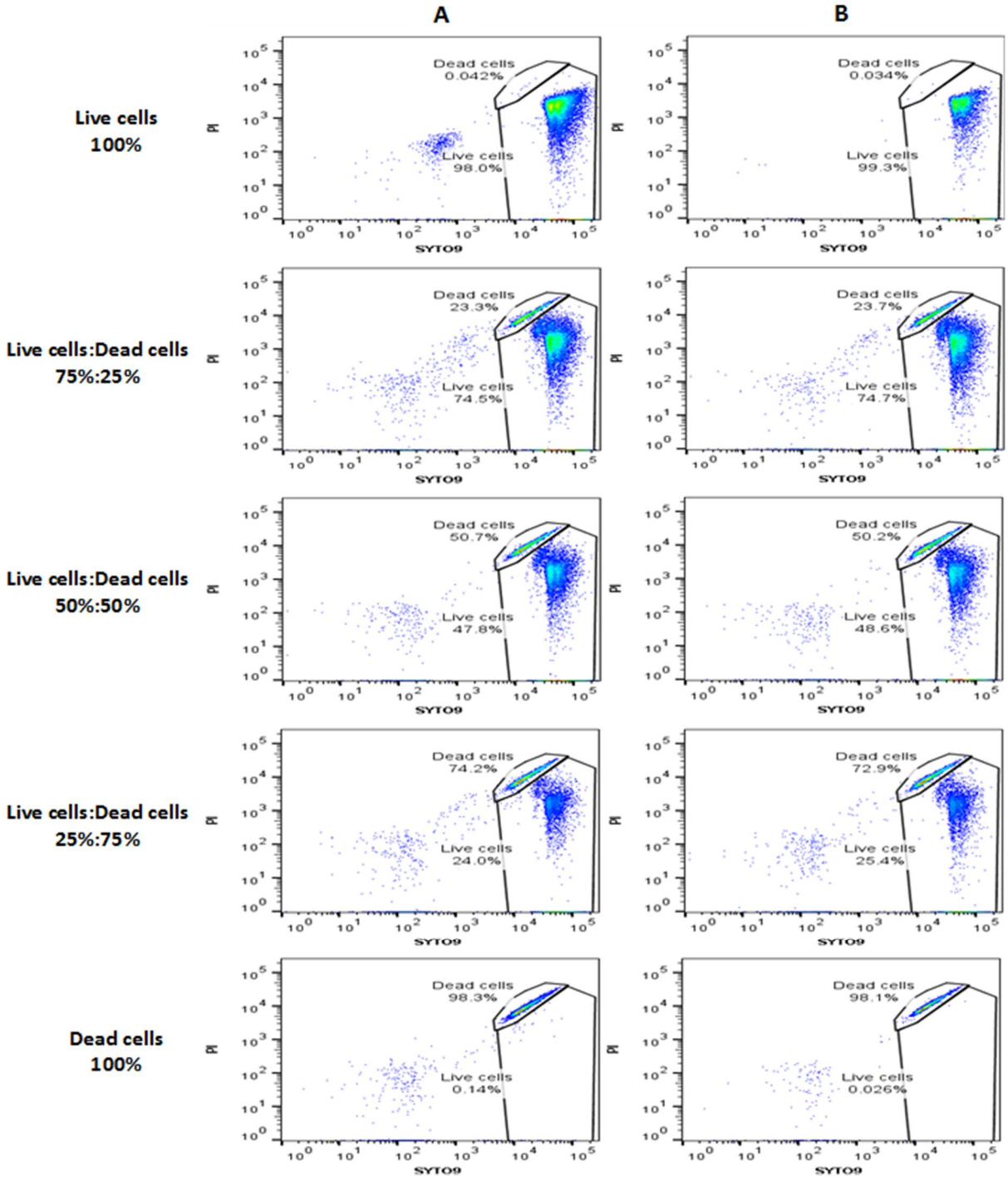

Fig 5.17. Enumeration of mixed samples. Dual-stained live and dead cells were accurately enumerated using reference beads in samples containing varying known ratios of live and dead bacteria, in duplicate. These results are representative of biological triplicates. Fixed bacteria were stained with 1.5 µl SYTO9 for 45 min, followed by staining with 1.5 µl PI for 15 min, treated with 1 mM EDTA. A and B represent samples in duplicate.

The input 100% live cell preparation was plated out in triplicate and the expected CFU value for the different ratios calculated based on this value. GraphPad Prism was used to perform a Pearson correlation which indicated a positive correlation between the bacteria/ml calculated from flow cytometry and the expected CFU/ml, r = 0.969, 2-tailed p value = 0.065, n = 5 (Fig 5.18).

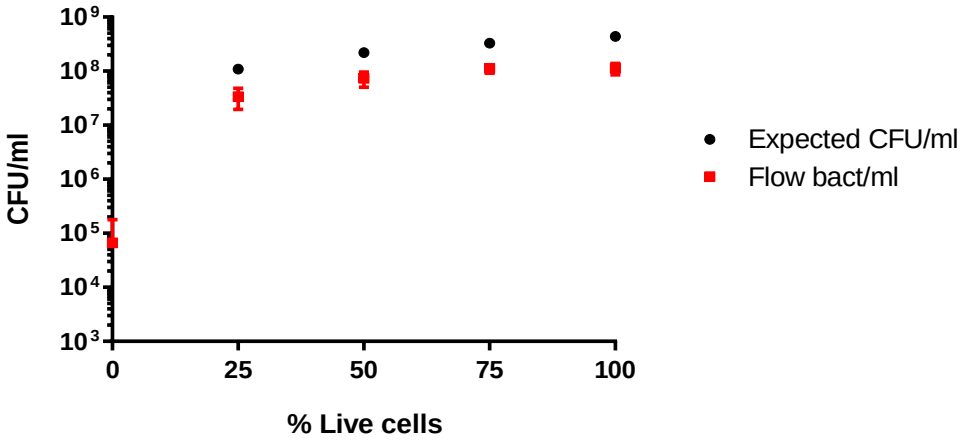

Fig 5.18. Correlation of cell counts for flow cytometry and plating. A positive correlation (r = 0.969) can be seen for viable bacteria/ml calculated from flow cytometry using reference beads versus the culturable CFU/ml from LB agar, however significant difference between these variables were seen (p=0.065). Results are representative of triplicates, with error bars indicating standard deviation.

5.3.4 TEM microscopy: Morphology of live and heat-killed cells

Live cells, live cells treated with 1 mM EDTA and heat-killed cells were sent for TEM analysis to determine the effect treatment has on the cell wall of *M. smegmatis* as this may influence the uptake and staining capabilities of SYTO9 and PI. These images were then sent in a blinded fashion to a microscopy expert (Dr. Ben Loos, Stellenbosch University) for analysis. Cell walls of live cells and live cells treated with 1 mM EDTA contained a well-defined membrane structure with a clear demarcated region between the membrane and the cytoplasm (Fig 5.19). Therefore, the addition of EDTA enhances uptake of SYTO9 without permeabilizing the cell membrane. Comparatively, the physiological abnormalities in heat-killed cells contributed to their undefined membrane structure and the non-equidistant region between the membrane and the cytoplasm appeared either enlarged or as a result of cytoplasm shrinkage.

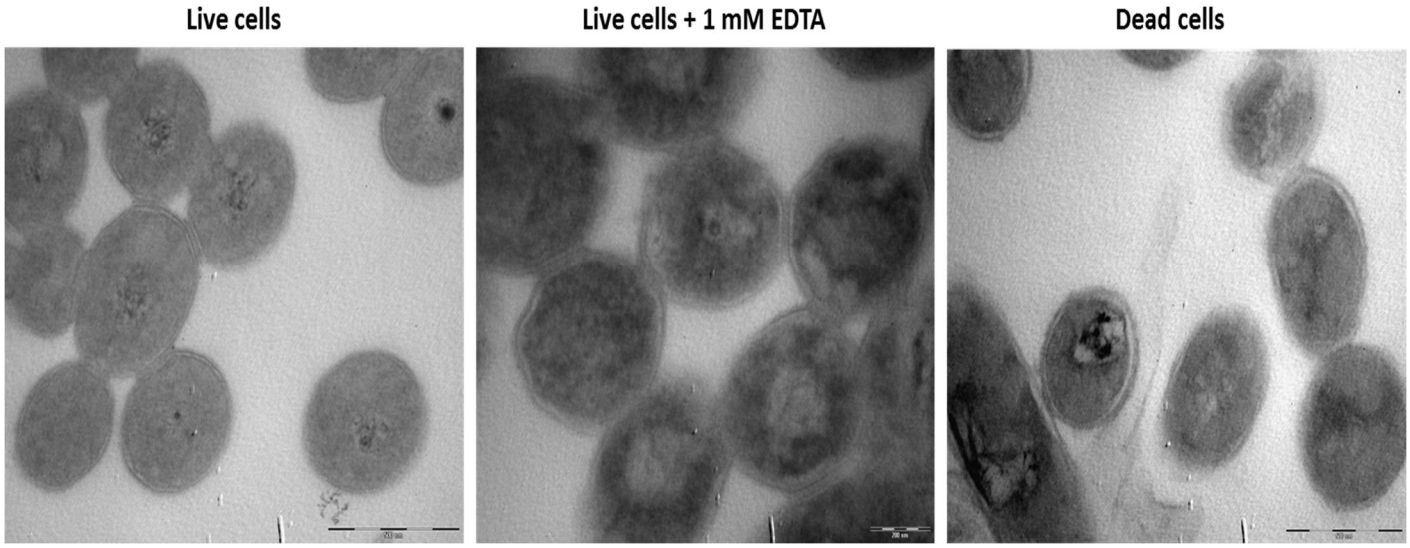

Fig 5.19. TEM images displaying morphology of live, live + 1 mM EDTA and heat-killed *M. smegmatis*.

5.3.5 Application of the optimized staining method in an attenuated strain of *Mycobacterium tuberculosis*

The optimized staining method was applied to *M. tuberculosis* to determine whether the optimized staining was applicable to *M. tuberculosis* (Fig 5.20). Positioning of the live and dead populations contrasted to results from *M. smegmatis,* indicating that organism-specific differences play a role in uptake or binding of the dyes. This contributed to the live and dead populations being less well defined in *M. tuberculosis.* Additionally, gating using an only live and only dead population was complicated by the relatively diffuse populations. Further optimization will be required to reliably distinguish between live and dead *M. tuberculosis,* however, these results suggest that this will be feasible.

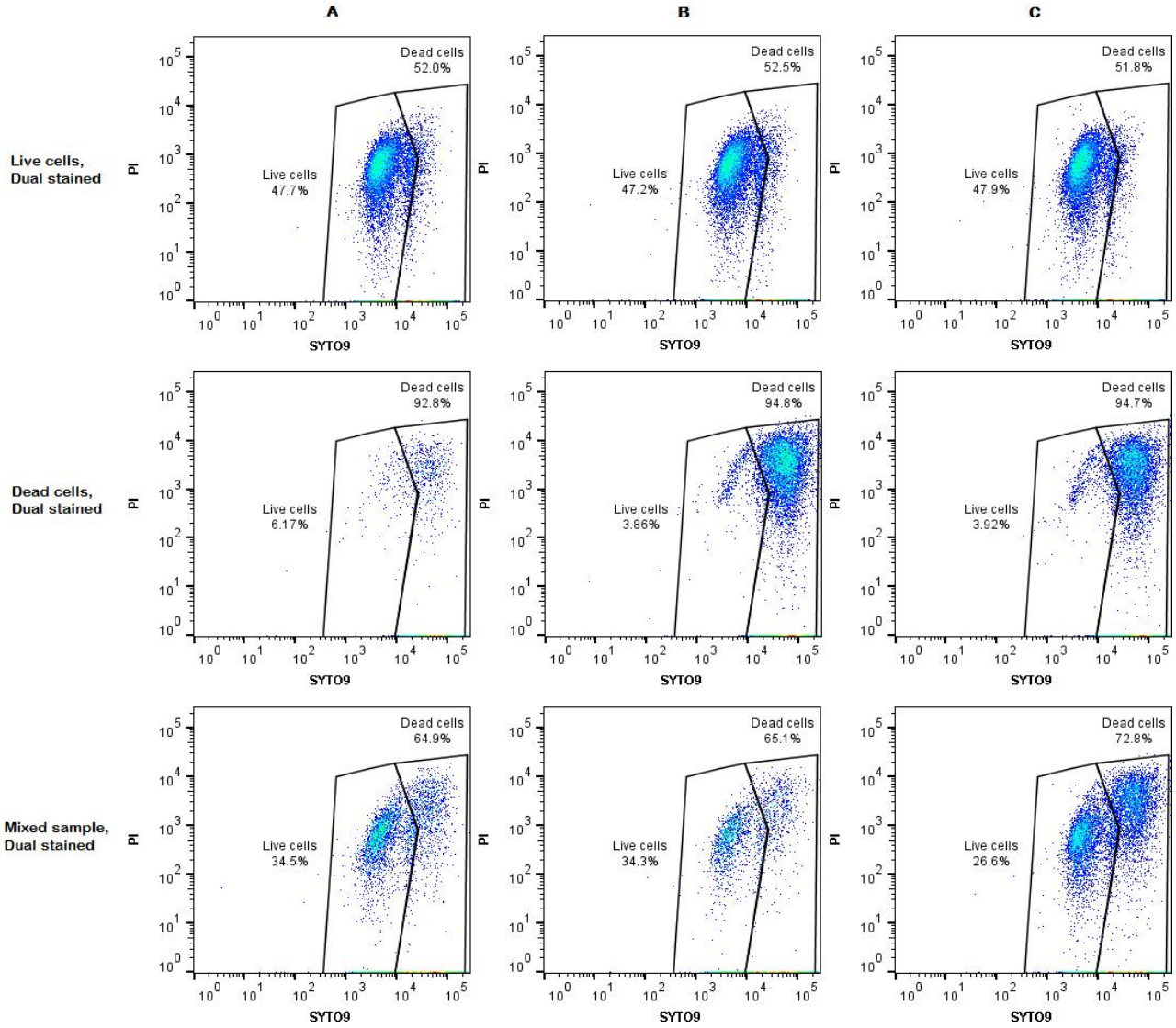

Fig 5.20. Applying the optimized staining method to *M. tuberculosis*. Organism specific differences in staining was displayed for *M. tuberculosis* and thus needs further optimization. Fixed bacteria were stained with 1.5 µl SYTO9 for 45 min, followed by staining with 1.5 µl PI for 15 min, treated with 1 mM EDTA. A, B and C represent samples in triplicate.

5.3.6 Validation of staining using *M. smegmatis* recovered from mock sputum

We next wished to recapitulate conditions expected to be encountered in a clinical setting. For example, samples to be analysed would frequently take the form of sputum. We therefore assessed the feasibility of recovering *M. smegmatis* from mock sputum, followed by staining with SYTO9 and PI, as this would be a valuable application for enumerating *M. tuberculosis* recovered from clinical samples.

Upon flow cytometric analysis of the stained samples recovered from sputum, we were able to distinguish live and dead bacterial populations. However, an unexpected intermediary population was identified in all NALC-treated samples recovered from mock sputum (Fig 5.21). This was not seen in

control samples not exposed to NALC or sputum. One possibility was that treatment with NALC contributes to cell injury, which would most likely result in a population intermediate to that of the live and dead population. We therefore examined *M. smegmatis* treated with NALC (in the absence of sputum) to determine whether this resulted in the same intermediary population. However, no intermediary population was observed in either live or dead *M. smegmatis* treated with NALC, suggesting that NALC treatment was not the cause of this intermediary population (Fig 5.22).

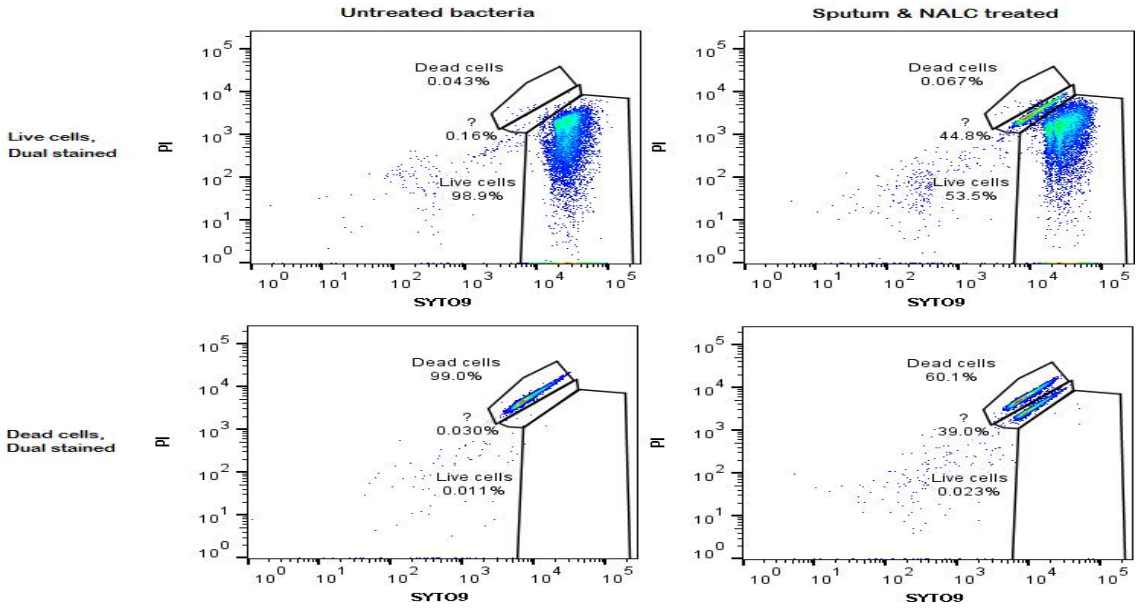

Fig 5.21. Applying the optimized staining to *M. smegmatis* recovered from mock sputum. *M. smegmatis* recovered from sputum and NALC treatment displayed an intermediary unknown population in comparison to the untreated samples (not exposed to NALC or sputum), representative of samples in triplicate. Fixed bacteria were stained with 1.5 µl SYTO9 for 45 min, followed by staining with 1.5 µl PI for 15 min, treated with 1 mM EDTA.

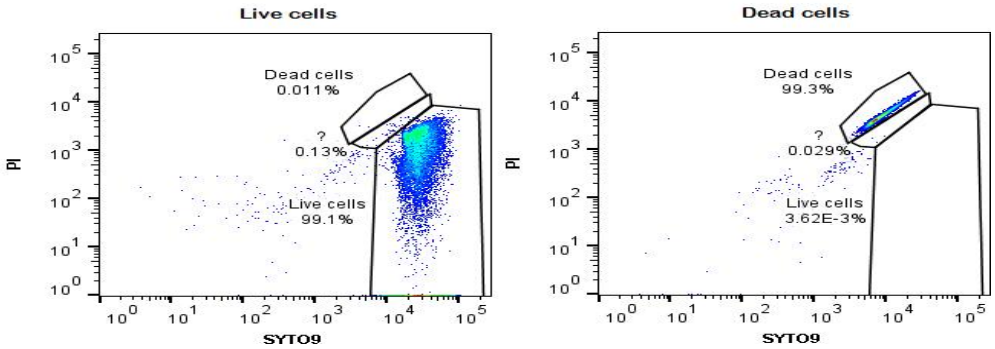

Fig 5.22. *M. smegmatis* treated with NALC resulted in no intermediary population. Fixed bacteria were stained with 1.5 µl SYTO9 for 45 min, followed by staining with 1.5 µl PI for 15 min, treated with 1 mM EDTA, representative of samples in triplicate

A second possibility was that the intermediary population was a contaminant in the sputum. Although plating of the autoclaved mock sputum displayed no bacterial growth (data not shown), this does not rule out the possibility of a contaminant. Since the live/dead stain is not specific for mycobacteria, any contaminant would also be detected. Staining mock sputum treated with NALC displayed the intermediary population (Fig 5.23). It was not possible to analyse untreated sputum, since this would be too viscous to allow flow cytometry. However, since the NALC-treated bacteria did not show any evidence of the intermediary population, we deduced that this was present in the mock sputum. The most likely source of contaminants would be from microorganisms in the egg as preparation of the mock sputum utilised autoclaved distilled water and was performed under sterile conditions.

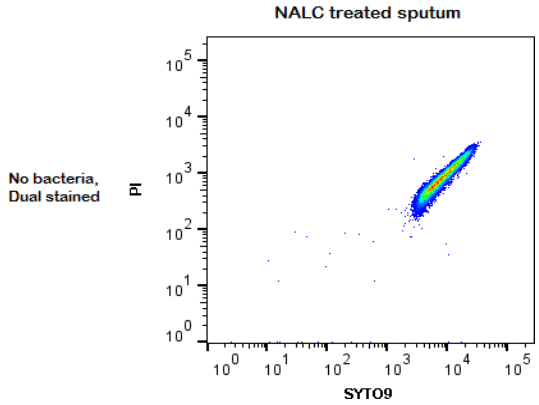

Fig 5.23. NALC treated sputum displayed the intermediary population. NALC treated sputum stained with 1.5 µl SYTO9 for 45 min, followed by staining with 1.5 µl PI for 15 min, treated with 1 mM EDTA displayed the intermediary population as a result from microorganisms in the egg.

In future work, we will test alternative mock sputum formulations. Nonetheless, we were still able to provide proof of concept that we could reliably differentiate live and dead *M. smegmatis* when recovered from mock sputum. To do this, we imposed an exclusion gate on the intermediate population (Fig 5.21), allowing clear distinction between the live and dead population when overlayed in FlowJo (Fig 5.24).

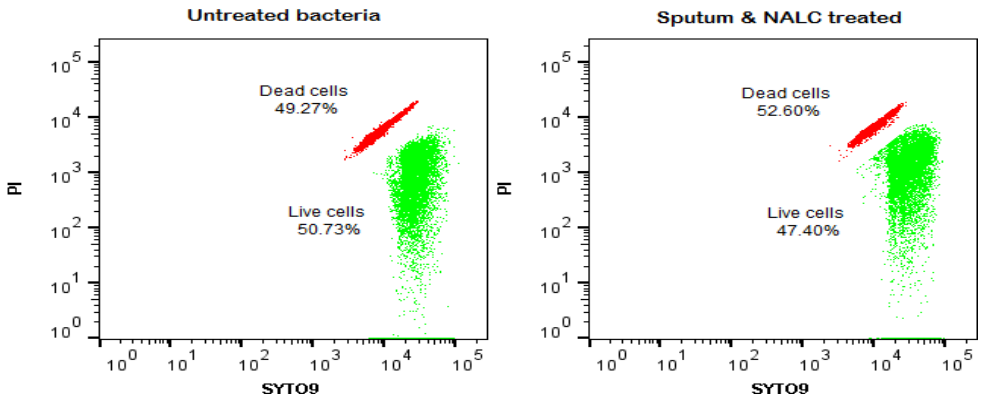

Fig 5.24. Live and dead *M. smegmatis* were differentiated following recovery from mock sputum. Exclusion of the intermediate population from *M. smegmatis* recovered from mock sputum displayed an accurate representation of live and dead cells, when overlayed, as compared to untreated bacteria.

5.4 DISCUSSION

5.4.1 Overview

Fluorescent staining in combination with flow cytometry offers a reliable method to investigate distinct functional properties of bacterial cells. The BacLight Bacterial Viability and Counting kit has proved to be an effective culture-free method for bacterial viability assessment and enumeration.

5.4.2 Killing methods

To optimize the staining protocol, a reliable method for generating consistent dead bacterial populations was required. The preparation of killed bacterial suspensions in other studies involved treatment with 70% alcohol (Stiefel *et al*., 2015), incubation in a boiling water bath for 32 min (Soejima *et al*., 2009), ultraviolet treatment (Maclean *et al*., 2009), and bleach (Mekonnen *et al*., 2015). Our attempt in using 70% absolute ethanol as a killing method resulted in cell lysis, which negatively affected bacterial numbers and increased the noise due to cell debris (Fig 5.4).

We next tested heat-killing. The complex cell structure of *M. smegmatis* is characterized by the length of the mycolic acids, reaching up to 90 carbon atoms (Liu *et al*., 1996), which contributes to the thickness of the mycobacterial cell wall. Thus higher temperatures are needed to increase the fluidity of the cell membrane by disrupting the arrangement of lipids, which impairs the cellular integrity. More specifically, high temperatures kill bacteria by denaturing the bacteria's proteins, causing them to be irreversibly altered and ineffective, but does not have an effect on the DNA integrity, as displayed by high quality whole genome sequencing data following heat-killing of *M. tuberculosis* for 50 min at 80°C (Brown *et al*., 2015). Therefore, it is likely that the binding capabilities of PI will not be affected. We initially treated *M. smegmatis* for 30 min at 95°C. This however was not sufficient to kill all bacteria, as detected by CFU plating and cells stained by SYTO9 (Fig 5.6).

Exposure to 95°C for a longer incubation time of 60 min indicated a loss of culturability and complete killing of *M. smegmatis,* as confirmed by CFU plating and flow cytometry (Fig 5.6). Morphological changes in the cell wall were observed by TEM analysis, with DNA contained either centrally or on the cell periphery as a result of disruption to the integrity of the cell membrane. (Fig 5.19).

5.4.3 PI and SYTO9 affinity

The exclusion of PI from live cells or cells with structurally intact cell membranes is due to the size and charge of the propidium molecule, whilst SYTO9 is able to penetrate cells with intact and disrupted cell membranes. The interaction between SYTO9 and PI was clearly seen in dual-stained samples, in comparison to PI-stained dead cells (Fig 5.7). A clear shift in the positioning of the dead cells was

observed in the presence of both dyes likely as a result of displacement of one dye by the other. The stronger binding affinity of PI for nucleic acids is supported by the association constant calculated by Stocks, who determined the binding affinity of SYTO9 at 1.8 x 10^5/M and PI at 3.7 x 10^5/M. The higher value for PI denotes stronger binding and thus leads to the displacement of SYTO9 by PI (Stocks, 2004).

Initially, grouping of the dead cell population overlapped the live cell population using an equal amount (1.5 µl) of SYTO9 and PI (as recommended by the manufacturer). Therefore, to improve the distinction between live and dead cells, different dye ratios were tested. Dual-stained mixed samples containing lower SYTO9 concentrations resulted in a complete overlap between the live and dead population (Fig 5.12). This could be due to SYTO9 binding to the dead cells as it is able to cross the comprised cell membrane with more ease.

Increasing the SYTO9 concentration to compensate for its displacement by PI, demonstrated an improvement in the distinction between live and dead populations. The higher SYTO9 concentrations appeared to downwardly shift the dead cell population in dual-stained dead samples when compared to the lower SYTO9 concentration. This shift was more prominent in samples with lower PI concentrations (0.5 µl) and could be attributed to the binding affinity of PI (Fig 5.12). The lowest SYTO9:PI amounts yielding the best separation between live and dead bacteria was 3:1.5 µl.

5.4.4 Influence of mycobacterial cell wall properties on uptake of dyes

The lack of the outer membrane in Gram-positive bacteria allows SYTO9 to enter the cells more easily than for gram negative bacteria (with outer and cytoplasmic membrane). However, *M. smegmatis* has a relatively thick cell wall, thus to allow optimal entry of SYTO9 into the cell, incubation of SYTO9 for 45 min was performed prior to incubation of PI for 15 min (Fig 5.8). Similarly, the Gram negative bacteria, *Salmonella*, has been shown to create an outer membrane barrier to SYTO9 in stationary phase (Berney *et al*., 2007).

The cell wall of *M. tuberculosis* may reach a thickness of 20 nm, which is almost twice as thick as that of *M. smegmatis.* Additionally, the low permeability of the mycobacterial cell wall aids in its resistance to many hydrophilic antibiotics and lipophilic solutes (Niederweis, 2003).

The mycobacterial outer membrane is assumed to contain two diffusion pathways; the lipid and the porin pathway. The former involves the interaction of the membrane lipids by dissolving hydrophobic solutes in the lipid bilayer, and the latter includes the diffusion of small hydrophilic solutes across water-filled channel proteins, spanning across the outer membrane (Mailaender *et al*., 2004). This property could also account for the staining affinity observed in our *M. tuberculosis* results. These

results clearly indicated the varying diffusion patterns of SYTO9 and PI for the 2 species, as the live and dead gating strategy used for *M. smegmatis* did not overlap with *M. tuberculosis* (Fig 5.20). There was considerable overlap between the live and dead *M. tuberculosis* population, thus further optimization would be needed. This is clearly an indication that the cell wall and membrane responsible for stability and protection from external stimuli influences the uptake of certain fluorescent dyes differently in different bacterial species. While active transport could influence uptake and intracellular concentration of dyes, such as ion permeable porin channels in *M. smegmatis* (Mailaender *et al.*, 2004), our protocol involves fixing cells before staining, therefore this is not applicable.

SYTO9 and PI are regarded as non-fixable dyes, however in our study bacteria were fixed, followed by staining; this did not affect fluorescence. Therefore following fixation *M. tuberculosis* can be removed from the bio-safety level 3 laboratory and staining may be implemented. This will allow staining to be achieved in flow cytometry facilities where high containment is not available.

Uptake of certain fluorescent dyes can be affected by the structure of the bacterial cell wall and the addition of the chelator ethylenediaminetetraacetate (EDTA) has shown to enhance its uptake into the cell (Jernaes and Steen, 1994; Sträuber and Müller, 2010). The addition of 5mM EDTA mimics the first step in membrane damage as it has shown to destabilize the outer membrane of the Gram-negative bacteria, *Escherichia coli* and *Salmonella typhimurium* (Berney *et al*., 2007). This process occurs through the chelation of divalent cations, which usually tightly cross-links the lipopolysaccharide layer on the outer membrane. Subsequently, this results in the release of a proportion of lipopolysaccharides, which disorganizes the outer membrane (Sträuber and Müller, 2010). In the Gram-positive bacteria *Enterococcus faecalis*, the destabilized outer membrane was shown to assist SYTO9 in entering cells more easily (Berney *et al*., 2007), although no known studies in *M. tuberculosis* have reported this.

In our study, 1mM EDTA was used to prevent complete permeabilization to the cell wall. TEM images indicated no morphological variations between live cells and live cells treated with EDTA, these cells displayed homogenous cytoplasm containing DNA central to the cell, which can be seen as electron dense material (Fig 5.19). Therefore, treatment with 1 mM EDTA improved the tighter grouping for SYTO9-stained live cells, resulting in a clearer distinction between live and dead cells in mixed samples (Fig 5.11), without permeabilizing the cell membrane of *M. smegmatis*.

Studies have reported that the structure and composition of the cell membrane following formaldehyde fixation affects the light scattering abilities of the cell, as this is impacted by the size, shape and refractive indices of the cell envelope (Giorgio *et al*., 1996). Additionally, a change in the

permeability of the cell membrane to the dye may also occur. Arguably, this only occurs if remaining in the fixative for lengthy time periods, such as longer than 30 min for *M. smegmatis* and *M. tuberculosis*. Using 4% formaldehyde fixation for *M. smegmatis* has shown to completely preserve the cell surface structure without having an effect on the cell morphology, whilst greater formaldehyde concentrations is known to cause cell shrinkage (Ren *et al.*, 2013).

5.4.5 Applying the BacLight kit for enumeration of *M. smegmatis*

Rapid counting could support both basic research and clinical applications. The ability to count live and dead *M. tuberculosis* in a culture-free manner will allow rapid and accurate assessment of the bacterial load in a sputum sample. This will allow the necessary action to be taken for administering antituberculosis drugs based on a patient specific level. This is essential due to the high emergence of drug resistant strains both locally and worldwide, based on reports by the World Health Organization (World Health Organization, 2015).

Using the optimized staining in *M. smegmatis* has allowed accurate detection of varying known ratios of live and dead bacteria (Fig 5.17), thus applying reference beads to these samples has proven a useful and rapid method for enumeration of live and dead *M. smegmatis*. These values have shown correlation to CFU results (Fig 5.18) and is thus a promising method for detection and distinguishing between live and dead *M. tuberculosis* and the once optimized, will fulfil the same applications in *M. tuberculosis.*

Following sample preparation, analysing and enumerating a *M. tuberculosis* sample could be attained within an hour. In contrast, culturing of *M. tuberculosis* by plating would take 3 weeks, followed by the time needed to manually count and calculate the CFU/ml. Additionally, samples were retained for 24h to give an indication on the feasibility of preparing and analysing samples the following day (Fig 5.13). As previously mentioned, SYTO9 slowly penetrates the cell wall, therefore the intracellular SYTO9 concentration could increase over 24h, resulting in the upwards shift of the live population. Similarly, this shift was noticed in *E. coli* containing an increased concentration of SYTO9, and occurred irrespective of staining with PI (Berney *et al.*, 2007). This corresponded to the shift occurring in our SYTO9-stained live control only and not in the PI-stained dead control (Fig 5.14). Therefore, samples cannot be retained following staining, but could be further investigated. Processed and fixed clinical samples can be stored and remain stable at 4°C for 2 weeks, followed by staining prior to analysis.

5.4.6 Applying the BacLight kit to *M. smegmatis* recovered from mock sputum

Using the optimized staining in a clinically relevant manner to providing an accurate culture-free estimation of the bacterial load directly from a patient's sputum sample will be highly beneficial.

Therefore, we tested the feasibility of applying the kit to perform characterise and enumerate bacteria recovered from mock sputum treated with the mucolytic agent, NALC.

An intermediary population, clearly distinct from the live and dead population was seen when analysing bacteria recovered from mock sputum (Fig 5.21). This was initially thought to be an injured population due to NALC treatment. However, staining the NALC-treated mock sputum with SYTO9 and PI displayed the additional population (Fig 5.23), which was not present when bacteria were treated with NALC (in the absence of mock sputum). This suggested that this population was most likely due to microorganisms in the egg. Plating of the autoclaved mock sputum displayed no growth, therefore the additional population killed by autoclaving was still stained by SYTO9 and PI.

It has been suggested that the chicken egg contains diverse microflora, as well as the pathogenic bacteria, *Salmonella* due to the porous nature of the egg shell (Stepień-Pyśniak, 2010). It is highly likely that a healthy person's sputum would resemble what is seen by mock sputum due to the broad range of natural microflora in the human oral cavity (Aas *et al.*, 2005). Currently no known studies have analysed the microflora in a healthy person's sputum using flow cytometry. Therefore in conjunction with staining with SYTO9 and PI, a *M. tuberculosis* specific antibody could be used to specifically select for *M. tuberculosis* following recovery from sputum.

NALC-sodium hydroxide (NALC-NaOH) is the accepted gold standard method for decontamination as it takes into account the high resistance of *M. tuberculosis* to acids and antibacterial agents by killing the contaminating natural flora or a variety of microorganisms likely to rapidly overgrow *M. tuberculosis.* This is essential for the isolation of *M. tuberculosis* as samples containing different types of bacteria will be more distributed in a FSC versus SSC plot, often seen in environmental samples. However, the addition of 1% NaOH has been shown to affect the viability of *M. tuberculosis* by reducing the amount of positive cultures by 10% (Burdz *et al.*, 2003; Peres *et al*., 2009), and was thus not incorporated into our study. Additionally, the bacterial numbers would be more greatly affected by NaOH in paucibacillary sputum samples than samples carrying a higher bacillary load (Peres *et al*., 2009), which will influence the accuracy in enumerating the total amount of live and dead bacteria in our samples.

5.4.7 Assessing the effect of antibiotics (INH/RIF) on *M. smegmatis* using the BacLight kit

Two out of the four first-line TB antibiotics, isoniazid (INH), and rifampicin (RIF) were used as an alternative killing method to assess the application of the kit. Both antibiotics target *M. tuberculosis* using a different mechanism of action; INH inhibits the synthesis of mycolic acids required for the

mycobacterial cell wall (Banerjee *et al*., 1994), and RIF inhibits RNA synthesis (Telenti *et al*., 1993). The MICs of INH and RIF were determined prior to testing of the kit (Results not shown). However, due to contamination we were unable to test staining of *M. smegmatis* killed via different mechanisms at this point.

5.4.8 Heterogeneity in the live population

A considerable amount of heterogeneity was observed in the live cell population by its more dispersed distribution (Fig 5.12). In our study, cells from stationary phase cultures were used and the distribution pattern seen in our results ranges from weak to strong green intensity for live cells. It would thus be interesting to stain cultures from different growth stages as the staining pattern from our live cells indicates that diffusion of SYTO9 across the cell wall and the different intracellular concentrations of SYTO9 and PI could be dependent on the physiological state of the cell. It has also been shown that cells containing an intact cell membrane display broader range in diffusion of SYTO9 in comparison to cells lacking an outer membrane (Berney *et al*., 2007). Previously, *E. coli* stained with both SYBR green and PI exhibited a higher intensity of green fluorescence in exponential phase than in stationary phase (Barbesti *et al*., 2000). Exponentially growing cells have shown to also possess higher RNA content as a result of increased metabolic activity (Bremer and Dennis, 2008), which could lead to increased green fluorescence intensity. In agreement, it was determined that faster growing *M. tuberculosis* displayed a 2-fold increase in the mean fluorescence intensity than slower growers (Hendon-Dunn *et al*., 2016). During stationary phase or slow growth of bacteria, cell wall alterations occur due to the scarcity of nutrients (Signoretto *et al*., 2002). In addition, *M. tuberculosis* experiencing hypoxic conditions *in vitro* and *in vivo* have shown to alter their metabolism by thickening their cell wall and expressing different cell surface proteins, contributing to differential staining. In stationary phase *M. tuberculosis* differential staining was noticed, but to a lesser degree than the hypoxic bacteria (Ryan *et al*., 2010).

5.4.9 Limitations

Defining viability remains complex as injured cells have a similar cell wall integrity as live cells, and thus cannot be distinguished from live cells using SYTO9. It was assumed that all membrane-compromised cells were dead, and cells containing an intact cell membrane as live. Distinction between injured cells can be made by addition of ethidium monoazide and ultraviolet light, as previously tested (Soejima *et al*., 2009). It is unknown whether injured cells would be able to form colonies on agar plates or repair and replicate. This could contribute to the overestimation of the amount of live cells in a population.

Stationary phase bacteria was used in our study, this may not reflect bacteria from clinical samples, which could influence staining. Additionally, dye:bacteria ratios may need to be tested to reflect actual numbers of bacteria in clinical samples. Only one killing method was used, this may differ from dead bacteria in clinical samples. The mock sputum used may not adequately replicate clinical samples as bacteria may behave differently in actual sputum.

The optimized staining method was also directly applied to *M. tuberculosis,* however a longer incubation time for SYTO9 could be required for *M. tuberculosis* as it possesses a thicker cell wall than *M. smegmatis.* SYTO9 may not have properly been taken up and this could have affected the results.

5.4.10 Further work

- Recovering *M. smegmatis* from sputum can be optimized in an alternative mock sputum protocol, prepared using bisacrylamide and acrylamide (Yamada *et al*., 2011) and upon ethics approval, using sputum from healthy participants.
- Staining with INH and RIF will be used as alternative killing methods.
- Testing of potentially novel compounds to determine the level of killing induced.
- Optimize staining in *M. tuberculosis.*
- Induce different types of cell injury to determine positioning on a SYTO9 vs. PI plot.
- Staining with SYTO9 and PI could be combined with additional dyes for labelling of distinct functional properties and to identify and understand the various physiological states of the cell.

5.5 CONCLUSION

The laborious and time-consuming procedures of traditional counting techniques emphasize the benefit of using flow cytometry for analysing mycobacterial viability in a heterogeneous population. This study has proven to yield reproducible results by providing a powerful tool for its rapid analysis in discriminating between live and dead cells, high sensitivity and its incorporation to a diverse range of applications. Additionally, this is the first time this method has successfully been applied for the enumeration of mycobacteria.

This approach supersedes the tedious nature of manual counting by providing rapid acquisition than CFU plating. Accurate determination and enumeration of live and dead bacteria offers valuable applications in terms of tuberculosis diagnostics by providing rapid high-throughput screening to determine the bacterial load in clinical samples, to determine bactericidal vs. bacteriostatic effects of novel antituberculosis agents, and to determine susceptibility to antituberculosis drugs prior to prescribing treatment or following completion of the standardized treatment regimen to provide early indication of drug-resistant strains.

Chapter 6:

GENERAL CONCLUSION

Flow cytometry has proven to be a powerful tool for its rapid analysis, high sensitivity and its incorporation to a diverse range of applications. A single-cell approach will be promising for exploring mechanisms underlying population-wide adaptation of *M. tuberculosis* in response to the host environment, to environmental stress, and to anti-tuberculosis drugs.

Adaptation to these conditions promotes diverse physiological changes in mycobacteria, contributing to population heterogeneity, which induces a subpopulation of VBNC bacteria and persisters. These subpopulations are undetectable on traditional CFU plating methods. The underrepresentation of the varying physiological states of mycobacteria poses a threat in the clinical setting as avirulent bacteria in the dormant state regain virulence after resuscitation under suitable conditions. Therefore, detection and isolation of these populations will provide an understanding to develop effective interventions.

Our optimized staining with SYTO9 and PI has yielded reproducible results in discriminating between live and dead cells using flow cytometry, and this method has successfully been applied for the enumeration of mycobacteria for the first time. Therefore this provides a culture-free manner to allow rapid and accurate assessment of *M. smegmatis.* Upon implementation to *M. tuberculosis,* clinical samples could be analysed and enumerated within an hour. In contrast, culturing of *M. tuberculosis* is hindered by the lengthy time needed to form visible colonies (3-4 weeks), followed by the time needed to manually count and calculate the CFU/ml. Additionally, CFU methods do not reveal the sensitivity or resistance to drug exposure, and this may result in the misconception of drug inhibition, tolerance and cell death (Hendon-Dunn *et al*., 2016).

In order to incorporate this technique as a replacement for CFU plating to improve the current routine tuberculosis tests in the clinical setting, flow cytometry can be exploited in combination with various fluorescent dyes to develop immune-based tests that offer greater specificity in detecting and targeting the various physiological states of *M. tuberculosis*, as recently described (Hendon-Dunn *et al*., 2016).

The fluorescence dilution technique adapted and optimised in mycobacteria (Mouton *et al.*, 2016), in combination with flow cytometry successfully revealed differentially replicating *M. smegmatis* in

macrophage infection models, which surprisingly revealed a replicating *M. smegmatis* population. Contrasting viewpoints have been reported on the intracellular survival of *M. smegmatis* (Johansson *et al*., 2015; Kuehnel *et al.*, 2001; Prakash *et al.*, 2010), therefore it will be valuable to understand the behaviour and adaptation of the replicating *M. smegmatis* and whether these results can be reliably extrapolated to *M. tuberculosis.* Flow cytometry offers the advantage that with correct controls, various gates could be applied to detect and select for bacteria within various physiological states. These populations can further be sorted for further characterization. These findings could assist in understanding whether *M. tuberculosis* undergoes an adaptive mechanism that allows it to persist in the host by evading host immune responses or whether this state is a result of damage inflicted by the macrophage.

REFERENCES

1. Aas, J.A., Paster, B.J., Stokes, L.N., Olsen, I., Dewhirst, F.E., 2005. Defining the Normal Bacterial Flora of the Oral Cavity. J. Clin. Microbiol. 43, 5721–5732. doi:10.1128/JCM.43.11.5721-5732.2005
2. Adams, K.N., Takaki, K., Connolly, L.E., Wiedenhoft, H., Winglee, K., Humbert, O., Edelstein, P.H., Cosma, C.L., Ramakrishnan, L., 2011. Drug Tolerance in Replicating Mycobacteria Mediated by a Macrophage-Induced Efflux Mechanism. Cell 145, 39–53. doi:10.1016/j.cell.2011.02.022
3. Aguilo, J.I., Alonso, H., Uranga, S., Marinova, D., Arbués, A., de Martino, A., Anel, A., Monzon, M., Badiola, J., Pardo, J., Brosch, R., Martin, C., 2013. ESX-1-induced apoptosis is involved in cell-to-cell spread of Mycobacterium tuberculosis. Cell. Microbiol. 15, 1994–2005. doi:10.1111/cmi.12169
4. Ambriz-Aviña, A, V., Contreras-Garduño, Jorge A., Pedraza-Reyes, M., 2014. Applications of Flow Cytometry to Characterize Bacterial Physiological Responses. BioMed Res. Int. 2014, e461941. doi:10.1155/2014/461941
5. Andries, K., Verhasselt, P., Guillemont, J., Göhlmann, H.W.H., Neefs, J.-M., Winkler, H., Van Gestel, J., Timmerman, P., Zhu, M., Lee, E., Williams, P., de Chaffoy, D., Huitric, E., Hoffner, S., Cambau, E., Truffot-Pernot, C., Lounis, N., Jarlier, V., 2005. A diarylquinoline drug active on the ATP synthase of Mycobacterium tuberculosis. Science 307, 223–227. doi:10.1126/science.1106753
6. Anes, E., Peyron, P., Staali, L., Jordao, L., Gutierrez, M.G., Kress, H., Hagedorn, M., Maridonneau-Parini, I., Skinner, M.A., Wildeman, A.G., Kalamidas, S.A., Kuehnel, M., Griffiths, G., 2006. Dynamic life and death interactions between Mycobacterium smegmatis and J774 macrophages. Cell. Microbiol. 8, 939–960. doi:10.1111/j.1462-5822.2005.00675.x
7. Anuchin, A.M., Mulyukin, A.L., Suzina, N.E., Duda, V.I., El-Registan, G.I., Kaprelyants, A.S., 2009. Dormant forms of Mycobacterium smegmatis with distinct morphology. Microbiology 155, 1071–1079. doi:10.1099/mic.0.023028-0
8. Balaban, N.Q., Gerdes, K., Lewis, K., McKinney, J.D., 2013. A problem of persistence: still more questions than answers? Nat. Rev. Microbiol. 11, 587–591.
9. Banerjee, A., Dubnau, E., Quemard, A., Balasubramanian, V., Um, K.S., Wilson, T., Collins, D., de Lisle, G., Jacobs, W.R., 1994. inhA, a gene encoding a target for isoniazid and ethionamide in Mycobacterium tuberculosis. Science 263, 227–230.
10. Barbesti, S., Citterio, S., Labra, M., Baroni, M.D., Neri, M.G., Sgorbati, S., 2000. Two and three-color fluorescence flow cytometric analysis of immunoidentified viable bacteria. Cytometry 40, 214–218. doi:10.1002/1097-0320(20000701)40:3<214::AID-CYTO6>3.0.CO;2-M
11. Barry, C.E., Boshoff, H., Dartois, V., Dick, T., Ehrt, S., Flynn, J., Schnappinger, D., Wilkinson, R.J., Young, D., 2009. The spectrum of latent tuberculosis: rethinking the goals of prophylaxis. Nat. Rev. Microbiol. 7, 845–855. doi:10.1038/nrmicro2236
12. Berens, C., Suess, B., 2015. Riboswitch engineering — making the all-important second and third steps. Curr. Opin. Biotechnol., Analytical Biotechnology 31, 10–15. doi:10.1016/j.copbio.2014.07.014
13. Berney, M., Hammes, F., Bosshard, F., Weilenmann, H.-U., Egli, T., 2007. Assessment and interpretation of bacterial viability by using the LIVE/DEAD BacLight Kit in combination with flow cytometry. Appl. Environ. Microbiol. 73, 3283–3290. doi:10.1128/AEM.02750-06
14. Berney, M., Weilenmann, H.-U., Egli, T., 2006. Flow-cytometric study of vital cellular functions in Escherichia coli during solar disinfection (SODIS). Microbiol. Read. Engl. 152, 1719–1729. doi:10.1099/mic.0.28617-0
15. Boehme, C.C., Nabeta, P., Hillemann, D., Nicol, M.P., Shenai, S., Krapp, F., Allen, J., Tahirli, R., Blakemore, R., Rustomjee, R., Milovic, A., Jones, M., O'Brien, S.M., Persing, D.H., Ruesch-Gerdes, S., Gotuzzo, E., Rodrigues, C., Alland, D., Perkins, M.D., 2010. Rapid Molecular Detection of

Tuberculosis and Rifampin Resistance. N. Engl. J. Med. 363, 1005–1015. doi:10.1056/NEJMoa0907847
16. Boldrin, F., Casonato, S., Dainese, E., Sala, C., Dhar, N., Palù, G., Riccardi, G., Cole, S.T., Manganelli, R., 2010. Development of a repressible mycobacterial promoter system based on two transcriptional repressors. Nucleic Acids Res. 38, e134. doi:10.1093/nar/gkq235
17. Bonecini-Almeida, M.G., 2000. Flow cytometry as a tool to identify Mycobacterium tuberculosis interaction with the immune system and drug susceptibility. Mem. Inst. Oswaldo Cruz 95, 491–494.
18. Braga, P.C., Bovio, C., Culici, M., Dal Sasso, M., 2003. Flow cytometric assessment of susceptibilities of Streptococcus pyogenes to erythromycin and rokitamycin. Antimicrob. Agents Chemother. 47, 408–412.
19. Brauner, A., Fridman, O., Gefen, O., Balaban, N.Q., 2016. Distinguishing between resistance, tolerance and persistence to antibiotic treatment. Nat. Rev. Microbiol. 14, 320–330. doi:10.1038/nrmicro.2016.34
20. Breeuwer, P., Abee, T., 2000. Assessment of viability of microorganisms employing fluorescence techniques. Int. J. Food Microbiol. 55, 193–200. doi:10.1016/S0168-1605(00)00163-X
21. Bremer, H., Dennis, P.P., 2008. Modulation of Chemical Composition and Other Parameters of the Cell at Different Exponential Growth Rates. EcoSal Plus 3. doi:10.1128/ecosal.5.2.3
22. Brown, A.C., Bryant, J.M., Einer-Jensen, K., Holdstock, J., Houniet, D.T., Chan, J.Z.M., Depledge, D.P., Nikolayevskyy, V., Broda, A., Stone, M.J., Christiansen, M.T., Williams, R., McAndrew, M.B., Tutill, H., Brown, J., Melzer, M., Rosmarin, C., McHugh, T.D., Shorten, R.J., Drobniewski, F., Speight, G., Breuer, J., 2015. Rapid Whole-Genome Sequencing of Mycobacterium tuberculosis Isolates Directly from Clinical Samples. J. Clin. Microbiol. 53, 2230–2237. doi:10.1128/JCM.00486-15
23. Bunthof, C.J., van Schalkwijk, S., Meijer, W., Abee, T., Hugenholtz, J., 2001. Fluorescent method for monitoring cheese starter permeabilization and lysis. Appl. Environ. Microbiol. 67, 4264–4271.
24. Burdz, T.V.N., Wolfe, J., Kabani, A., 2003. Evaluation of sputum decontamination methods for Mycobacterium tuberculosis using viable colony counts and flow cytometry. Diagn. Microbiol. Infect. Dis. 47, 503–509. doi:10.1016/S0732-8893(03)00138-X
25. Carroll, P., Schreuder, L.J., Muwanguzi-Karugaba, J., Wiles, S., Robertson, B.D., Ripoll, J., Ward, T.H., Bancroft, G.J., Schaible, U.E., Parish, T., 2010. Sensitive Detection of Gene Expression in Mycobacteria under Replicating and Non-Replicating Conditions Using Optimized Far-Red Reporters. PLoS ONE 5, e9823. doi:10.1371/journal.pone.0009823
26. Chao, M.C., Rubin, E.J., 2010. Letting sleeping dos lie: does dormancy play a role in tuberculosis? Annu. Rev. Microbiol. 64, 293–311. doi:10.1146/annurev.micro.112408.134043
27. Claudi, B., Spröte, P., Chirkova, A., Personnic, N., Zankl, J., Schürmann, N., Schmidt, A., Bumann, D., 2014. Phenotypic variation of Salmonella in host tissues delays eradication by antimicrobial chemotherapy. Cell 158, 722–733. doi:10.1016/j.cell.2014.06.045
28. Clemens, D.L., Horwitz, M.A., 1995. Characterization of the Mycobacterium tuberculosis phagosome and evidence that phagosomal maturation is inhibited. J. Exp. Med. 181, 257–270.
29. Comas, J., Vives-Rego, J., 1998. Enumeration, viability and heterogeneity in Staphylococcus aureus cultures by flow cytometry. J. Microbiol. Methods 32, 45–53. doi:10.1016/S0167-7012(98)00003-7
30. Daniel, T.M., Janicki, B.W., 1978. Mycobacterial antigens: a review of their isolation, chemistry, and immunological properties. Microbiol. Rev. 42, 84–113.
31. Dartois, V., 2014. The path of anti-tuberculosis drugs: from blood to lesions to mycobacterial cells. Nat. Rev. Microbiol. 12, 159–167. doi:10.1038/nrmicro3200
32. Davey, H.M., Kell, D.B., 1996. Flow cytometry and cell sorting of heterogeneous microbial populations: the importance of single-cell analyses. Microbiol. Rev. 60, 641–696.

33. Davidow, A., Kanaujia, G.V., Shi, L., Kaviar, J., Guo, X., Sung, N., Kaplan, G., Menzies, D., Gennaro, M.L., 2005. Antibody Profiles Characteristic of Mycobacterium tuberculosis Infection State. Infect. Immun. 73, 6846–6851. doi:10.1128/IAI.73.10.6846-6851.2005
34. de Smit, M.H., van Duin, J., 1990. Secondary structure of the ribosome binding site determines translational efficiency: a quantitative analysis. Proc. Natl. Acad. Sci. U. S. A. 87, 7668–7672.
35. Desai, S.K., Gallivan, J.P., 2004. Genetic Screens and Selections for Small Molecules Based on a Synthetic Riboswitch That Activates Protein Translation. J. Am. Chem. Soc. 126, 13247–13254. doi:10.1021/ja048634j
36. Du, M., Chen, J., Zhang, X., Li, A., Li, Y., Wang, Y., 2007. Retention of Virulence in a Viable but Nonculturable Edwardsiella tarda Isolate. Appl. Environ. Microbiol. 73, 1349–1354. doi:10.1128/AEM.02243-06
37. Elliott, T.O.J.P., Owolabi, O., Donkor, S., Kampmann, B., Hill, P.C., Ottenhoff, T.H.M., Haks, M.C., Kaufmann, S.H.E., Maertzdorf, J., Sutherland, J.S., 2015. Dysregulation of apoptosis is a risk factor for TB disease progression. J. Infect. Dis. jiv238. doi:10.1093/infdis/jiv238
38. Fowler, C.C., Brown, E.D., Li, Y., 2008. A FACS-based approach to engineering artificial riboswitches. Chembiochem Eur. J. Chem. Biol. 9, 1906–1911. doi:10.1002/cbic.200700713
39. Freud, A.G., Becknell, B., Roychowdhury, S., Mao, H.C., Ferketich, A.K., Nuovo, G.J., Hughes, T.L., Marburger, T.B., Sung, J., Baiocchi, R.A., Guimond, M., Caligiuri, M.A., 2005. A Human CD34(+) Subset Resides in Lymph Nodes and Differentiates into CD56brightNatural Killer Cells. Immunity 22, 295–304. doi:10.1016/j.immuni.2005.01.013
40. Garst, A.D., Edwards, A.L., Batey, R.T., 2011. Riboswitches: Structures and Mechanisms. Cold Spring Harb. Perspect. Biol. 3. doi:10.1101/cshperspect.a003533
41. Gefen, O., Gabay, C., Mumcuoglu, M., Engel, G., Balaban, N.Q., 2008. Single-cell protein induction dynamics reveals a period of vulnerability to antibiotics in persister bacteria. Proc. Natl. Acad. Sci. U. S. A. 105, 6145–6149. doi:10.1073/pnas.0711712105
42. Gillespie, S.H., 2002. Evolution of Drug Resistance in Mycobacterium tuberculosis: Clinical and Molecular Perspective. Antimicrob. Agents Chemother. 46, 267–274. doi:10.1128/AAC.46.2.267-274.2002
43. Giorgio, P.A. del, Bird, D.F., Prairie, Y.T., Planas, D., 1996. Flow cytometric determination of bacterial abundance in lake plankton with the green nucleic acid stain SYTO 13. Limnol. Oceanogr. 41, 783–789. doi:10.4319/lo.1996.41.4.0783
44. Goletti, D., Petruccioli, E., Joosten, S.A., Ottenhoff, T.H.M., 2016. Tuberculosis Biomarkers: From Diagnosis to Protection. Infect. Dis. Rep. 8. doi:10.4081/idr.2016.6568
45. Gunasekera, T.S., Attfield, P.V., Veal, D.A., 2000. A Flow Cytometry Method for Rapid Detection and Enumeration of Total Bacteria in Milk. Appl. Environ. Microbiol. 66, 1228–1232. doi:10.1128/AEM.66.3.1228-1232.2000
46. Hatfull, G.F., Jacobs, W.R., 2014. Molecular Genetics of Mycobacteria. American Society for Microbiology Press.
47. Helaine, S., Cheverton, A.M., Watson, K.G., Faure, L.M., Matthews, S.A., Holden, D.W., 2014. Internalization of Salmonella by macrophages induces formation of nonreplicating persisters. Science 343, 204–208. doi:10.1126/science.1244705
48. Helaine, S., Kugelberg, E., 2014. Bacterial persisters: formation, eradication, and experimental systems. Trends Microbiol. 22, 417–424. doi:10.1016/j.tim.2014.03.008
49. Helaine, S., Thompson, J.A., Watson, K.G., Liu, M., Boyle, C., Holden, D.W., 2010. Dynamics of intracellular bacterial replication at the single cell level. Proc. Natl. Acad. Sci. 107, 3746–3751. doi:10.1073/pnas.1000041107
50. Hendon-Dunn, C.L., Doris, K.S., Thomas, S.R., Allnutt, J.C., Marriott, A.A.N., Hatch, K.A., Watson, R.J., Bottley, G., Marsh, P.D., Taylor, S.C., Bacon, J., 2016. A flow cytometry method for rapidly assessing M. tuberculosis responses to antibiotics with different modes of action. Antimicrob. Agents Chemother. doi:10.1128/AAC.02712-15

51. Henkin, T.M., 2008. Riboswitch RNAs: using RNA to sense cellular metabolism. Genes Dev. 22, 3383–3390. doi:10.1101/gad.1747308
52. Hernlem, B.J., Ravva, S.V., 2007. Application of flow cytometry and cell sorting to the bacterial analysis of environmental aerosol samples. J. Environ. Monit. JEM 9, 1317–1322. doi:10.1039/b710512f
53. Herzenberg, Leonard A., Parks, D., Sahaf, B., Perez, O., Roederer, M., Herzenberg, Leonore A., 2002. The History and Future of the Fluorescence Activated Cell Sorter and Flow Cytometry: A View from Stanford. Clin. Chem. 48, 1819–1827.
54. Hoefel, D., Grooby, W.L., Monis, P.T., Andrews, S., Saint, C.P., 2003. Enumeration of water-borne bacteria using viability assays and flow cytometry: a comparison to culture-based techniques. J. Microbiol. Methods 55, 585–597.
55. Holani, A.G., Ganvir, S.M., Shah, N.N., Bansode, S.C., Shende, I., Jawade, R., Bijjargi, S.C., 2014. Demonstration of Mycobacterium Tuberculosis in Sputum and Saliva Smears of Tuberculosis Patients Using Ziehl Neelsen and Flurochrome Staining- A Comparative Study. J. Clin. Diagn. Res. JCDR 8, ZC42-ZC45. doi:10.7860/JCDR/2014/9764.4587
56. Hong, J., Guan, W., Jin, G., Zhao, H., Jiang, X., Dai, J., 2015. Mechanism of tachyplesin I injury to bacterial membranes and intracellular enzymes, determined by laser confocal scanning microscopy and flow cytometry. Microbiol. Res. 170, 69–77. doi:10.1016/j.micres.2014.08.012
57. Janko, C., Jeremic, I., Biermann, M., Chaurio, R., Schorn, C., Muñoz, L.E., Martin Herrmann, 2013. Cooperative binding of Annexin A5 to phosphatidylserine on apoptotic cell membranes. Phys. Biol. 10, 065006. doi:10.1088/1478-3975/10/6/065006
58. Jarzembowski, T., Wiśniewska, K., Józwik, A., Bryl, E., Witkowski, J., 2008. Flow cytometry as a rapid test for detection of penicillin resistance directly in bacterial cells in Enterococcus faecalis and Staphylococcus aureus. Curr. Microbiol. 57, 167–169. doi:10.1007/s00284-008-9179-8
59. Jernaes, M.W., Steen, H.B., 1994. Staining of Escherichia coli for flow cytometry: influx and efflux of ethidium bromide. Cytometry 17, 302–309. doi:10.1002/cyto.990170405
60. Johansson, J., Karlsson, A., Bylund, J., Welin, A., 2015. Phagocyte interactions with Mycobacterium tuberculosis--Simultaneous analysis of phagocytosis, phagosome maturation and intracellular replication by imaging flow cytometry. J. Immunol. Methods 427, 73–84. doi:10.1016/j.jim.2015.10.003
61. Joux, F., Lebaron, P., 2000. Use of fluorescent probes to assess physiological functions of bacteria at single-cell level. Microbes Infect. Inst. Pasteur 2, 1523–1535.
62. Kalir, N., Özkütük, A.A., Esen, N., Özkütük, N., 2013. Pyrazinamide monoresistance in clinical isolates. Turk. J. Med. Sci. 43, 163–167.
63. Keeler, E., Perkins, M.D., Small, P., Hanson, C., Reed, S., Cunningham, J., Aledort, J.E., Hillborne, L., Rafael, M.E., Girosi, F., Dye, C., 2006. Reducing the global burden of tuberculosis: the contribution of improved diagnostics. Nature 444, 49–57. doi:10.1038/nature05446
64. Keer, J.T., Birch, L., 2003. Molecular methods for the assessment of bacterial viability. J. Microbiol. Methods 53, 175–183.
65. Koopman, G., Reutelingsperger, C.P., Kuijten, G.A., Keehnen, R.M., Pals, S.T., Oers, M. van, 1994. Annexin V for flow cytometric detection of phosphatidylserine expression on B cells undergoing apoptosis. Blood 84, 1415–1420.
66. Kuehnel, M.P., Goethe, R., Habermann, A., Mueller, E., Rohde, M., Griffiths, G., Valentin-Weigand, P., 2001. Characterization of the intracellular survival of Mycobacterium avium ssp. paratuberculosis: phagosomal pH and fusogenicity in J774 macrophages compared with other mycobacteria. Cell. Microbiol. 3, 551–566.
67. Langemann, T., Mayr, U.B., Meitz, A., Lubitz, W., Herwig, C., 2016. Multi-parameter flow cytometry as a process analytical technology (PAT) approach for the assessment of bacterial ghost production. Appl. Microbiol. Biotechnol. 100, 409–418. doi:10.1007/s00253-015-7089-9

68. Langsrud, S., Sundheim, G., 1996. Flow cytometry for rapid assessment of viability after exposure to a quaternary ammonium compound. J. Appl. Bacteriol. 81, 411–418. doi:10.1111/j.1365-2672.1996.tb03527.x
69. Lawn, S.D., Wilkinson, R., 2006. Extensively drug resistant tuberculosis. BMJ 333, 559–560. doi:10.1136/bmj.38971.587222.AB
70. Lee, H.R., Seo, J.-W., Kim, M.J., Song, S.H., Park, K.U., Song, J., Han, K.-S., 2012. Rapid Detection of Bacterial Contamination of Platelet-Rich Plasma-Derived Platelet Concentrates Using Flow Cytometry. Ann. Clin. Lab. Sci. 42, 174–181.
71. Lee, J., Remold, H.G., Ieong, M.H., Kornfeld, H., 2006. Macrophage Apoptosis in Response to High Intracellular Burden of Mycobacterium tuberculosis Is Mediated by a Novel Caspase-Independent Pathway. J. Immunol. 176, 4267–4274. doi:10.4049/jimmunol.176.7.4267
72. Lewis, K., 2010. Persister Cells. Annu. Rev. Microbiol. 64, 357–372. doi:10.1146/annurev.micro.112408.134306
73. Li, H., Zhou, L.-P., Luo, J., Yu, J.-P., Yang, H., Wei, H.-P., 2016. Rapid colorimetric pyrazinamide susceptibility testing of Mycobacterium tuberculosis. Int. J. Tuberc. Lung Dis. 20, 462–467. doi:10.5588/ijtld.15.0745
74. Li, L., Mendis, N., Trigui, H., Oliver, J.D., Faucher, S.P., 2014. The importance of the viable but non-culturable state in human bacterial pathogens. Front. Microbiol. 5, 258. doi:10.3389/fmicb.2014.00258
75. Lin, M.Y., Reddy, T.B.K., Arend, S.M., Friggen, A.H., Franken, K.L.M.C., Meijgaarden, K.E. van, Verduyn, M.J.C., Schoolnik, G.K., Klein, M.R., Ottenhoff, T.H.M., 2009. Cross-Reactive Immunity to Mycobacterium tuberculosis DosR Regulon-Encoded Antigens in Individuals Infected with Environmental, Nontuberculous Mycobacteria. Infect. Immun. 77, 5071–5079. doi:10.1128/IAI.00457-09
76. Liu, J., Barry, C.E., Besra, G.S., Nikaido, H., 1996. Mycolic acid structure determines the fluidity of the mycobacterial cell wall. J. Biol. Chem. 271, 29545–29551.
77. Loeuillet, C., Martinon, F., Perez, C., Munoz, M., Thome, M., Meylan, P.R., 2006. Mycobacterium tuberculosis Subverts Innate Immunity to Evade Specific Effectors. J. Immunol. 177, 6245–6255. doi:10.4049/jimmunol.177.9.6245
78. López-Amorós, R., Comas, J., García, M.T., Vives-Rego, J., 1998. Use of the 5-cyano-2,3-ditolyl tetrazolium chloride reduction test to assess respiring marine bacteria and grazing effects by flow cytometry during linear alkylbenzene sulfonate degradation. FEMS Microbiol. Ecol. 27, 33–42. doi:10.1111/j.1574-6941.1998.tb00523.x
79. Lynch, S.A., Desai, S.K., Sajja, H.K., Gallivan, J.P., 2007. A high-throughput screen for synthetic riboswitches reveals mechanistic insights into their function. Chem. Biol. 14, 173–184. doi:10.1016/j.chembiol.2006.12.008
80. Lynch, S.A., Gallivan, J.P., 2009. A flow cytometry-based screen for synthetic riboswitches. Nucleic Acids Res. 37, 184–192. doi:10.1093/nar/gkn924
81. Machtel, P., Bąkowska-Żywicka, K., Żywicki, M., 2016. Emerging applications of riboswitches – from antibacterial targets to molecular tools. J. Appl. Genet. 57, 531–541. doi:10.1007/s13353-016-0341-x
82. Maclean, M., MacGregor, S.J., Anderson, J.G., Woolsey, G., 2009. Inactivation of Bacterial Pathogens following Exposure to Light from a 405-Nanometer Light-Emitting Diode Array. Appl. Environ. Microbiol. 75, 1932–1937. doi:10.1128/AEM.01892-08
83. Maglica, Ž., Özdemir, E., McKinney, J.D., 2015. Single-Cell Tracking Reveals Antibiotic-Induced Changes in Mycobacterial Energy Metabolism. mBio 6, e02236-14. doi:10.1128/mBio.02236-14
84. Mailaender, C., Reiling, N., Engelhardt, H., Bossmann, S., Ehlers, S., Niederweis, M., 2004. The MspA porin promotes growth and increases antibiotic susceptibility of both Mycobacterium bovis BCG and Mycobacterium tuberculosis. Microbiology 150, 853–864. doi:10.1099/mic.0.26902-0

85. Manina, G., Dhar, N., McKinney, J.D., 2015. Stress and Host Immunity Amplify Mycobacterium tuberculosis Phenotypic Heterogeneity and Induce Nongrowing Metabolically Active Forms. Cell Host Microbe 17, 32–46. doi:10.1016/j.chom.2014.11.016
86. Mason, D.J., Lloyd, D., 1997. Acridine orange as an indicator of bacterial susceptibility to gentamicin. FEMS Microbiol. Lett. 153, 199–204. doi:10.1111/j.1574-6968.1997.tb10482.x
87. Mekonnen, D., Admassu, A., Wassie, B., Biadglegne, F., 2015. Evaluation of the efficacy of bleach routinely used in health facilities against Mycobacterium tuberculosis isolates in Ethiopia. Pan Afr. Med. J. 21, 317. doi:10.11604/pamj.2015.21.317.5456
88. Monici, M., 2005. Cell and tissue autofluorescence research and diagnostic applications. Biotechnol. Annu. Rev. 11, 227–256. doi:10.1016/S1387-2656(05)11007-2
89. Morishige, Y., Fujimori, K., Amano, F., 2015. Use of Flow Cytometry for Quantitative Analysis of Metabolism of Viable but Non-culturable (VBNC) Salmonella. Biol. Pharm. Bull. 38, 1255–1264. doi:10.1248/bpb.b15-00005
90. Mouton, J.M., Helaine, S., Holden, D.W., Sampson, S.L., 2016. Elucidating population-wide mycobacterial replication dynamics at the single-cell level. Microbiol. Read. Engl. doi:10.1099/mic.0.000288
91. Müller, S., Davey, H., 2009. Recent advances in the analysis of individual microbial cells. Cytometry A 75A, 83–85. doi:10.1002/cyto.a.20702
92. Müller, S., Nebe-von-Caron, G., 2010. Functional single-cell analyses: flow cytometry and cell sorting of microbial populations and communities. FEMS Microbiol. Rev. 34, 554–587. doi:10.1111/j.1574-6976.2010.00214.x
93. Niederweis, M., 2003. Mycobacterial porins – new channel proteins in unique outer membranes. Mol. Microbiol. 49, 1167–1177. doi:10.1046/j.1365-2958.2003.03662.x
94. Novo, D.J., Perlmutter, N.G., Hunt, R.H., Shapiro, H.M., 2000. Multiparameter flow cytometric analysis of antibiotic effects on membrane potential, membrane permeability, and bacterial counts of Staphylococcus aureus and Micrococcus luteus. Antimicrob. Agents Chemother. 44, 827–834.
95. Nuding, S., 2013. Detection, Identification, and Susceptibility Testing of Bacteria by Flow Cytometry. J. Bacteriol. Parasitol. 01. doi:10.4172/2155-9597.S5-005
96. O'Donnell, M.R., Pym, A., Jain, P., Munsamy, V., Wolf, A., Karim, F., Jacobs, W.R., Larsen, M.H., 2015. A Novel Reporter Phage To Detect Tuberculosis and Rifampin Resistance in a High-HIV-Burden Population. J. Clin. Microbiol. 53, 2188–2194. doi:10.1128/JCM.03530-14
97. Olenych, S.G., Claxton, N.S., Ottenberg, G.K., Davidson, M.W., 2007. The fluorescent protein color palette. Curr. Protoc. Cell Biol. Chapter 21, Unit 21.5. doi:10.1002/0471143030.cb2105s36
98. Oliver, J.D., 2010. Recent findings on the viable but nonculturable state in pathogenic bacteria. FEMS Microbiol. Rev. 34, 415–425. doi:10.1111/j.1574-6976.2009.00200.x
99. Ordóñez, J.V., Wehman, N.M., 1993. Rapid flow cytometric antibiotic susceptibility assay for Staphylococcus aureus. Cytometry 14, 811–818. doi:10.1002/cyto.990140714
100. Ozanne, V., Ortalo-Magne, A., Vercellone, A., Fournie, J.J., Daffe, M., 1996. Cytometric detection of mycobacterial surface antigens: exposure of mannosyl epitopes and of the arabinan segment of arabinomannans. J. Bacteriol. 178, 7254–7259.
101. Pandey, S., Congdon, J., McInnes, B., Pop, A., Coulter, C., 2017. Evaluation of the GeneXpert MTB/RIF assay on extrapulmonary and respiratory samples other than sputum: a low burden country experience. Pathology (Phila.) 49, 70–74. doi:10.1016/j.pathol.2016.10.004
102. Parish, T., Mahenthiralingam, E., Draper, P., Davis, E.O., Colston, M.J., 1997. Regulation of the inducible acetamidase gene of Mycobacterium smegmatis. Microbiol. Read. Engl. 143 (Pt 7), 2267–2276. doi:10.1099/00221287-143-7-2267
103. Peres, R.L., Maciel, E.L., Morais, C.G., Ribeiro, F.C.K., Vinhas, S.A., Pinheiro, C., Dietze, R., Johnson, J.L., Eisenach, K., Palaci, M., 2009. Comparison of two concentrations of NALC-NaOH for decontamination of sputum for mycobacterial culture [Technical note]. Int. J. Tuberc. Lung Dis. 13, 1572–1575.

104. Perez, O.D., Nolan, G.P., 2006. Phospho-proteomic immune analysis by flow cytometry: from mechanism to translational medicine at the single-cell level. Immunol. Rev. 210, 208–228. doi:10.1111/j.0105-2896.2006.00364.x
105. Pinto, D., Almeida, V., Almeida Santos, M., Chambel, L., 2011. Resuscitation of Escherichia coli VBNC cells depends on a variety of environmental or chemical stimuli. J. Appl. Microbiol. 110, 1601–1611. doi:10.1111/j.1365-2672.2011.05016.x
106. Piuri, M., Jacobs, W.R., Jr., Hatfull, G.F., 2009. Fluoromycobacteriophages for Rapid, Specific, and Sensitive Antibiotic Susceptibility Testing of Mycobacterium tuberculosis. PLoS ONE 4, e4870. doi:10.1371/journal.pone.0004870
107. Prakash, H., Lüth, A., Grinkina, N., Holzer, D., Wadgaonkar, R., Gonzalez, A.P., Anes, E., Kleuser, B., 2010. Sphingosine Kinase-1 (SphK-1) Regulates Mycobacterium smegmatis Infection in Macrophages. PLOS ONE 5, e10657. doi:10.1371/journal.pone.0010657
108. Prax, M., Bertram, R., 2014. Metabolic aspects of bacterial persisters. Front. Cell. Infect. Microbiol. 4. doi:10.3389/fcimb.2014.00148
109. Ramakrishnan, L., Federspiel, N.A., Falkow, S., 2000. Granuloma-specific expression of Mycobacterium virulence proteins from the glycine-rich PE-PGRS family. Science 288, 1436–1439.
110. Ramamurthy, T., Ghosh, A., Pazhani, G.P., Shinoda, S., 2014. Current Perspectives on Viable but Non-Culturable (VBNC) Pathogenic Bacteria. Front. Public Health 2, 103. doi:10.3389/fpubh.2014.00103
111. Rao, S.P.S., Alonso, S., Rand, L., Dick, T., Pethe, K., 2008. The protonmotive force is required for maintaining ATP homeostasis and viability of hypoxic, nonreplicating Mycobacterium tuberculosis. Proc. Natl. Acad. Sci. U. S. A. 105, 11945–11950. doi:10.1073/pnas.0711697105
112. Ren, K., Banaei, N., Zare, R.N., 2013. Sorting Inactivated Cells Using Cell-Imprinted Polymer Thin Films. ACS Nano 7, 6031–6036. doi:10.1021/nn401768s
113. Rizzo, M.A., Davidson, M.W., Piston, D.W., 2009. Fluorescent Protein Tracking and Detection: Fluorescent Protein Structure and Color Variants. Cold Spring Harb. Protoc. 2009, pdb.top63. doi:10.1101/pdb.top63
114. Roberts, G., Muttucumaru, D.G.N., Parish, T., 2003. Control of the acetamidase gene of Mycobacterium smegmatis by multiple regulators. FEMS Microbiol. Lett. 221, 131–136.
115. Rottenberg, H., Wu, S., 1998. Quantitative assay by flow cytometry of the mitochondrial membrane potential in intact cells. Biochim. Biophys. Acta BBA - Mol. Cell Res. 1404, 393–404. doi:10.1016/S0167-4889(98)00088-3
116. Ryan, G.J., Hoff, D.R., Driver, E.R., Voskuil, M.I., Gonzalez-Juarrero, M., Basaraba, R.J., Crick, D.C., Spencer, J.S., Lenaerts, A.J., 2010. Multiple M. tuberculosis Phenotypes in Mouse and Guinea Pig Lung Tissue Revealed by a Dual-Staining Approach. PLoS ONE 5. doi:10.1371/journal.pone.0011108
117. Sakula, A., 1982. Robert Koch: centenary of the discovery of the tubercle bacillus, 1882. Thorax 37, 246–251. doi:10.1136/thx.37.4.246
118. Sampson, S.L., Dascher, C.C., Sambandamurthy, V.K., Russell, R.G., Jacobs, W.R., Bloom, B.R., Hondalus, M.K., 2004. Protection Elicited by a Double Leucine and Pantothenate Auxotroph of Mycobacterium tuberculosis in Guinea Pigs. Infect. Immun. 72, 3031–3037. doi:10.1128/IAI.72.5.3031-3037.2004
119. Sánchez, A., Espinosa, P., Garcia, T., Mancilla, R., 2012. The 19 kDa Mycobacterium tuberculosis Lipoprotein (LpqH) Induces Macrophage Apoptosis through Extrinsic and Intrinsic Pathways: A Role for the Mitochondrial Apoptosis-Inducing Factor. Clin. Amp Dev. Immunol. 2012, 950503. doi:10.1155/2012/950503
120. Sandilos, J.K., Chiu, Y.-H., Chekeni, F.B., Armstrong, A.J., Walk, S.F., Ravichandran, K.S., Bayliss, D.A., 2012. Pannexin 1, an ATP Release Channel, Is Activated by Caspase Cleavage of Its Pore-associated C-terminal Autoinhibitory Region. J. Biol. Chem. 287, 11303–11311. doi:10.1074/jbc.M111.323378

121. Saper, C.B., 2009. A Guide to the Perplexed on the Specificity of Antibodies. J. Histochem. Cytochem. 57, 1–5. doi:10.1369/jhc.2008.952770
122. Sauvat, A., Y, W., F, S., S, S., K, M., H, Z., L, G., O, K., G, K., 2015. Quantification of cellular viability by automated microscopy and flow cytometry. Oncotarget 6, 9467–9475.
123. Seeliger, J.C., Topp, S., Sogi, K.M., Previti, M.L., Gallivan, J.P., Bertozzi, C.R., 2012. A Riboswitch-Based Inducible Gene Expression System for Mycobacteria. PLoS ONE 7, e29266. doi:10.1371/journal.pone.0029266
124. Sester, U., Fousse, M., Dirks, J., Mack, U., Prasse, A., Singh, M., Lalvani, A., Sester, M., 2011. Whole-Blood Flow-Cytometric Analysis of Antigen-Specific CD4 T-Cell Cytokine Profiles Distinguishes Active Tuberculosis from Non-Active States. PLoS ONE 6, e17813. doi:10.1371/journal.pone.0017813
125. Sevastsyanovich, Y., Alfasi, S., Overton, T., Hall, R., Jones, J., Hewitt, C., Cole, J., 2009. Exploitation of GFP fusion proteins and stress avoidance as a generic strategy for the production of high-quality recombinant proteins. FEMS Microbiol. Lett. 299, 86–94. doi:10.1111/j.1574-6968.2009.01738.x
126. Shaner, N.C., Campbell, R.E., Steinbach, P.A., Giepmans, B.N.G., Palmer, A.E., Tsien, R.Y., 2004. Improved monomeric red, orange and yellow fluorescent proteins derived from Discosoma sp. red fluorescent protein. Nat. Biotechnol. 22, 1567–1572. doi:10.1038/nbt1037
127. Shleeva, M.O., Bagramyan, K., Telkov, M.V., Mukamolova, G.V., Young, M., Kell, D.B., Kaprelyants, A.S., 2002. Formation and resuscitation of "non-culturable" cells of Rhodococcus rhodochrous and Mycobacterium tuberculosis in prolonged stationary phase. Microbiology 148, 1581–1591. doi:10.1099/00221287-148-5-1581
128. Shu, Z., Weigel, K.M., Soelberg, S.D., Lakey, A., Cangelosi, G.A., Lee, K.-H., Chung, J.-H., Gao, D., 2012. Cryopreservation of Mycobacterium tuberculosis Complex Cells. J. Clin. Microbiol. 50, 3575–3580. doi:10.1128/JCM.00896-12
129. Signoretto, C., Lleò, M.M., Canepari, P., 2002. Modification of the peptidoglycan of Escherichia coli in the viable but nonculturable state. Curr. Microbiol. 44, 125–131.
130. Singh, K.K., Dong, Y., Belisle, J.T., Harder, J., Arora, V.K., Laal, S., 2005. Antigens of Mycobacterium tuberculosis Recognized by Antibodies during Incipient, Subclinical Tuberculosis. Clin. Diagn. Lab. Immunol. 12, 354–358. doi:10.1128/CDLI.12.2.354-358.2005
131. Sliwinska, E., Zielinska, E., Jedrzejczyk, I., 2005. Are seeds suitable for flow cytometric estimation of plant genome size? Cytometry A 64A, 72–79. doi:10.1002/cyto.a.20122
132. Snapper, S.B., Melton, R.E., Mustafa, S., Kieser, T., Jacobs, W.R., 1990. Isolation and characterization of efficient plasmid transformation mutants of Mycobacterium smegmatis. Mol. Microbiol. 4, 1911–1919.
133. Soejima, T., Iida, K., Qin, T., Taniai, H., Yoshida, S., 2009. Discrimination of live, anti-tuberculosis agent-injured, and dead Mycobacterium tuberculosis using flow cytometry. FEMS Microbiol. Lett. 294, 74–81. doi:10.1111/j.1574-6968.2009.01549.x
134. Steingart, K.R., Ng, V., Henry, M., Hopewell, P.C., Ramsay, A., Cunningham, J., Urbanczik, R., Perkins, M.D., Aziz, M.A., Pai, M., 2006. Sputum processing methods to improve the sensitivity of smear microscopy for tuberculosis: a systematic review. Lancet Infect. Dis. 6, 664–674. doi:10.1016/S1473-3099(06)70602-8
135. Stellmach, J., Severin, E., 1987. A fluorescent redox dye. Influence of several substrates and electron carriers on the tetrazolium salt—formazan reaction of Ehrlich ascites tumour cells. Histochem. J. 19, 21–26. doi:10.1007/BF01675289
136. Stepień-Pyśniak, D., 2010. Occurrence of gram-negative bacteria in hens' eggs depending on their source and storage conditions. Pol. J. Vet. Sci. 13, 507–513.
137. Stiefel, P., Schmidt-Emrich, S., Maniura-Weber, K., Ren, Q., 2015. Critical aspects of using bacterial cell viability assays with the fluorophores SYTO9 and propidium iodide. BMC Microbiol. 15. doi:10.1186/s12866-015-0376-x

138. Stocks, S.M., 2004. Mechanism and use of the commercially available viability stain, BacLight. Cytom. Part J. Int. Soc. Anal. Cytol. 61, 189–195. doi:10.1002/cyto.a.20069
139. Sträuber, H., Müller, S., 2010. Viability states of bacteria--specific mechanisms of selected probes. Cytom. Part J. Int. Soc. Anal. Cytol. 77, 623–634. doi:10.1002/cyto.a.20920
140. Sun, Y., Booker, C.F., Kumari, S., Day, R.N., Davidson, M., Periasamy, A., 2009. Characterization of an orange acceptor fluorescent protein for sensitized spectral fluorescence resonance energy transfer microscopy using a white-light laser. J. Biomed. Opt. 14. doi:10.1117/1.3227036
141. Tan, M.P., Sequeira, P., Lin, W.W., Phong, W.Y., Cliff, P., Ng, S.H., Lee, B.H., Camacho, L., Schnappinger, D., Ehrt, S., Dick, T., Pethe, K., Alonso, S., 2010. Nitrate Respiration Protects Hypoxic Mycobacterium tuberculosis Against Acid- and Reactive Nitrogen Species Stresses. PLOS ONE 5, e13356. doi:10.1371/journal.pone.0013356
142. Telenti, A., Imboden, P., Marchesi, F., Lowrie, D., Cole, S., Colston, M.J., Matter, L., Schopfer, K., Bodmer, T., 1993. Detection of rifampicin-resistance mutations in Mycobacterium tuberculosis. Lancet Lond. Engl. 341, 647–650.
143. Topp, S., Reynoso, C.M.K., Seeliger, J.C., Goldlust, I.S., Desai, S.K., Murat, D., Shen, A., Puri, A.W., Komeili, A., Bertozzi, C.R., Scott, J.R., Gallivan, J.P., 2010. Synthetic Riboswitches That Induce Gene Expression in Diverse Bacterial Species. Appl. Environ. Microbiol. 76, 7881–7884. doi:10.1128/AEM.01537-10
144. Tracy, B.P., Gaida, S.M., Papoutsakis, E.T., 2010a. Flow cytometry for bacteria: enabling metabolic engineering, synthetic biology and the elucidation of complex phenotypes. Curr. Opin. Biotechnol., Analytical Biotechnology 21, 85–99. doi:10.1016/j.copbio.2010.02.006
145. Tracy, B.P., Gaida, S.M., Papoutsakis, E.T., 2010b. Flow cytometry for bacteria: enabling metabolic engineering, synthetic biology and the elucidation of complex phenotypes. Curr. Opin. Biotechnol. 21, 85–99. doi:10.1016/j.copbio.2010.02.006
146. Tundup, S., Mohareer, K., Hasnain, S.E., 2014. Mycobacterium tuberculosis PE25/PPE41 protein complex induces necrosis in macrophages: Role in virulence and disease reactivation? FEBS Open Bio 4, 822–828. doi:10.1016/j.fob.2014.09.001
147. Van Vlack, E.R., Seeliger, J.C., 2015. Chapter Twelve - Using Riboswitches to Regulate Gene Expression and Define Gene Function in Mycobacteria, in: Burke-Aguero, D.H. (Ed.), Methods in Enzymology, Riboswitches as Targets and Tools. Academic Press, pp. 251–265.
148. Vermes, I., Haanen, C., Reutelingsperger, C., 2000. Flow cytometry of apoptotic cell death. J. Immunol. Methods, Flow Cytometry 243, 167–190. doi:10.1016/S0022-1759(00)00233-7
149. Vilchèze, C., Weisbrod, T.R., Chen, B., Kremer, L., Hazbón, M.H., Wang, F., Alland, D., Sacchettini, J.C., Jacobs, W.R., 2005. Altered NADH/NAD+ Ratio Mediates Coresistance to Isoniazid and Ethionamide in Mycobacteria. Antimicrob. Agents Chemother. 49, 708–720. doi:10.1128/AAC.49.2.708-720.2005
150. Vives-Rego, J., Lebaron, P., Nebe-von Caron, G., 2000. Current and future applications of flow cytometry in aquatic microbiology. FEMS Microbiol. Rev. 24, 429–448. doi:10.1111/j.1574-6976.2000.tb00549.x
151. Wachsmuth, M., Domin, G., Lorenz, R., Serfling, R., Findeiß, S., Stadler, P.F., Mörl, M., 2015. Design criteria for synthetic riboswitches acting on transcription. RNA Biol. 12, 221–231. doi:10.1080/15476286.2015.1017235
152. Wachsmuth, M., Findeiß, S., Weissheimer, N., Stadler, P.F., Mörl, M., 2013. De novo design of a synthetic riboswitch that regulates transcription termination. Nucleic Acids Res. 41, 2541–2551. doi:10.1093/nar/gks1330
153. Walter, N.D., Dolganov, G.M., Garcia, B.J., Worodria, W., Andama, A., Musisi, E., Ayakaka, I., Van, T.T., Voskuil, M.I., de Jong, B.C., Davidson, R.M., Fingerlin, T.E., Kechris, K., Palmer, C., Nahid, P., Daley, C.L., Geraci, M., Huang, L., Cattamanchi, A., Strong, M., Schoolnik, G.K., Davis, J.L., 2015. Transcriptional Adaptation of Drug-tolerant Mycobacterium tuberculosis During Treatment of Human Tuberculosis. J. Infect. Dis. 212, 990–998. doi:10.1093/infdis/jiv149

154. World Health Organization, 2015. Global tuberculosis report 2015. Geneva World Health Organ.
155. Yamada, H., Mitarai, S., Wahyunitisari, M.R., Mertaniasih, N.M., Sugamoto, T., Chikamatsu, K., Aono, A., Matsumoto, H., Fujiki, A., 2011. Improved Polyacrylamide-Based Artificial Sputum with Formalin-Fixed Tubercle Bacilli for Training of Tuberculosis Microscopists. J. Clin. Microbiol. 49, 3604–3609. doi:10.1128/JCM.00370-11
156. Zuker, M., 2003. Mfold web server for nucleic acid folding and hybridization prediction. Nucleic Acids Res. 31, 3406–3415.
157. Zumla, A., Abubakar, I., Raviglione, M., Hoelscher, M., Ditiu, L., McHugh, T.D., Squire, S.B., Cox, H., Ford, N., McNerney, R., Marais, B., Grobusch, M., Lawn, S.D., Migliori, G.-B., Mwaba, P., O'Grady, J., Pletschette, M., Ramsay, A., Chakaya, J., Schito, M., Swaminathan, S., Memish, Z., Maeurer, M., Atun, R., 2012. Drug-resistant tuberculosis--current dilemmas, unanswered questions, challenges, and priority needs. J. Infect. Dis. 205 Suppl 2, S228-240. doi:10.1093/infdis/jir858